

# Electrochemical C–H/C–C Bond Oxygenation: A Potential Technology for Plastic Depolymerization

Sadia Rani,<sup>[a]</sup> Samina Aslam,<sup>[a]</sup> Kiran Lal,<sup>[a]</sup> Sobia Noreen,<sup>[b]</sup> Khadeeja Ali Mohammed Alsader,<sup>[c]</sup> Riaz Hussain,<sup>[d]</sup> Bahareh Shirinfar,<sup>[e]</sup> and Nisar Ahmed<sup>\*[c]</sup>

**Abstract:** Herein, we provide eco-friendly and safely operated electrocatalytic methods for the selective oxidation directly or with water, air, light, metal catalyst or other mediators serving as the only oxygen supply. Heavy metals, stoichiometric chemical oxidants, or harsh conditions were drawbacks of earlier oxidative cleavage techniques. It has recently come to light that a crucial stage in the deconstruction of plastic waste and the utilization of biomass is the selective activation of inert C(sp<sup>3</sup>)–C/H(sp<sup>3</sup>) bonds, which continues to be a significant obstacle in the chemical upcycling of resistant polyolefin waste. An appealing alternative to chemical oxidations using oxygen and catalysts is direct or indirect electrochemical conversion. An essential transition in the chemical and pharmaceutical industries is the electrochemical oxidation of C–H/C–C bonds. In this review, we discuss cutting-edge approaches to chemically recycle commercial plastics and feasible C–C/C–H bonds oxygenation routes for industrial scale-up.

**Keywords:** Electrochemical oxygenation, C–H oxygenation, C–C bond cleavage, Plastic depolymerization, eco-friendly electrocatalysis

[a] S. Rani, S. Aslam, K. Lal

Department of Chemistry, The Women University Multan, Multan 60000, Pakistan

[b] S. Noreen

Institute of Chemistry, University of Sargodha, Sargodha 40100, Pakistan

[c] K. A. M. Alsader, N. Ahmed

School of Chemistry, Cardiff University, Main Building, Park Place, Cardiff, CF10 3AT, United Kingdom

E-mail: AhmedN14@cardiff.ac.uk

nisarhej@gmail.com

AhmedN03@outlook.com

[d] R. Hussain

Department of Chemistry, University of Education Lahore, D.G. Khan Campus 32200, Pakistan

[e] B. Shirinfar

West Herts College – University of Hertfordshire, Watford, WD17 3EZ, London, United Kingdom

## 1. Introduction

Functional groups made of carbon-oxygen (C–O) bonds are a common feature of complex compounds. The conversion of relatively inert carbon-hydrogen (C–H) bonds, which are common in basic precursor compounds, to C–O bonds by a procedure known as C–H oxygenation is a particularly attractive method for the synthesis of such molecules. The synthetic world has recently paid a lot of attention to organic electro-oxidation as a potent and sustainable method.<sup>[1–9]</sup> With the potential to eliminate the need for expensive and harmful oxidants or reductants,<sup>[1,10–13]</sup> electrosynthesis has become a more and more practical method for molecular synthesis, lowering the environmental impact of unwanted, toxic byproducts.<sup>[14–15]</sup> Electric current is more environmentally friendly and greener than conventional chemical oxidants.<sup>[16–21]</sup> In the existing structure of the chemical industry, the production of feedstock depends critically on the effective and selective oxidation of the C–H bond in organic compounds.<sup>[22–24]</sup> Aldehydes and ketones, two crucial intermediates needed to meet the need for products with significant value like fragrances, agrochemicals, and pharmaceuticals, can

© 2023 The Authors. The Chemical Record published by The Chemical Society of Japan and Wiley-VCH GmbH. This is an open access article under the terms of the Creative Commons Attribution Non-Commercial NoDerivs License, which permits use and distribution in any medium, provided the original work is properly cited, the use is non-commercial and no modifications or adaptations are made.

be produced by a conventional oxidation.<sup>[25–27]</sup> Low polarity and strong bond energy of C–H bond, however, make it difficult to activate it using mild and controlled methods. It is common practice to use harsh operating conditions, such as high oxygen pressures,<sup>[28]</sup> high temperatures,<sup>[29]</sup> stoichiometric additives,<sup>[30]</sup> powerful oxidants (H<sub>2</sub>O<sub>2</sub>, *t*-BuOOH, O<sub>2</sub>, etc.)<sup>[31]</sup> and acidic solvents.<sup>[32]</sup> Electrochemical oxidation, in contrast, is a reliable and sustainable substitute.<sup>[1,12,33–34]</sup> Under favorable circumstances, organic substrates that are electrically driven can lose electrons at the surface of anode (positive electrode), resulting in the formation of products.<sup>[35–36]</sup> Catalysts are essential for electrochemical oxidation because they have a significant impact on the reaction rate, selectivity, and Faraday efficiency.<sup>[37–40]</sup> Inert C–C bonds can be activated under mild conditions via electrochemical oxidation, which is a promising method.<sup>[35,41–45]</sup>

An important step in the deconstruction of plastic waste and the valorization of biomass, the selective activation of carbon (sp<sup>3</sup>)-carbon(sp<sup>3</sup>) bonds is a difficult problem in organic chemistry.<sup>[46–51]</sup> However, the inertness of the C–C associations prevents selective and energy-efficient bond activation of these compounds.<sup>[51–53]</sup> Indeed, a number of thermodynamic and kinetic restrictions,<sup>[54–58]</sup> such as high bond dissociation energies (BDEs) of about 90 kcalmol<sup>-1</sup> for C–H bonds and unfavorable orbital directionality towards cleavage, which necessitates the rotation of two carbon sp<sup>3</sup> orbitals, make it difficult to activate C–C bonds.<sup>[59]</sup> Studies show that as the C–C bond dissociation energy decreases, the selectivity of the C–C bond cleavage rises. To this goal, electrochemical oxidation offers a viable method for mildly activating inactive C–C bonds.<sup>[35,41–45]</sup>

Such electrochemical methods can be divided into direct and indirect electrochemical C–H/C–C bond oxygenation. The substrate diffuses to the electrode surfaces in a direct electro-oxidation configuration, where it receives an electron transfer. Although the inert C–C bonds must be activated by strongly anodic potentials, which can also induce adverse side

effects such solvent oxidation, direct electro-oxidation is inefficient at converting energy.<sup>[6,60]</sup> The efficient cleavage and functionalization of C–C bonds would be advantageous in a variety of processes, including the conversion of biomass, the production of pharmaceuticals, and polymer degradation.<sup>[61–69]</sup> For example, visible light driven C–C bond cleavage is used in recycling of plastics and other organic transformations.<sup>[70]</sup>

Due to its widespread use in the production of pharmaceuticals and fine chemicals, direct oxidation of benzylic C(sp<sup>3</sup>)-H bonds to produce carbonyl compounds is one of the most useful conversions.<sup>[71–76]</sup> Even so, a lot of progress has been made toward achieving site-selective, regulated C–H oxygenation reactions in challenging environments.<sup>[77–88]</sup>

Using water as the only oxygen source is an environmentally friendly electro-catalytic method. The anodic C–H oxidation onset potential can be lowered by adding water. Using air as an only oxygen source is also eco-friendly and green electrochemical C–H/C–C bond oxygenation protocol because air is the purest and safest oxidant. However, difficult oxidative processes can be carried out selectively using electro-photocatalysis. Mediated electrochemical C–H/C–C bond oxygenation lowers the anodic potential and it provides high selectivity. However, recycling challenges have to be faced and mediators are required in this strategy. Transition metal catalysis has become one of the most significant channels for selectivity control in contemporary synthetic chemistry. In modern synthetic chemistry, transition metal catalyzed C–H/C–C bond oxygenation has emerged as one of the key mechanisms for selectivity regulation.

We suggest the review article by Gerhard Hilt<sup>[89]</sup> that highlights the fundamental concepts and various applications in organic electrochemistry, as well as the article by Charlotte Willans and coworkers<sup>[90]</sup> that aims to make electrosynthesis more accessible to beginners, in order to help the reader understand the technique of electrosynthesis.

Recent investigations have concentrated on looking for a green oxygen source in electrochemical C–H/C–C bond



Nisar Ahmed obtained his PhD in organic chemistry with Brain Korea BK21 fellowship from POSTECH, Korea. Then, he moved to the University of Zurich, Switzerland for a postdoctoral stay with an Innovative Novartis Fellowship. Subsequently, he joined the University of Bristol as a senior research associate. Further, he started his independent research & academic career at Cardiff University, United Kingdom. He also holds an Adjunct position (Visiting Professor) at HEJ Research Institute of Chemistry, ICCBS. He is (co-)author of ~60 peer-reviewed publications & 4 book chapters. His fields of research include synthesis of value-added chemicals, fine chemicals, green fuels, and pharmaceuticals with special focus on inert bonds activations & cleavage using a renewable energy source rather than fossil fuels (green chemistry) & modern synthetic tools such as electrochemistry, photochemistry, sonochemistry, flow technology, digital & automation chemistry, and reaction engineering. These methods require fewer reaction steps, consume less energy, and generate less or zero waste and are environmentally benign to achieve goal of Zero/Net carbon future. Furthermore, novel synthetic derivatives are used in molecular recognition (supramolecular chemistry), drug delivery & drug discovery (pharmaceutical & medicinal chemistry).

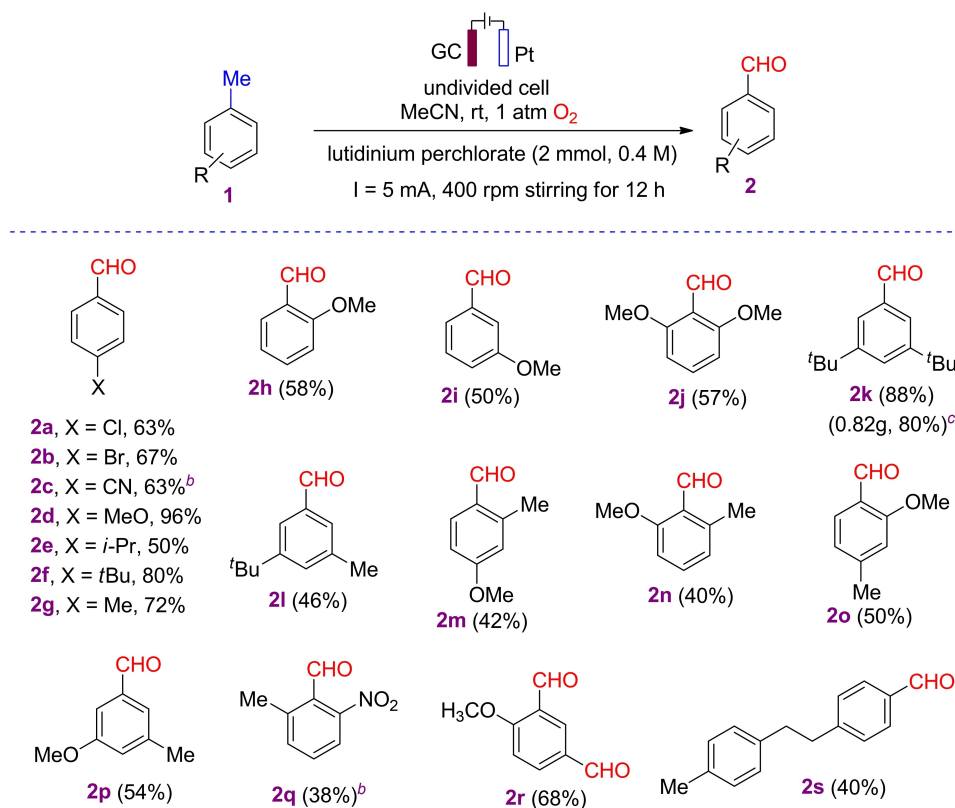
oxygenation. This study has revealed direct,<sup>[91]</sup> water-aided,<sup>[92–93]</sup> air-intended,<sup>[94]</sup> transition metal-catalyzed,<sup>[54,57–58,95–98]</sup> photo-induced,<sup>[99–104]</sup> and other mediated electrochemical C–H/C–C bond oxygenation.

## 2. Direct Electrochemical C–H/C–C Bond Oxygenation

For the oxidation of benzylic C(sp<sup>3</sup>)–H bonds, an effective electrochemical technique has been suggested. Using O<sub>2</sub> as the oxygen source and 0.4 M lutidinium perchlorate as the electrolyte, a range of methylarenes, methylheteroarenes, and benzylic (hetero)methylens could be converted into the required aryl aldehydes and aryl ketones in moderate to good yields (up to 96% yield). When the reaction conditions were first optimized in an undivided cell using *p*-chlorotoluene **1**,

the required aldehyde **2** at room temperature was produced (Scheme 1). It is metal and base free gram scale strategy. Glassy carbon plate was used as anode and platinum plate was used as cathode, the current applied during this electrochemical process was 5 mA.

In order to produce the corresponding aldehydes in good yields **2a–2g**, both electron-withdrawing and electron-donating substituted methylarenes underwent efficient oxidation. Furthermore, the reaction was unhindered for substrates with various aryl ring substitution patterns **2h–2k**. In modest yields **2g** and **2l–2q**, bismethylbenzenes were selectively oxidized to the corresponding monoaldehydes. Bisaldehyde **2r** was produced in a 68% yield when 1-methoxy-2,4-dimethylbenzene **1r** was utilized in the process. It was reasoned that both the methyl groups on the *ortho*- and *para*-positions can be oxidized because the methoxy group can effectively stabilize the benzyl radical through resonance at the *ortho*- and *para*- positions.



<sup>a</sup>Standard conditions: 0.5 mmol of substrate, 5 mL of acetonitrile, 0.4M [LutH]<sup>+</sup>ClO<sub>4</sub><sup>-</sup>, and a constant current of 5 mA (**2a**, **2b**, **2d–2p**, **2r**, and **2s**). <sup>b</sup>With 0.4 mmol of substrate, 4 mL of acetonitrile, 0.01 M M [LutH]<sup>+</sup>ClO<sub>4</sub><sup>-</sup>, 20 mol % NHPI, and a constant current of 2 mA. Isolated yields. <sup>c</sup>With 5 mmol of **1k**, 10 mL of acetonitrile, 0.4M M [LutH]<sup>+</sup>ClO<sub>4</sub><sup>-</sup>, and a constant current of 5 mA. Isolated yields.

**Scheme 1.** Electrochemical production of aldehydes **2** by direct C–H bond oxygenation.

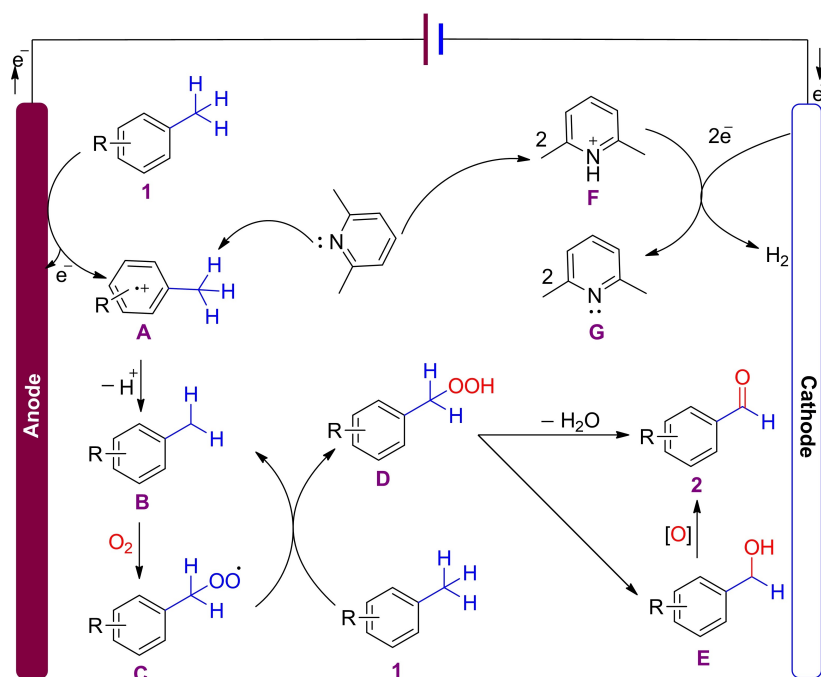
Monoaldehyde **2s** was obtained in a 40% yield during the oxidation of symmetrical 1,2-dip-tolyethane **1s**, but no ketone or bisaldehyde was produced. By oxidizing substrate **1k** on a 5 mmol scale to produce the desired product **2k** was produced in 80% yield. **2k** is an important synthon for the production of porphyrins or porphyrin nano-rings.<sup>[105–106]</sup>

A potential single electron transfer mechanism (scheme 2) for the electro-oxidation reaction has been put forth on the basis of cyclic voltammetry studies, <sup>18</sup>O labeling experiments, and radical trapping experiments. Lutidine **F** undergoes cathodic reduction at the cathode electrolyte to produce H<sub>2</sub> and lutidine **G**. In contrast, the anodic oxidation of substrate **1** results in the formation of the radical cation **A** via single electron transfer (SET), and the subsequent loss of a benzylic proton results in the generation of the benzyl radical **B** with the help of lutidine **E**. This radical could be captured by molecular oxygen to form peroxy radical **C**, which then takes a hydrogen atom from benzylic acid to create hydroperoxide intermediate **D**. After dehydration, this intermediate gives rise to aldehyde product **2**. In order to get the final product, the hydroperoxide intermediate **D** can potentially change into benzyl alcohol **E** and then go through anodic oxidation.<sup>[91]</sup>

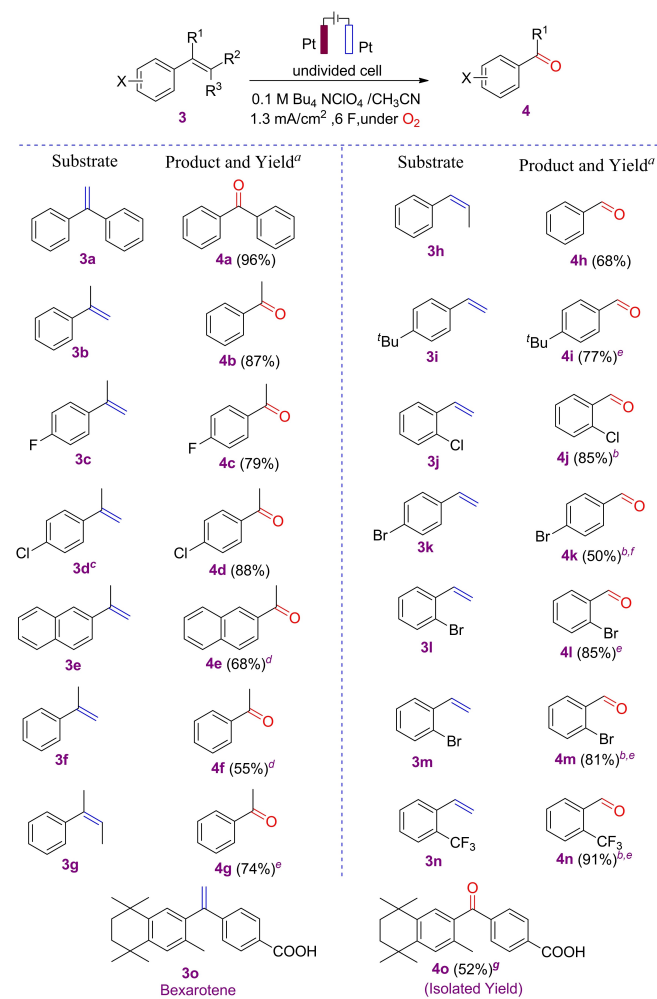
The composition of the electrodes can significantly affect how an electrolysis reaction plays out. The ability of various electrodes to produce various products from the same substrate is very intriguing. The selective molecular oxygen reactions of styrene derivatives with electrode materials have been reported.

Tetrahydrofuran is formed using carbon electrodes while carbonyl compounds can be produced by cleaving olefins using platinum electrodes. For both reactions, a range of styrenes are available. Metal- and oxidant-free, simple and mild chemical transformations are made possible by electrolysis. The distinct ways that platinum and carbon electrodes affect styrene are revealed by electrochemical tests. The fact that the oxidation potentials of the substrates are lower (greater HOMO energy) on carbon electrodes than on platinum electrodes is likely the determining factor in the different reactions. Tetrahydrofuran synthesis may be aided by the adsorption of the substrates on carbon electrodes. Selective transformation of styrenes **3** with molecular oxygen (O<sub>2</sub>) into carbonyls **4** and tetrahydrofurans (THF) **5** was demonstrated using electrode material (platinum and carbon).

At room temperature, Pt-electrodes were placed in an undivided cell containing 10 mL of O<sub>2</sub>-saturated solution containing 0.5 mmol of substrate. The extent of the olefin cleavage using the optimal conditions was illustrated (Scheme 3). In this reaction, a number of styrenes were produced in yields ranging from 50 to 96%. The corresponding ketones **4b–4e** were produced in good yields from  $\alpha$ -methylstyrene derivatives **3b–3e**. Both  $\beta$ -*cis/trans*-methylstyrene and styrene **3f** were tolerated. The conversion of a bulky substituent **3i** is possible. Halogen substituents (**3j–3n**) and electron-withdrawing groups provided the required products in moderate to high yields. Surprisingly, 52% of



**Scheme 2.** Proposed mechanism for electrochemical production of aldehyde **2** by direct C–H bond oxygenation.

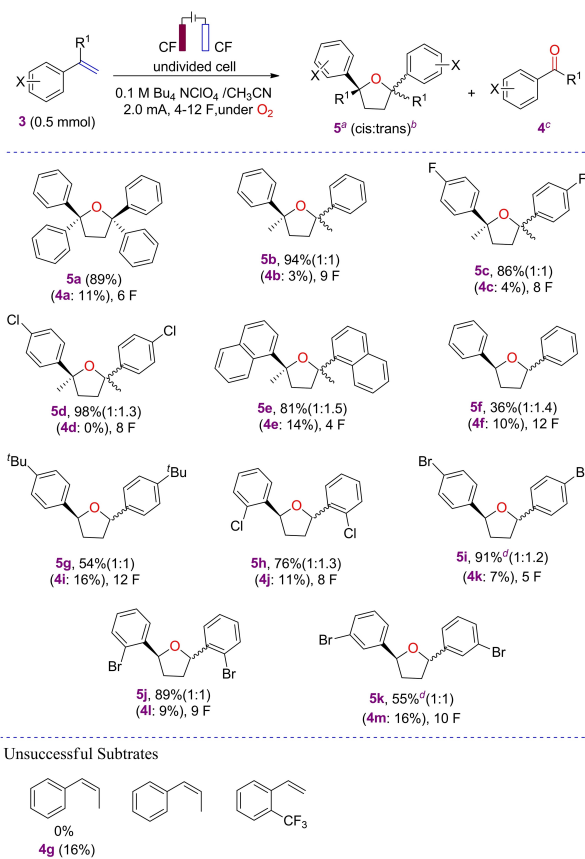


<sup>a</sup> Yields were determined by GC-MS integration. <sup>b</sup> CH<sub>3</sub>NO<sub>2</sub> was used as solvent. <sup>c</sup> 7 F was applied. <sup>d</sup> 3 F was applied. <sup>e</sup> 4 F was applied. <sup>f</sup> 5 F was applied. <sup>g</sup> 0.1 mmol substrate was used due to solubility issues.

**Scheme 3.** Electrochemical production of carbonyl **4**.

Bexarotene (Targretin), an anti-cancer drug for cutaneous T-cell lymphoma, was successfully changed **4o**.

Carbon electrodes have been investigated for an unexpected THF synthesis (Scheme 4). In natural substances like lignans, the structural moiety of 2,5-diaryltetrahydrofuran is frequently present.<sup>[107]</sup> Selective THF production over C=C cleavage was done using a range of substrates in yields ranging from 36–98%, while excellent stereoselectivity was not attained. Importantly, column chromatography allowed for the separation of the products' stereoisomers, with the exception of **5h** and **5j**. Excellent yields **5a–5e** of  $\alpha$ -substituted styrenes were converted into the desired THF products. Even though there was only limited oxidative cleavage of the olefins, **3f** and **3i** were transformed in low to moderate yields **5f** and **5g** because the starting materials could not be consumed fully. The

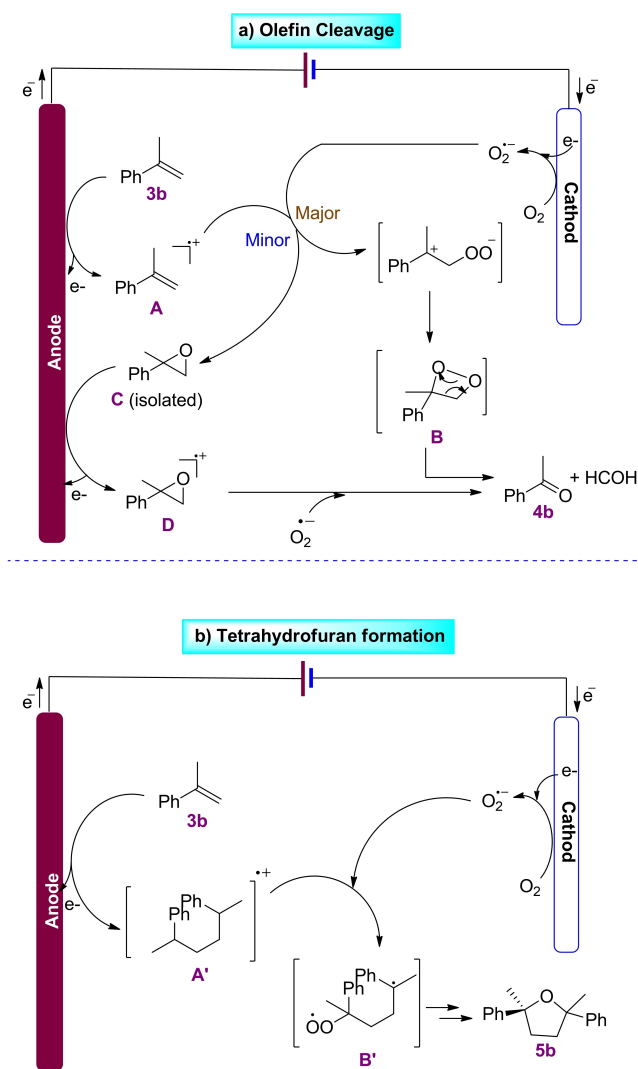


<sup>a</sup>Yields of isolated product. <sup>b</sup>Ratios of stereoisomers (cis/trans) were determined by GC analysis. <sup>c</sup>Yields were determined by GC-MS integration. <sup>d</sup>CH<sub>3</sub>NO<sub>2</sub> was used as solvent.

**Scheme 4.** Electrochemical production of carbonyl **4** and tetrahydrofuran **5**.

transformation of halogenated styrene with good chemo-selectivity **5h–5k** was achieved. The fact that **3g**, **3h**, and **3n** did not respond is remarkable. Sometimes an excessive amount of charge was required, maybe as a result of the superoxide radical anion's competitive oxidation ( $E_{ox}O_2^{\bullet-}/O_2 = -0.56$  V vs. Ag wire) or the reduction of the radical cation at the cathode.<sup>[108]</sup>

Scheme 5a depicts two possible carbonyl product formation routes from the olefin cleavage. Due to its long lifetime in aprotic solvents and the fact that it can be produced via the reduction of  $O_2 \cdot O_2^{\bullet-}$  would serve as a trap for the radical cation intermediate **A**. The dioxetane **B** and epoxide **C** intermediates are produced on the major and secondary pathways, respectively. Formaldehyde was identified by GC-MS, indicating that the dioxetane was rapidly degraded into the intended carbonyl compounds. The THF synthesis requires **A** to be trapped by **3b** at the  $\beta$ -position after **3b** has been anodically oxidised on the carbon electrode.  $O_2^{\bullet-}$  then forms a connection with **A'**, forming **5b** (Scheme 5b).<sup>[109]</sup>



**Scheme 5.** Suggested mechanism for electrochemical production of carbonyl **4b** and tetrahydrofuran **5b**.

Trifluoromethoxylated aromatics ( $\text{ArOCF}_3$ ) are significant structural motifs in the field of drug discovery because the addition of the trifluoromethoxy group ( $\text{CF}_3\text{O}$ ) enhances their desired physicochemical qualities. Despite recent major advancements in the  $\text{CF}_3\text{O}$  group insertion into aromatic compounds, current techniques necessitate for the employment of pricey trifluoromethoxylation reagents or harsh reaction conditions. The direct C–H trifluoromethoxylation of (hetero)aromatics by the combination of the widely accessible trifluoromethylating reagent and oxygen under electrochemical reaction conditions has been addressed in a conceptually novel and straightforward practical methodology. Trifluoromethoxylated aromatics are being used in more and more pharmaceutical products.<sup>[110–111]</sup> For instance, the FDA only recently approved Sonidegib (anticancer)<sup>[112]</sup> and Pretomanid

(antituberculosis)<sup>[113–114]</sup> in 2015 and 2019, respectively, while MI-09 is a superb SARS-CoV-2 Mpro inhibitor with antiviral effectiveness in a transgenic mouse model.<sup>[115]</sup>

This innovative trifluoromethoxylation could offer  $\text{ArOCF}_3$  a practical, step- and atom-efficient, convenient, and practical technique. There were reportedly many difficulties with this  $\text{O}_2$ -involved radical trifluoromethoxylation. First,  $\text{O}_2$  might prevent the trifluoromethylating reagents from producing  $\text{CF}_3$  radicals. Second, the electrophilic and highly active  $\text{CF}_3$  radical would combine with aromatics to produce the competitive trifluoromethylated product. Third, the unstable and highly active  $\text{CF}_3\text{OO}^\bullet$  radical may not readily yield the trifluoromethoxy radical.<sup>[116]</sup>

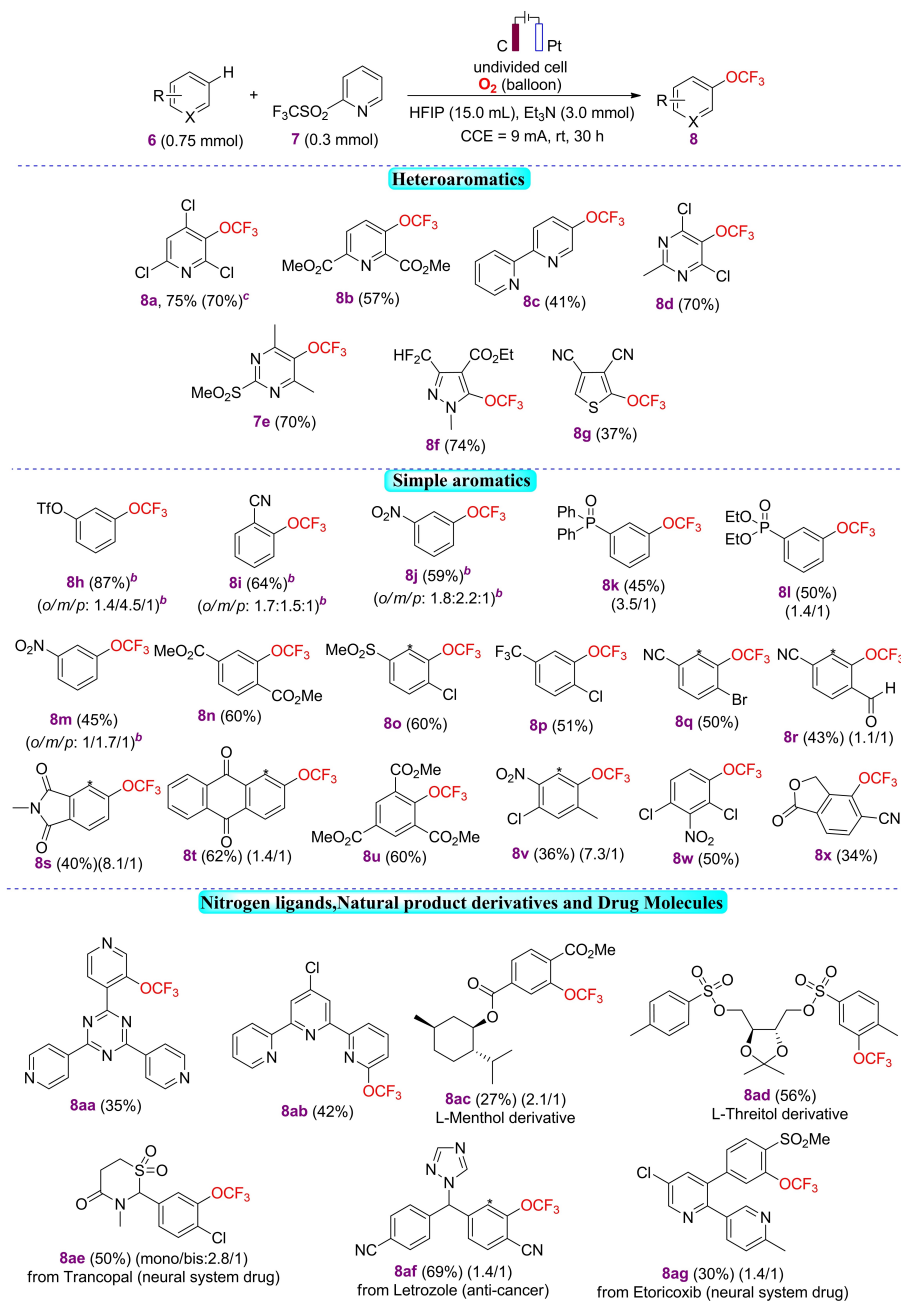
The reaction was conducted in an undivided cell possessing graphite anode and platinum cathode with  $\text{O}_2$  atmosphere and constant current electrolysis.  $\text{MeCN}/\text{H}_2\text{O}$  was used as the solvents, and  $\text{Bu}_4\text{NClO}_4$  as the electrolyte.<sup>[117]</sup> After determining the ideal reaction conditions, the electrochemical C–H trifluoromethoxylation process's substrate range was investigated. First, integrating the  $\text{OCF}_3$  group into heteroaromatics was concentrated. Pyridines with chloro, bromo, and ester substituents, were well tolerated and gave rise to the compounds (**8a–8c**) in moderate to high yields. Smooth reactions occurred between electro-donating and electro-withdrawing substituents in pyrimidine derivatives (**8d** and **8e**). Thiophene and imidazole could be combined to produce the equivalent trifluoromethoxylated compounds (**8f** and **8g**).

Mono-substituted aromatics with phosphonate, sulfonate, nitro, phosphine oxide, cyano, and sulfonyl groups all converted satisfactorily and in good yields into the required products (**8h–8m**). Furthermore, the synthesis of highly functionalized trifluoromethoxylated aromatics (**8o–8w**) was made possible by the compatibility of sulfonyl, chloro, bromo, ester, cyano, trifluoromethyl, aldehyde, and ketone substituents. In modest yields phthalimide **8s** and anthraquinone **8t** underwent regioselective trifluoromethoxylation. Tri- or tetra-substituted aromatics that were sterically inhibited took part in the reaction with good selectivity as well (**8u–8x**). The regioisomers were often isolated as a mixture for those substrates containing several reaction sites. The competitive hexafluoroisopropoxylation reaction, however, prevented the relatively electro-rich aromatics from being useful in this synthesis.<sup>[118]</sup> The trifluoromethoxylation of the complex and bio-relevant compounds was focused at to further highlight the usefulness of this electrochemical procedure. The trifluoromethoxylated compounds **8aa**, **8ab** were readily produced from the nitrogen-containing ligands in average yields. Additionally, this reaction was easily carried out with natural product derivatives made from l-menthol and l-threitol (**8ac**, **8ad**). This approach was also effectively used to produce the trifluoromethoxylated compounds (**8ae–8ag**) in synthetically useful yields from commercially accessible pharmaceut-

icals such as the neural system drug Etoricoxib, the neural system drug Trancopal, and anti-cancer drug Letrozole (Scheme 6). To produce product **8** in a 70% isolated yield,

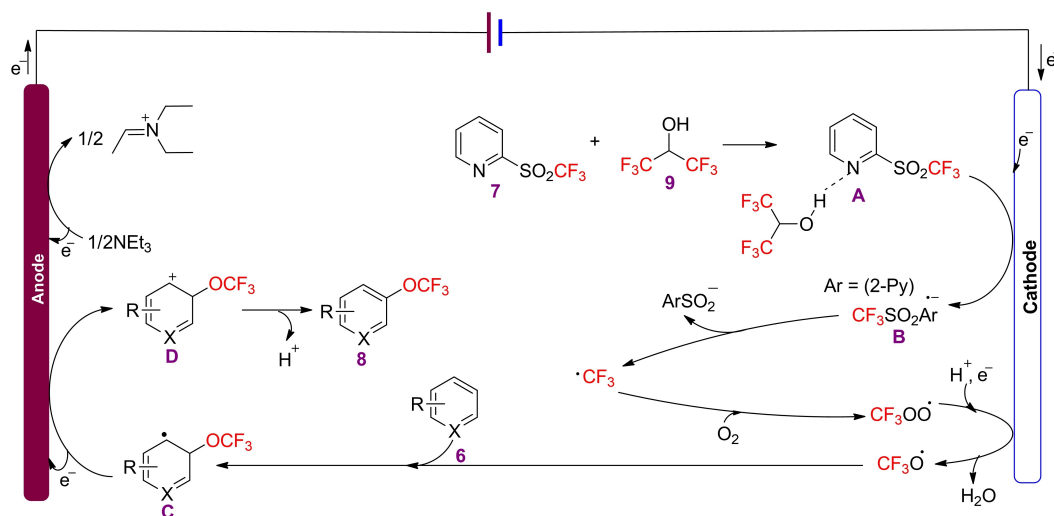
the electrochemical trifluoromethoxylation reaction could be stepped up to 3.0 mmol.<sup>[119]</sup>

On the basis of relevant data from earlier research,<sup>[120–123]</sup> a possible reaction mechanism was suggested in scheme 7. To



<sup>a</sup>Standard reaction conditions, <sup>b</sup>The isomer ratio and yield determined by <sup>19</sup>F NMR spectroscopy using trifluoromethylbenzene as an internal standard. <sup>\*</sup>The minor regioisomeric position is labeled with the respective carbon atom number. <sup>c</sup>Reaction conditions: **6** (7.5 mmol), **7** (3.0 mmol), Et<sub>3</sub>N (30.0 mmol), HFIP (150 mL), 50 mA, oxygen atmosphere, constant current, RT, 53 h, isolated yield.

**Scheme 6.** Electrochemical production of trifluoromethoxylated compounds **8 a–8 z** and **8 aa–8 ag**.



**Scheme 7.** Proposed mechanism for electrochemical production of trifluoromethoxylated compound **8**.

create **A**, HFIP **9** must first bind to the nitrogen atom in **7**. The radical anion **B** is then produced by the cathodic reduction of **A**. Sulfinate ion and the  $\text{CF}_3$  radical are released when the radical anion **B** collapses.<sup>[124]</sup> After  $\text{CF}_3$  radical and  $\text{O}_2$  combine,  $\text{CF}_3\text{OO}$  radical is produced,<sup>[125]</sup> which can then be reduced at the cathode to produce the crucial  $\text{CF}_3\text{O}$  radical intermediate.<sup>[126]</sup> The dearomatized intermediate **C** is produced when (hetero)aromatics are combined with the  $\text{CF}_3\text{O}$  radical. After re-aromatization and anodic oxidation of **C**, the required trifluoromethoxylated compounds **8** are produced. In the meanwhile, anodic oxidation is used to change the sacrificial electron donor  $\text{Et}_3\text{N}$  into the appropriate iminium cation.

### 3. Indirect Electrochemical C–H/C–C Bond Oxygenation

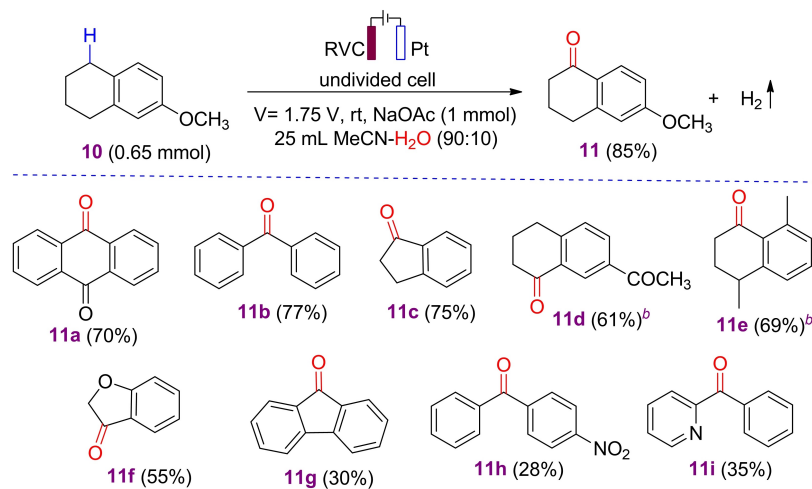
This type is further categorized into following subtypes:

#### 3.1. Electrochemical C–H/C–C Bond Oxygenation Using Water

For the production of feedstock in the chemical industry, the selective oxidation of the C–H bond is essential. The use of oxygen or peroxide as the oxidation reagent under high temperatures in current techniques poses significant problems to the sustainability of production and industrial safety. Here, M. Ding et al., show how to use water as the only oxygen source and an eco-friendly electrocatalytic method to selectively oxidize benzyl groups to ketones under ambient conditions (Scheme 8). Water addition lowers the anodic C–H oxidation onset potential and yields 1-tetralone **9** with

excellent ketone to alcohol ratio and satisfying conversion. The water affinity is further adjusted and the oxidation is facilitated by layered  $\text{MnO}_2$  catalysts (rich in oxygen vacancies), which results in a much higher faradaic efficiency. Reaction was performed in an undivided cell possessing reticulated vitreous carbon (RVC) as anode and platinum plate as cathode. 6-methoxy-3,4-dihydronaphthalen-1(2H)-one product **11** is obtained in 85% yield. The water molecules can then attack the cation intermediate created at the anode to form a C–O bond, leading to the production of ketone products with high conversion and high ketone to alcohol ratio. More importantly, this water-assisted method avoids the use of mediators or chemical oxidants such as gaseous oxygen or hydrogen peroxide, which prevents the creation of the potentially explosive alkyl hydroperoxide intermediate. It also functions at normal temperature and ambient pressure. As a result, it offers an environmentally friendly, abundant, and secure source of oxygen, which greatly lowers the cost and possible risks for use in industrial production. To understand the electro-kinetics and reaction mechanism, systematic experiments are made. Further research is being done on functional methods to modify the water affinity of the electrode materials in order to improve the catalytic performance of electrodes. A variety of compounds with benzyl groups were used as substrates to demonstrate the adaptability of this electro-oxidation arrangement (Scheme 8). Due to the relative stability of the aromatic ring and the electron-rich nature of the C=C bonds, the corresponding ketones (**11a–11i**) were produced under the same conditions. Alcohols were also absent from the reaction mixture. Additionally, the activity and selectivity for the electro-oxidation of compounds containing pyridyl and furan rings were assessed; the activities were generally weak, possibly





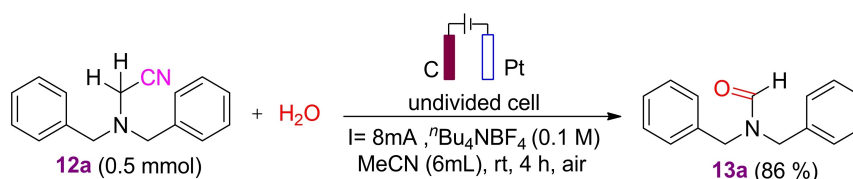
<sup>a</sup>Standard conditions. <sup>b</sup>GC yield using dodecane as the internal standard

**Scheme 8.** Electrochemical production of 1-tetralone **11**.

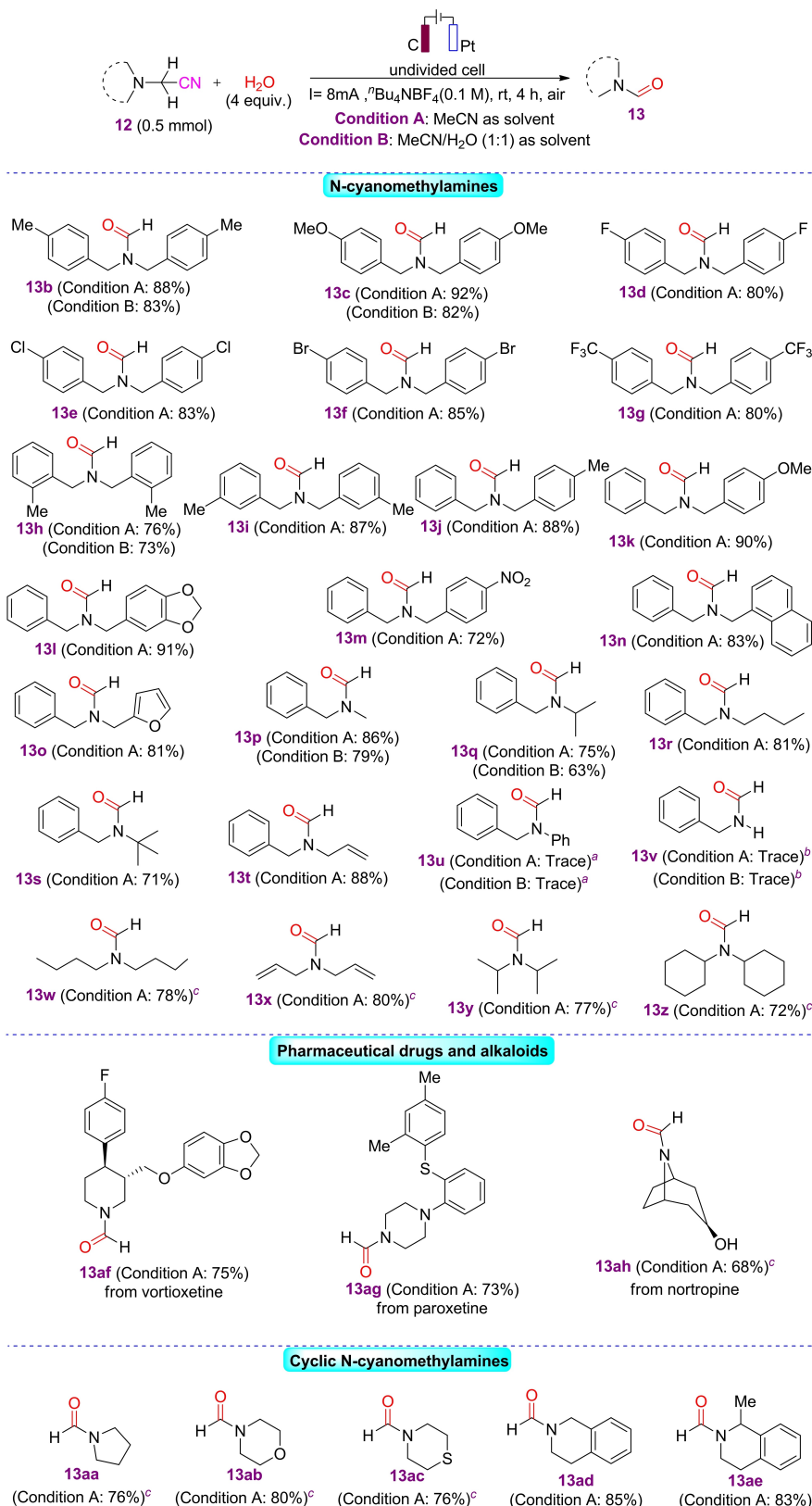
due to the unfavorable effects of the heteroatoms inside the rings.<sup>[93]</sup>

A novel and sustainable method for electrochemically assisted decyanative C(sp<sup>3</sup>)–H oxygenation of tertiary amines was developed. This strategy includes incorporating cyano groups into the substrates, which serve a dual purpose of removing groups. The major goal of this technology was to overcome the issues associated with formamide electrosynthesis. Research demonstrated that the oxygen atom essential for carbonyl production comes from H<sub>2</sub>O rather than molecular O<sub>2</sub>. This novel decyanative C(sp<sup>3</sup>)–H oxygenation approach is notable for its harmonic compatibility with common techniques such as external oxidant-mediated, transition metal-catalyzed, and photo catalyzed formylation processes. The electrochemical decyanative formylation reaction was developed using 2-(dibenzylamino) acetonitrile **12a** and H<sub>2</sub>O as model reaction partners. A decyanative N-formylation product **13** was formed by electrolyzing nBu<sub>4</sub>NBF<sub>4</sub> and MeCN at 8 mA constant current in an undivided cell with a graphite rod anode and a platinum plate cathode for 4 hours at room temperature. The product yielded 86% of N,N-dibenzylformamide **13a** (Scheme 9).

The evaluation of the applicability and limitations of this electrochemically driven decyanative C(sp<sup>3</sup>)–H oxygenation process with respect to several N-cyanomethylamines was concentrated after the optimal conditions had been determined, as shown in scheme 10. In the beginning, (**12b–12g**), the electronic effects of substituents on the benzene ring moiety of 2-(dibenzylamino)acetonitriles were assessed. It was discovered that the various substituents, such as Me, MeO, F, Cl, Br, and CF<sub>3</sub>, could participate in this selective electrochemical decyanative C(sp<sup>3</sup>)–H oxygenation very well to produce the corresponding formamides **13b** and **13g**, respectively, in moderate to excellent yields (80–92%). A methyl group was present at either the 2- or 3-position of the benzene ring moiety in the substrates, these substrates **12h** and **12i** smoothly produced the corresponding formamides **13h** and **13i** in yields of 76% and 87%, respectively. In this electrochemical system, asymmetric 2-(dibenzylamino)acetonitrile derivatives were also studied further, and a series of substrates from **12j** to **12n** effectively carried out the decyanative formylation process to generate a variety of functionalized formamides **13j–13n** in good yields. Fortunately, the required products **13b**, **13c**, and **13h** were



**Scheme 9.** Electrochemical production of N,N-dibenzylformamide **13a**.

Scheme 10. Electrochemical production of decyanative N-formylation products **13 b–13 ah**.

produced in pretty excellent yields (73–83 %), but with slightly lower efficiencies than those using MeCN as the solvent, by switching from MeCN to a mixed solvent of H<sub>2</sub>O/MeCN (1:1). In general, the electron-donating or electron-withdrawing groups substituted on the benzene ring moiety have no discernible effect on the selectivity and reactivity of these 2-(dibenzylamino)acetonitrile derivatives.

The required compounds **13p** and **13t** were then produced, respectively, in high yields (75–88 %), from a variety of 2-(alkyl(benzyl)amino)acetonitriles **12p** and **12t**, including methyl, isopropyl, n-butyl, tert-butyl, and allyl. Unfortunately, the substrate 2-(benzyl(phenyl)amino)acetonitrile **12u** was inert, and more than 90 % of the substrate **12u** was recovered. In addition, corresponding formamide **13v** could not be seen since 2-(benzylamino)acetonitrile **12v** was quickly broken down. This electrocatalysisdecyanative method was also compatible with other 2-(dialkylamino) acetonitriles. Different 2-(dialkylamino)acetonitriles with n-butyl, allyl, isopropyl, or cyclohexyl groups smoothly interacted with water to produce the corresponding formamides **13w–13z** in high yields (72–80 %).

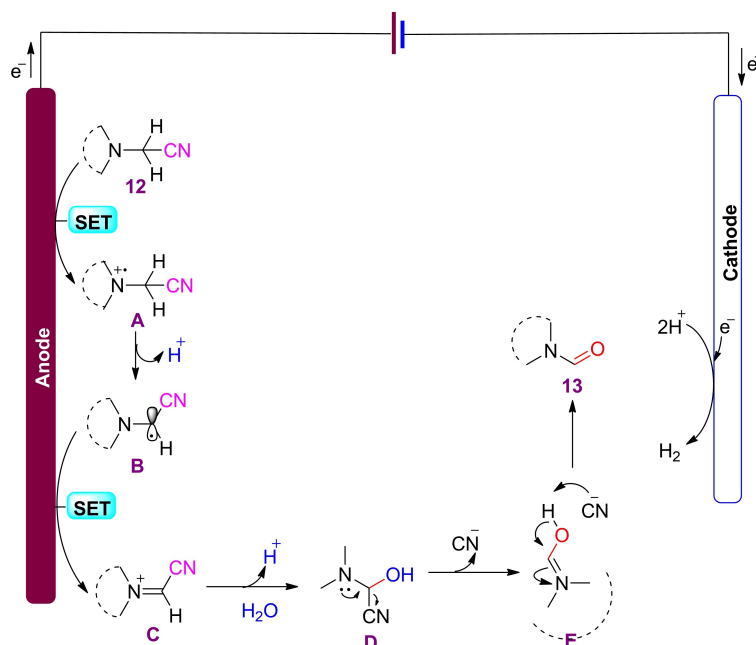
With regard to several cyclic N-cyanomethylamines, It was focused on the viability of this electrochemical decyanative C(sp<sup>3</sup>)–H oxygenation procedure. The simple conversion of the five-membered N-cyanomethyltetrahydropyrrole **12aa** to the N-formyl tetrahydropyrrole **13aa** produced a 76 % yield. Similarly, an array of six-membered cyclic N-cyanomethylamines, such as N-

cyanomethylmorpholine **12ab**, N-cyanomethylthiomorpholine **12ac**, 2-(3,4-dihydroiso-quinolin-2(1H-yl)acetonitrile **12ad**, and 2-(1-methyl-3,4-dihydroiso-quinolin-2(1H-yl)acetonitrile **12ae**, were also suitable for this transformation, giving the corresponding cyclic formamides (**13ab–13ae**) in moderate to excellent yields (76%–85%). Notably, the incorporation of N-formyl into some significant bioactive molecules, such as vortioxetine, paroxetine, and nortropine, was successfully accomplished using this electrochemical approach.

Scheme 11 demonstrates the mechanism that includes the anodic single electron oxidation of tertiary amine **12** to produce nitrogen-centered radical cation **A**, which swiftly loses one proton (H<sup>+</sup>) to produce carbon-centered radical **B**. Following that, the radical intermediate **B** oxidized at the anode surface to create the crucial iminium ion intermediate **C**. The addition of H<sub>2</sub>O to the iminium ion result in the formation of intermediate **D**. Finally, the cyano group was removed to provide the iminium ion intermediate **E**, and the desired product **13** is achieved while the created cyano anion is present.<sup>[127]</sup>

### 3.2. Electrochemical C–H/C–C Bond Oxygenation Using Metal-Free Electrocatalysts

Ethylbenzene **14** oxidation is a crucial chemical process that yields valuable chemicals like styrene **3**, acetophenone **15**, and N-(1-phenethyl) acetamide **16**. Polyoxometalates (POMs) are



**Scheme 11.** Proposed mechanism for electrochemical production of N-formylation product **13**.

anionic metal-oxide clusters made from abundant earth elements like Mo, V, W, Ta, and Nb. POMs are interesting electrocatalysts due to their tunable redox characteristics and rapid electron transport behavior. Recent research suggests that porous cationic covalent triazine frameworks (CTFs) are ideal for POM-based electrodes. The POM@CTF proved to be highly active for selective benzyl alcohol oxidation and H<sub>2</sub> production. Li et al performed Ethylbenzene (EB) oxidation by employing PMo<sub>10</sub>V<sub>2</sub>@CTF, a noble metal-free electrocatalysts. Using water as the oxygen source, 65% of ethylbenzene **14** transformed to three value-added products with a total Faraday efficiency of 90.4% while operating at room temperature and humidity.

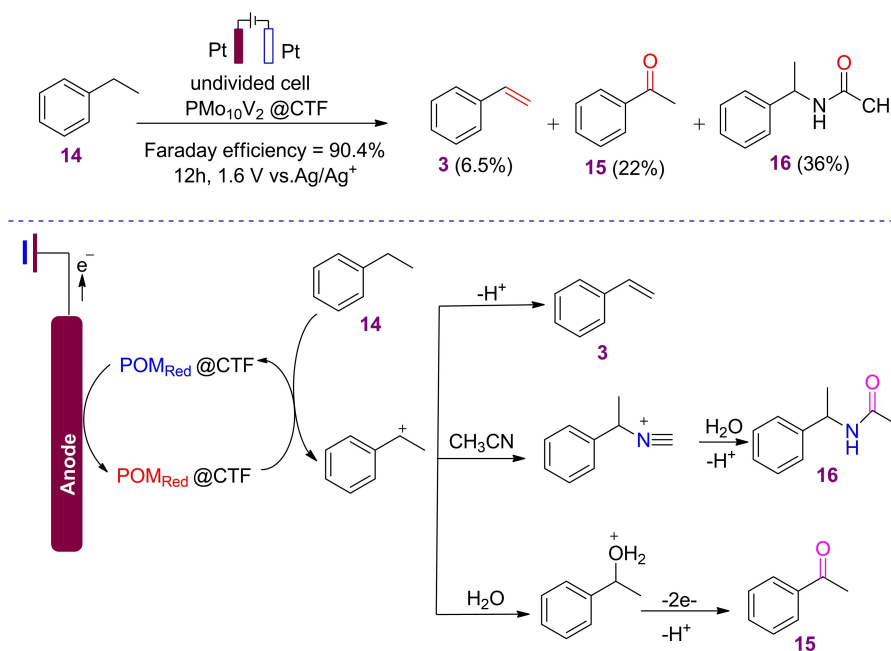
A feasible mechanism was developed (Scheme 12). The  $-1e^-/-1H^+$  reaction on the anode oxidizes the benzylic C–H bond of **14**, yielding a benzylic radical after one electron oxidation, resulting in a carbocation intermediate. Next, styrene was created by removing  $\beta$ -H atoms. Nucleophiles trap carbocation. Acetonitrile attack produces nitrile cations, resulting in **16** that follows hydrolysis, while H<sub>2</sub>O attack produces ACE with phenyl ethanol as an intermediate. In addition to aiding in the electron transfer oxidation of EB, the uniformly distributed PMo<sub>10</sub>V<sub>2</sub> that serves as the major catalytic active sites also helps stabilize the carbocation intermediate. It opened up a sustainable route for the oxidative improvement of alkylaromatic chemicals.<sup>[128]</sup>

### 3.3. Electrochemical C–H/C–C Bond Oxygenation Using Air

Heavy metal pollution, excessive chemical oxidants, transition metal catalysts, and severe reaction conditions are common problems with traditional approaches. The oxidative cleavage of the aromatic C=C bond in indoles has been studied in depth by scientists who were motivated to do so by previous reports<sup>[45,56,62–64,66–69,129–135]</sup> and efforts on selective cleavage of C=C bond. Since air is the purest and safest oxidant, they began by investigating terminal oxidant situations using air. The C(2)=C(3)/C(2)–N bonds in indoles can be broken apart using an aerobic oxidative cleavage driven by electrochemistry. This method is used to synthesize many *ortho*-amino aryl ketones, which are used often in the synthesis of pharmaceuticals and other natural compounds. It was simple to scale up, did not require any metals, and used air as the oxidant.

The corresponding products **18** were isolated in good yields by successive cleavage of the C(2)=C(3) and C(2)–N bonds of N-Boc-indoles **17** under mild conditions. Graphite felts (GF) were used as both anode and cathode, Et<sub>4</sub>NBF<sub>4</sub> as electrolyte, acetonitrile-water as co-solvent, constant current, room temperature, in an undivided cell. Et<sub>4</sub>NBF<sub>4</sub> was discovered to be more efficient in a screening of supporting electrolytes.<sup>[94]</sup>

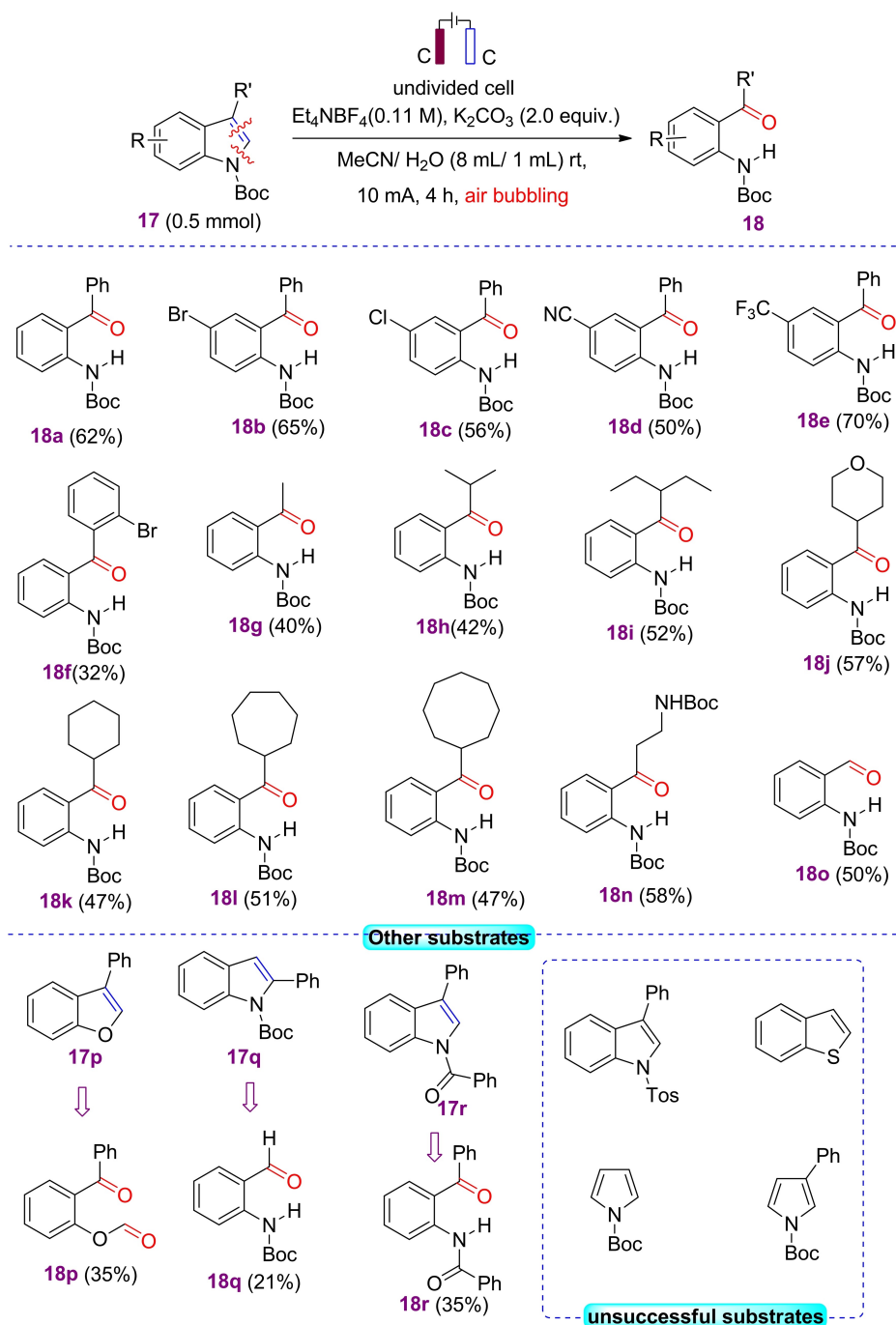
As a result of the aforementioned optimization conditions, applications of N-Boc-indoles and its derivatives are displayed



**Scheme 12.** Electrochemical production of styrene **3**, acetophenone **15**, and N-(1-phenethyl) acetamide **16** and proposed mechanism for the electrocatalytic oxidation of ethylbenzene **14** by PMo<sub>10</sub>V<sub>2</sub>@CTF.

in scheme 13. It was discovered that the target products could be produced in moderate to good yields (**18a–18e**) with a phenyl group on C3, regardless of whether the substituent on the indole core was electron-withdrawing or electron-donating. Additionally, C3-arylated indole was efficient substrate **18f**. The yield decreased for substrates with more steric hindrance

**18f**. In addition, indoles containing an alkyl group on the C3 atom easily gave rise to the desired compounds **18g–18h**. In addition, the indoles **18j–18m** with cycloalkyl and tetrahydropyran substituents were compatible with this system. Notably, considerable yields of the required compounds may also be obtained through the oxidation of tryptamine and



**Scheme 13.** Electrochemical production of *ortho*-amino aryl ketones **18a–18r**.

azazindole derivatives (**18n** and **18o**). It is interesting to note that benzofuran may also be compatible with this electrochemical system (**18p**), which showed promise for use in other heterocycles.

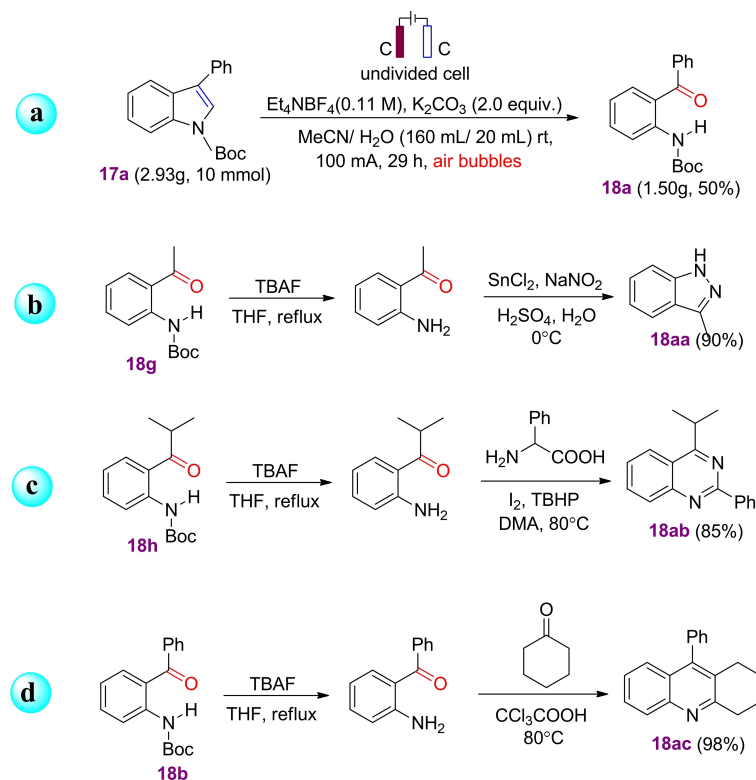
However, with heterocycles like benzothiophene and pyrroles, no desirable product was observed. Tert-butyl(2-formylphenyl)carbamate (**18q**), which was produced in 21% yield by the C2-aryl-N-Boc indole, suggesting that a decarbonylation should take place. Different N-protective groups produced various results. While N-Tos indole was a poor substrate, N-Benzoyl indole produced a 35% yield of the desired product (**18r**). The raw materials were almost always entirely used up, and the low yields could be the result of excessive substrate oxidation.

This method can easily be scaled up to the gram level, as shown in scheme 14a. It suggests that the chemical and pharmaceutical industries might use this technology. The products also serve as valuable building blocks that are easily transformed into a variety of bioactive heterocycles (scheme 14b–14d).<sup>[94,136]</sup>

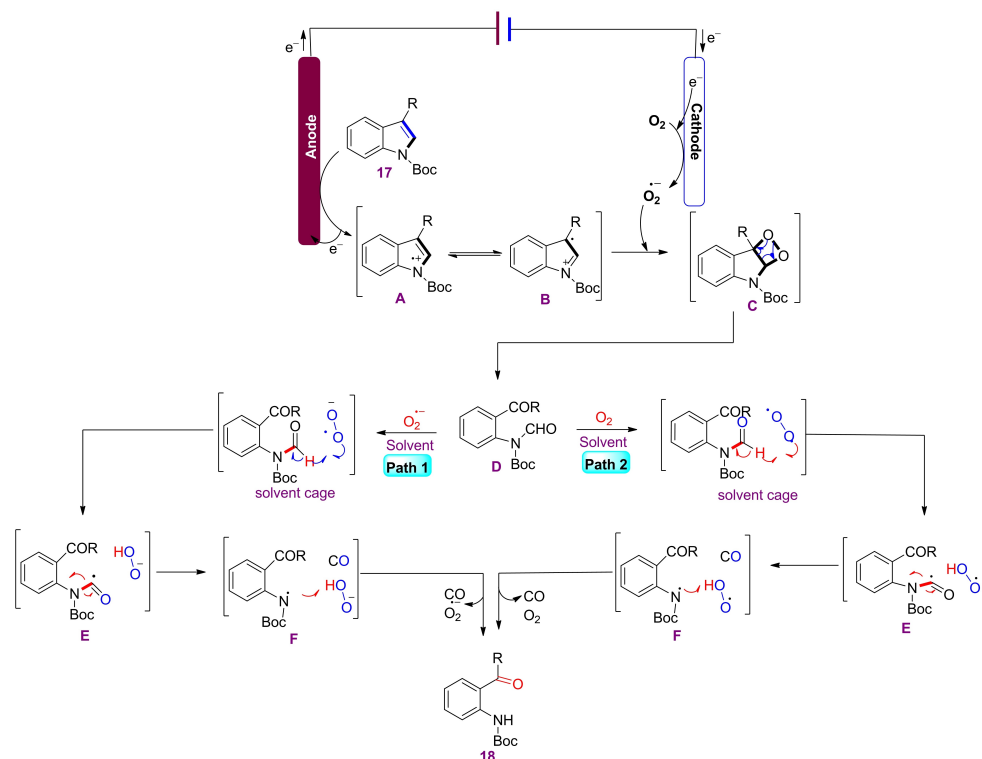
At first, indoles **17** were oxidized on the anode to a radical cation **A** that could resonate with **B**. Cathodic oxidation of oxygen led to the formation of the superoxide radical anion, which was then trapped by the **B** to yield the four-membered

peroxide **C**. The ring-opening ketone **D** could be obtained via fragmentation of **C**. Then, there would be two routes through. In scenario **I**, radical **E** is produced when hydrogen is transferred from **D** to the superoxide radical anion in the solvent cage. When **E** is deformed, CO and the radical **F** are produced; **F** then abstracts a hydrogen atom back into HOO<sup>-</sup>, producing the end product and regenerating O<sub>2</sub><sup>-</sup> in the process. The second possible route begins with **D** and ends with molecular oxygen via the same procedures described earlier (scheme 15).

It has been revealed that an inert C(sp<sup>3</sup>)–C(sp<sup>3</sup>) bond in alkylarenes can be broken by electrochemistry. A wide variety of aryl alkanes can be transformed into ketones and/or aldehydes, which are useful building blocks for synthetic processes, by simply bubbling air into an undivided cell. More importantly, this technique might offer a workable concept for polymer degradation and biomass conversion. To test this theory, Z. Liu and coworkers first investigated the conditions of the reaction using the template substrate 4-isopropylphenyl benzoate **19** and air as the terminal oxidant (Scheme 16). When graphite felt was used as the anode and Platinum plate was used as the cathode in an undivided cell with air bubbling, CF<sub>3</sub>NaSO<sub>3</sub> as the electrolyte acetonitrile (CH<sub>3</sub>CN) as the solvent, and stirring at room temperature and constant voltage,



**Scheme 14.** Gram scale electrochemical production of *ortho*-amino aryl ketone **18a** and electrochemical production of bioactive heterocycles **18aa–18ac**.



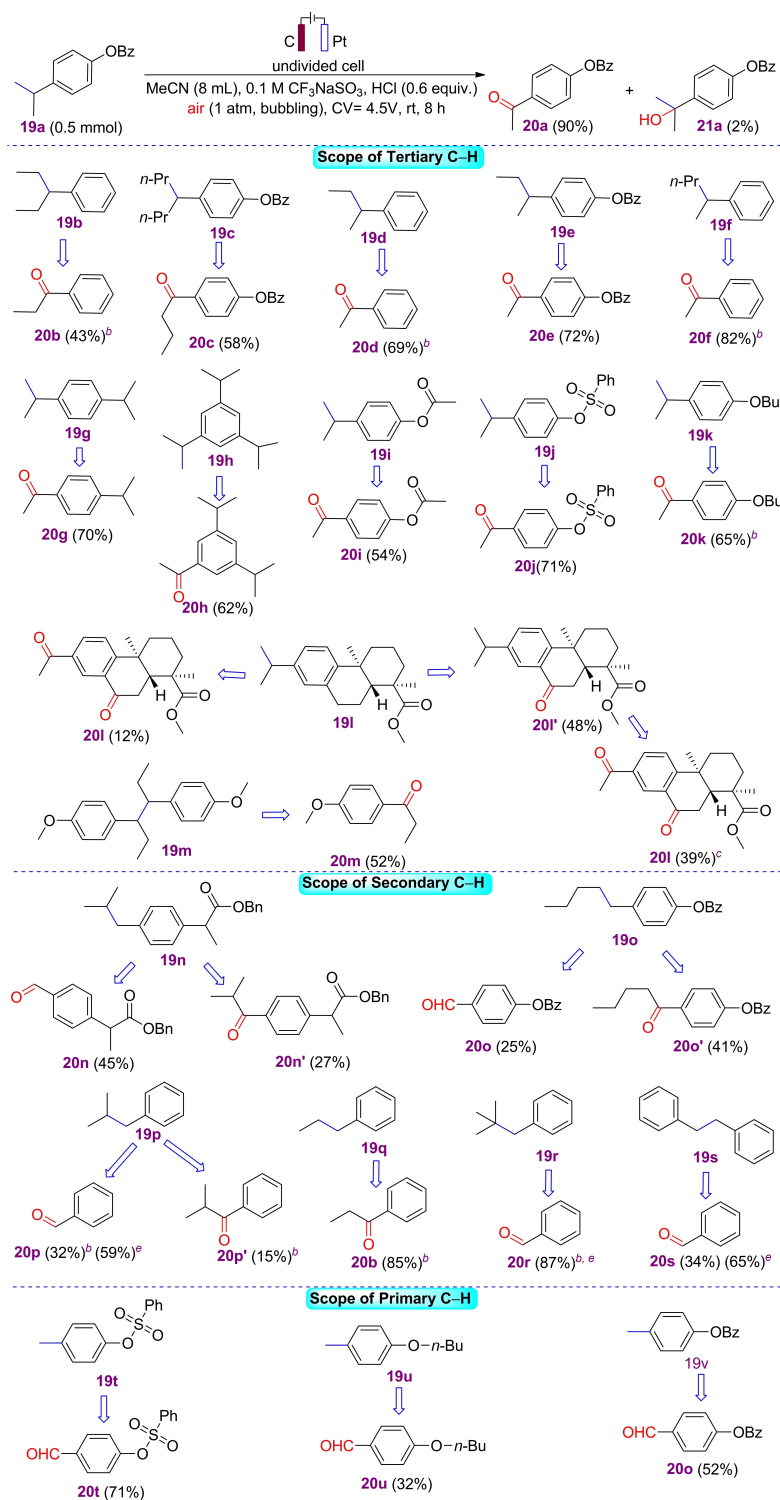
**Scheme 15.** Suggested mechanism for electrochemical production of *ortho*-amino aryl ketone **18**.

the desired product **20a** was produced in 90% yield. In this case 0.6 equivalent of HCl was used as an additive. Additionally, it was discovered that this reaction may be scaled up to grams level.<sup>[137]</sup>

These early results motivated an investigation into the practicability of this electrochemical oxidation system. Under the predetermined reaction conditions, a variety of functionalized alkylbenzenes **19** were used as substrates (Scheme 16). Notably, moderate to high yields of the target products can be obtained from unsubstituted alkylbenzenes and electron-rich substrates (**19a–19k**). The target product **20b** was discovered along with ethanal during the course of the GC–MS detection of **20b**, which was used to confirm the oxidative product of the releasing alkyl group. It is interesting to note that in substrates with two branches at the same benzyl position (**19d–19f**), only the longer chain will be cut off selectively. This selectivity may be a result of the corresponding leaving alkyl radicals' stability, which are produced when a C–C bond is broken. It was thrilling to learn that numerous compounds found in natural products and medications, such as methyl dehydroabietate, hexestrol, and derivatives of ibuprofen, suffered selective cleavage of the C–C bond (**19l**, **20l**, **19m**, and **19n**). Several substrates containing primary or secondary C–H bonds in the benzyl position have been calculated under standard circumstances (**19n–19v**) in order to examine the

range of this transition. Both benzyl C–H and C–C oxidation happened in the case of secondary methylene-containing substrates (**19n–19s**). Furthermore, the stability of the departing C-centered radicals was crucial for the principal products. The more stable secondary, tertiary and benzyl radicals would lead to C–C oxidation (**19n**, **19p**, **19r**, and **19s**), whereas the active primary radical would mostly contribute to C–H oxidation (**19o** and **19q**). From this finding, it was concluded that C–C oxidative products would develop more frequently if the leaving alkyl radicals were more stable tertiary C-centered radicals. Moreover, the crucial intermediary that causes the C–C cleavage is not the four-membered ring peroxide but rather the alkoxy radical. Additionally, the associated aldehydes, which were primary by-products of toluenes (**19t–19v**) in this system, were identified.

Furthermore, it was assessed the electro-oxidative conditions with a derivative of estrone named 3-methoxy-estrone (**19w**), taking into account the practical applicability and universality of this approach. Recovering 30% of the original substance, this steroid was cheerfully transformed into **20w** in 35% yield (Scheme 17a). In addition, the yield of ketones produced by the oxidation of CH<sub>2</sub> that is benzylic was noticed. In addition, it was discovered that this reaction may be increased up to the level of grams (Scheme 17b).

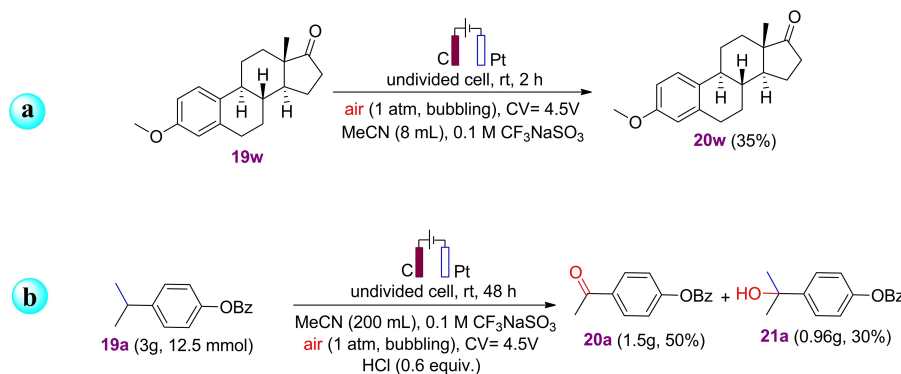


<sup>a</sup>Standard conditions. <sup>b</sup>Reaction time was 4 h. <sup>c</sup>NaOH (0.5 equiv) instead of HCl, voltage value = 3.0 V.

<sup>d</sup>Substrate (1 mmol) was estimated during 24 h. <sup>e</sup>Yields are based on <sup>1</sup>H NMR analysis.

**Scheme 16.** Electrochemical production of ketone derivatives **20 a–20 u**.

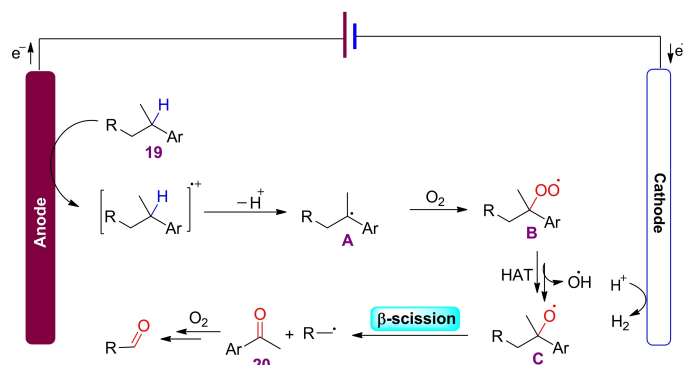




**Scheme 17.** Electrochemical production of estrone **20w** and gram scale electrochemical production of ketone derivative **20a** and alcohol derivative **21a**.

A potential mechanism in scheme 18 based on the findings of earlier research investigations is suggested. Alkylarene **19** was first oxidized on the anode to a radical cation, which then released a proton to create a benzyl radical **A**. **A** was able to obtain peroxide radical **B** by capturing molecular oxygen. After that, the homolysis of **B** and hydrogen-atom transfer would produce an alkoxy radical **C** and a hydroxyl radical. The corresponding ketone and an alkyl radical were produced by the  $\beta$ -scission of **C**, which also produced the other oxidation result by forming a bond with O<sub>2</sub>.

A supplementary cathode oxygen reduction process allowed for the development of a method for electrochemically oxygenating indoles to produce isatins. This green protocol's characteristics include exogenous oxidant free preparation, molecular oxygen as the only oxidant, and the absence of an electron transfer mediator. Its gram scale's set up consists of flow-cell. The two oxygen atoms in the isatins were likely both derived from molecular oxygen, according to mechanistic analyses that supported a radical process. To improve the electrolysis conditions, the authors began researching the electrolytic aerobic oxidation of 1-methyl-1H-indole **22a**.



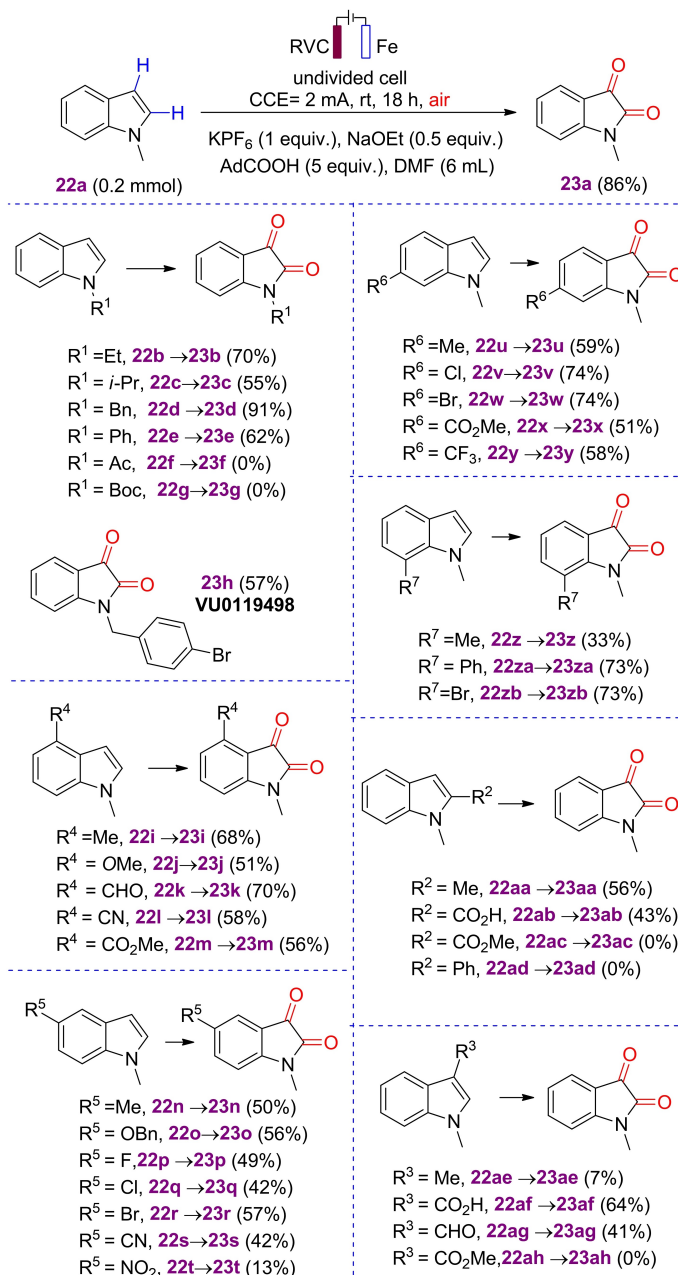
**Scheme 18.** Suggested mechanism for electrochemical production of ketone derivative **20**.

Reticulated vitreous carbon (RVC) served as the anode and an iron plate served as the cathode in the electrochemical setup, which was a single undivided cell. 1-adamantane carboxylic acid (AdCOOH (5 equiv)), sodium ethoxide (NaOEt (0.5 equiv)), and KPF<sub>6</sub> (1 equiv) were used as the supporting electrolytes in DMF at ambient temperature, an air environment, and a continuous current of 2 mA for 18 hours to produce N-Methyl Isatin **23a** in 86% yield.

The substrate scope for the electrolytic aerobic oxidation of indoles was then investigated (Scheme 19), using the optimum conditions as a guide. It went well to produce N-methylisatin **23a** from N-methylindoles bearing CH<sub>3</sub> and COOH at position C2 (Scheme 19, **22aa** and **22ab**).

The approach, however, was unable to successfully oxidize the indoles (**22ac** or **22ad**, respectively), which were substituted with either C2-CO<sub>2</sub>Me or C2-Ph. Only 7% of **23a** was separated due to the presence of a methyl substituent at position C3. In low yields, the carbaldehyde and the C3-substituted indole carboxylic acid were converted into **23a**. Additionally, C3-CO<sub>2</sub>Me **22ah** failed to deliver the expected outcome. Next, it was also looked into how substituents affected the nitrogen atom in indoles. N-alkyl or N-phenyl indoles typically interacted effectively to produce desired products **23b–23e** in high yields. In contrast, under the prescribed conditions, indoles replaced with electron-withdrawing groups like Ac and Boc failed to provide the expected results. The similar procedure was used to create VU0119498, a medication with a reputation for acting as a neuroprotective agent, with a 57% yield. In addition to the N1-, C2-, and C3-substituted indoles, a number of other substituents, including OR (R = Me or Bn), Ph, CHO, CN, CO<sub>2</sub>Me, F, Cl, Br, and CF<sub>3</sub>, were all tolerably tolerated at positions C4–C7 of the N-methylindoles, yielding a variety of N-methylisatins in acceptable to good amounts. The one exception is that only 13% of 5-nitro-N-methylisatin **23t** could be extracted.<sup>[138]</sup>

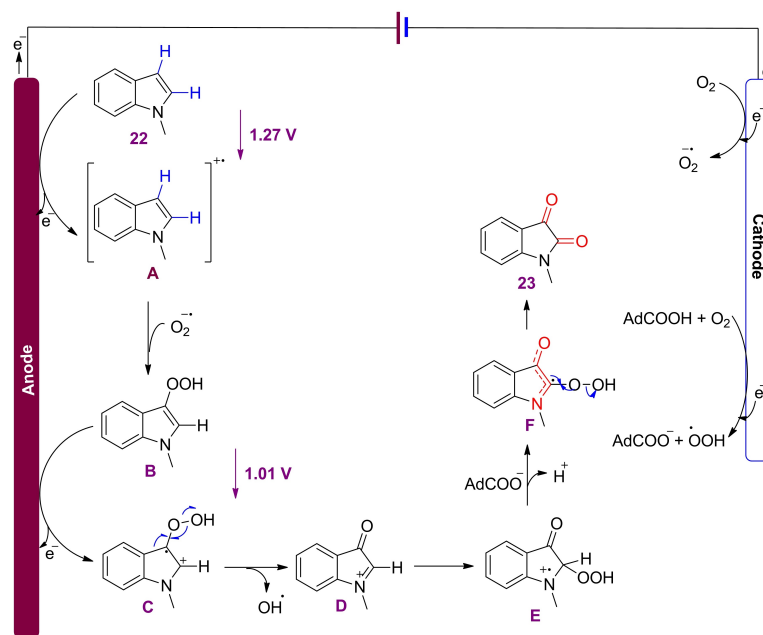
A mechanism for the electrochemical aerobic oxidation of indoles has been proposed (Scheme 20) based on the extensive



Scheme 19. Electrochemical production of N-alkyl Isatin 23.

experimental mechanistic studies described above. First, a single electron oxidation of 1-methylindole **22** with a calculated oxidation potential of 1.27 V versus SCE generated the radical cation intermediate **A**. At the same time, superoxide ions  $\text{O}_2^{\bullet-}$  are produced by oxygen's one-electron reduction. Intermediate **B** is produced by additional anode single-electron oxidation with a predicted oxidation potential of 1.01 V vs SCE, which is then followed by radical coupling between **A** and  $\text{O}_2^{\bullet-}$  to produce intermediate **C**. The 1-methylindolin-3-

one cation **D** and a hydroxyl radical are produced as a result of the homolytic cleavage of the oxygen oxygen bond of **C** via transition state with a free energy barrier of 11.3 kcal/mol. To create the radical cation **E**, **D** would be attacked by  $\text{HO}_2^{\bullet}$ , which is produced from  $\text{O}_2^{\bullet-}$  and a proton. This step's estimated total activation free energy is 18.3 kcal/mol. Then, **F** will be produced by the deprotonation of  $\text{AdCOO}^-$ , which is generated from the deprotonation of  $\text{AdCOOH}$  by superoxide ions  $\text{O}_2^{\bullet-}$  or  $\text{NaOEt}$ . According to the predicted outcomes,



**Scheme 20.** Proposed mechanism for electrochemical production of N-alkylisatin **23**.

this deprotonation by  $\text{AdCOO}^-$  is thermodynamically efficient ( $G^\circ = 38.5$  kcal/mol).

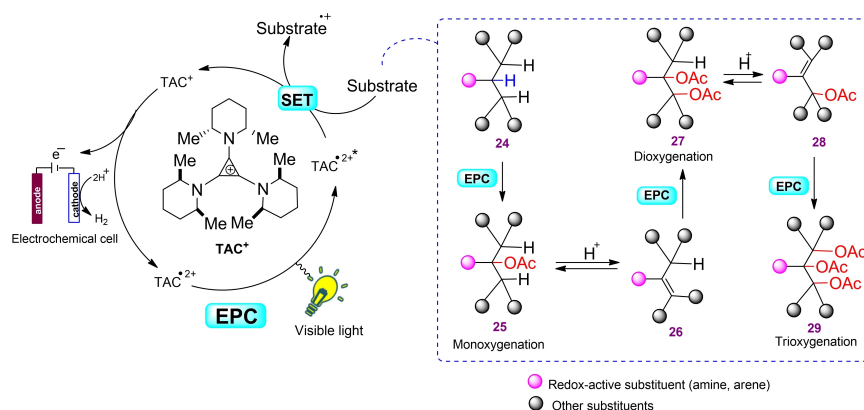
### 3.4. Photo-Induced Electrochemical C–H/C–C Bond Oxygenation

Functional groups containing oxygen are always found in complicated small molecules. Although it would be exceedingly important, the establishing of numerous C–O bonds by the simultaneous, selective oxygenation of adjacent C–H bonds has generally been the domain of biosynthesis. Synthetically generating several, contemporaneous C–H bond oxygenation processes is difficult,<sup>[77–82]</sup> especially given the possibility of over-oxidation. It has been observed that dehydrogenation and oxygenation can selectively oxygenate two or three adjacent C–H bonds, allowing the conversion of simple alkylarenes or trifluoroacetamides to their corresponding di- or triacetoxyates. The technique uses a powerful oxidative catalyst repeatedly to carry out these conversions, but only when the circumstances are sufficiently selective to prevent damaging over-oxidation.

Electrophotocatalysis (EPC),<sup>[83,139–154]</sup> which uses both electrochemical<sup>[11,3,11–12,45]</sup> and photochemical energy to induce reactions, has recently been used to selectively carry out a range of difficult oxidative processes. It is noteworthy that careful acid selection enables the selective synthesis of either di- or trioxygenated compounds. A trisaminocyclopropenium ion ( $\text{TAC}^+$ )<sup>[143]</sup> has been demonstrated to be a robust oxidative electrophotocatalyst that may facilitate a variety of C–H bond

functionalizations and other transformations.<sup>[83,142–146]</sup> In these processes, the deep red TAC radical dication ( $\text{TAC}^{\bullet 2+}$ ) is created by oxidizing the TAC cation ( $\text{TAC}^+$ ) in an electrochemical cell at a relatively low anodic potential (1.26 V versus standard calomel electrode (SCE)). Although this species is not strong enough to oxidize the substrate on its own, it becomes a potent oxidant when photoexcited ( $\text{TAC}^{\bullet 2+*}$ , 3.33 V against SCE).<sup>[143]</sup> By using single electron transfer (SET) to oxidize even weakly reactive substrates, irradiation of an electrochemical cell containing  $\text{TAC}^+$  can produce the appropriate radical cations, which are highly reactive intermediates and can result in a variety of beneficial reaction consequences. It has been proposed that TAC EPC could provide a novel method to accomplish such difficult conversions using affordable acetic acid (AcOH) as the oxygen source (Scheme 21).<sup>[155]</sup>

In particular, it was argued that a substrate **24** containing a redox-active substituent, such as an arene or amine derivative, might be transformed into the monooxygenated intermediate **25** at suitable EPC circumstances in the presence of AcOH. Acidic EPC conditions may allow for the gradual, reversible removal of **24** to produce olefin **25**. This olefin would be susceptible to a second round of EPC oxidation in order to create the dioxygenated adduct **27** because of its conjugation to the redox-active substituent. It was also thought that repeating similar elimination/oxidation procedures with a different nearby C–H bond may produce elusive trioxygenation products like **29**. This idea for the controlled oxygenation of two or three continuous C–H bonds of alkylarenes



**Scheme 21.** Mechanistic rationale of electrophotocatalytic oxygenation of multiple C–H bonds. **Ac**, acetyl; **Me**, methyl.

and trifluoroacetamides has been implemented in this case (Scheme 21).<sup>[87]</sup>

Alkylated arenes **30** were electrophotocatalytically dioxygenated using catalytic  $\text{TAC}^+\text{ClO}_4^-$  (8 mol%) in the presence of acetic anhydride, acetic acid, and trifluoroacetic acid (TFA) for branched substrates or trifluoromethanesulfonic acid (HOTf) for unbranched substrates in methylene chloride, with tetraethylammonium tetrafluoroborate as an electrolyte. An undivided electrolytic cell with a carbon cloth anode and a platinum plate cathode was used for the reaction, which was carried out at a constant current of 5 mA while being illuminated by two compact fluorescent lamps (CFLs). A wide variety of branched and unbranched alkylarenes with a variety of functionalities were affected by these circumstances by vicinal C–H dioxygenation. For example, product with unbranched alkylarenes **31a–31h** is obtained containing moderate to good yield while branched alkylarene product **31i–31o** contains good yield (Scheme 22). It was possible to access products with electron-donating or electron-withdrawing substituents in a low yield.

A wide variety of branched and unbranched alkylarenes with a variety of functionalities were affected by these circumstances by vicinal C–H dioxygenation (Scheme 22). For some substrates, a hydrolytic work-up to produce a 1,2-diol product, such as **31a**, achieved a greater yield. In 68% yield and with a 2.3:1 d.r.,<sup>[156]</sup> the dihydroxylation of *n*-pentylbenzene produced 1,2-diol **31b**, a known precursor to a beta-secretase 2 (BACE2) inhibitor. While this was going on, a trifluoroacetamide substituent was successfully incorporated into the creation of **31c**. Products **31d** and **31e**, which have benzylic vicinal C–H bonds on both sides, were also reachable. Additionally, a number of heteroaromatic compounds **31f** and **31g** might be provided. Although other ester **31h** could be accessed, acetic acid is the most practical oxygen donor.

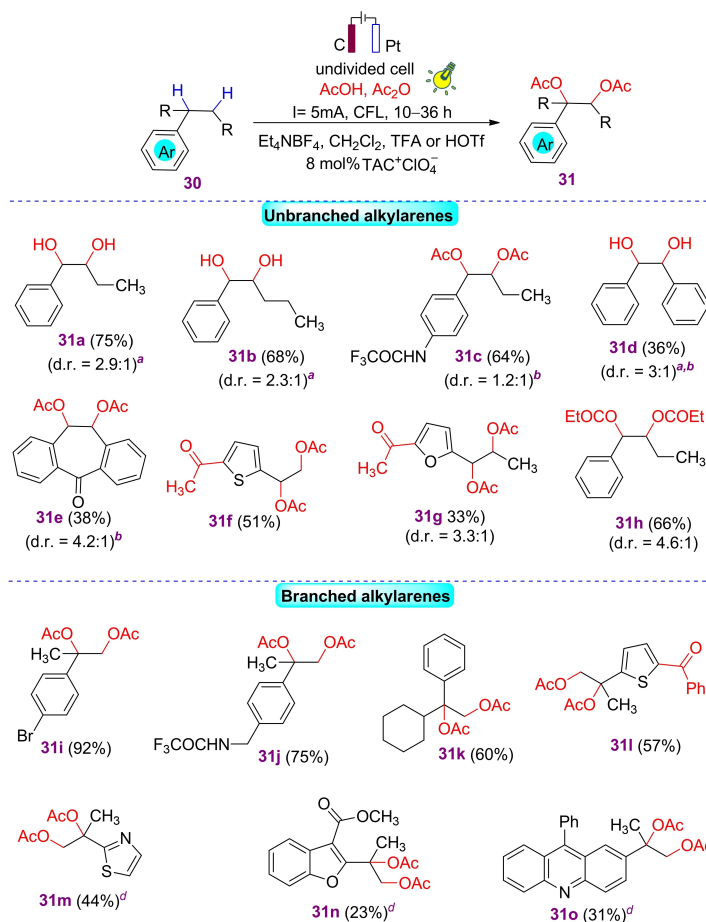
With the introduction of a weaker acid (TFA), benzylic-branched substrates, in addition to unbranched substrates,

readily participated in the transformation. Halogenated derivative of cumene **31i** was produced with a 92% yield. Alcohol functionality or the presence of oxidatively sensitive benzylic trifluoroacetamide proved compatible, producing adducts **31j**. **31k** was produced only by a substrate that was  $\beta$ -branched. It was also noted that these reactions could produce a few heteroaromatic substrates (**31l–31n** and **31o**).

We are not aware of any reports of a continuous C–H tri-oxygenation occurring inside a single reaction flask. In keeping with this, it is claimed that this postulated mechanism might be expanded to offer the first illustration of this elusive change. It is therefore hypothesized that branching substrates, which are more capable of ionization than unbranched substrates, might be vulnerable to additional oxidation after the initial dioxygenation reaction as an E1-type elimination is thought to be a crucial step in this chemistry. In actual fact, it was discovered that utilizing the more potent HOTf acid with this particular class of substrate **32** allowed to achieve a third C–H oxygenation, which resulted in a brand-new tri-oxygenation of three adjacent C–H bonds. By applying the same reaction conditions as mentioned in scheme 22 and replacing the reaction time 10–36 hours with 12–15 hours triacetates having good yield are formed from halogenated cumenes. However for raising the yield of the reaction, working was done with supporting electrolytes such as  $\text{Na}_2\text{CO}_3$  (aq.)/ $\text{CH}_3\text{OH}$  (Scheme 23).

This transformation demonstrated to be possible on a variety of substrates. For instance, the synthesis of triacetate **33a** from the oxidation of 1,1-diphenylethane resulted from the twofold oxygenation of the methyl group. A cyclic substrate was additionally changed into adduct **33b** in 44% yield. Additionally, the responses of heteroaromatic substances such as benzofuran **33c**, thiophene **33d**, and acridine **33e** were studied.

A number of more intricate and biologically significant structures were derivatized in order to further highlight the



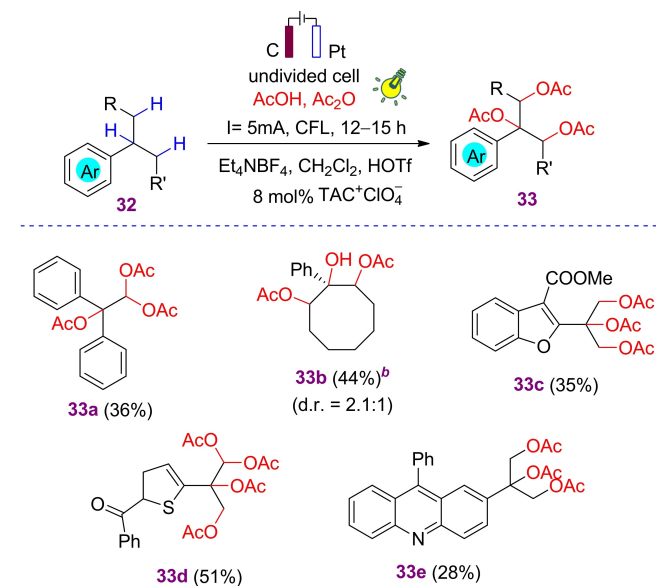
**Scheme 22.** Electrophotocatalytic vicinal C–H deoxygenation.

usefulness of this new peroxygenation chemistry (Scheme 24). The flavor and aroma ingredient celestolide was easily dioxygenated under our usual conditions, producing analogue **34a** in 82% yield on a small scale or at 69% yield on a larger scale (2.5 g, 10 mmol). This process was also used to create analogues of the sigma ( $\alpha$ )-receptor agonist **34b**<sup>[157]</sup> and a fluorobiphenyl structure linked to the nonsteroidal anti-inflammatory medication flurbiprofen **34c**. In addition, compounds **34d** and **34e**, which are di- and trioxygenated analogues of a retinoic acid receptor agonist,<sup>[158]</sup> respectively, were produced in yields that were useful for synthetic purposes in 58% and 41%, respectively. It is interesting to note that the antidepressant medication substrate **34f**, a modified form of sertraline, produced diacetate ketone **34g** in 47% yield after undergoing 12-electron oxidation. The formation of the tetra-, penta-, and hexa-acetate products **34h–34j** resulted from eight-, ten-, and twelve-electron oxidations, respectively.

### 3.5. Electrochemical C–H/C–C Bond Oxygenation Using Mediators

Mediated electro-oxidation uses a homogeneous, redox-active species that first undergoes reversible oxidation at the electrode, then selectively oxidizes the target substrate in solution, and finally is regenerated at the electrode to repeat the cycle (Scheme 25). Easy electron transport of mediators considerably reduces the oxidation potential. Additionally, mediators can be made to only react with a certain substrate, reducing many negative effects.<sup>[159]</sup> Modified TEMPO/<sup>[160]</sup> NHPI,<sup>[16,82]</sup> DDQ,<sup>[161]</sup> nitrate,<sup>[162]</sup> imidazoles,<sup>[163]</sup> and halogens<sup>[160]</sup> are common mediators that provide an effective mediated C–H oxidation pathway.<sup>[11]</sup>

In electrocatalysis, a wide range of redox potentials and reactivity of organic molecules, transition metal complexes, and inorganic salts have been investigated as redox mediators.<sup>[6,11,60]</sup> For instance, 2,2,6,6-tetramethylpiperidine-N-oxyl (TEMPO) mediates hydride transfer for the oxidation of alcohols;<sup>[164]</sup> transition metal salts mediate



<sup>a</sup>Worked up with Na<sub>2</sub>CO<sub>3</sub> (aq.)/CH<sub>3</sub>OH. <sup>b</sup>The syn product was major.

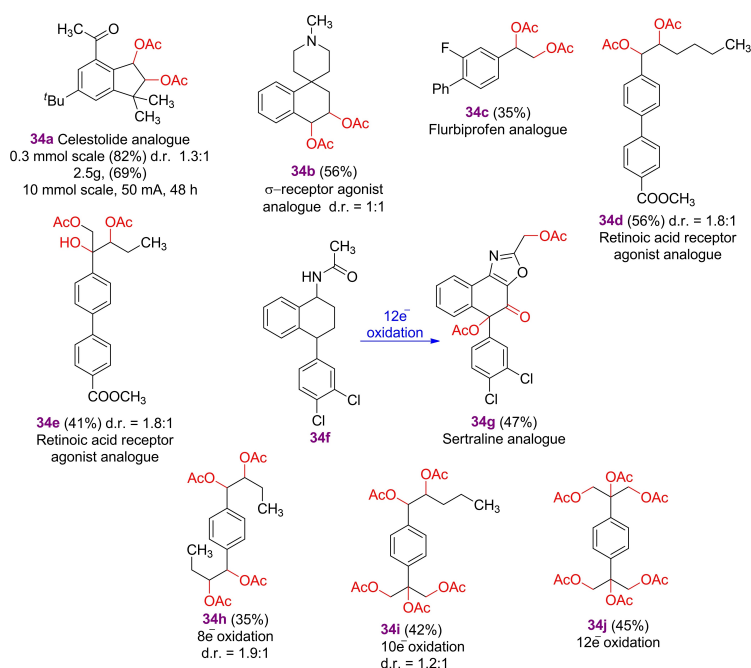
**Scheme 23.** Electrophotocatalytic vicinal C–H trioxygenation.

oxygen transfer or electron transfer to oxidize olefins and aromatics;<sup>[11]</sup> and Ni- and Co-salen complexes mediate electron transfer for the reductive cyclization of unsaturated aldehydes, ketones, and esters.<sup>[11]</sup> N-hydroxyphthalimide (NHPI), one of

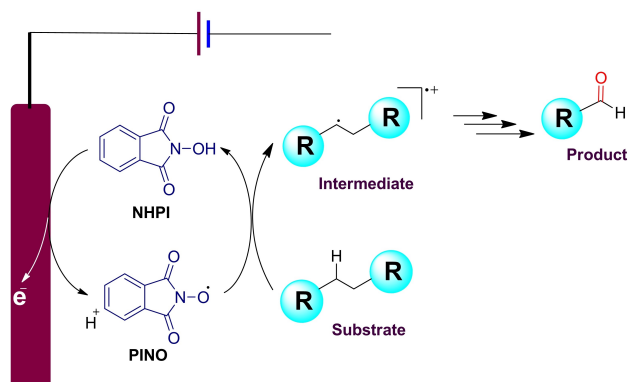
the redox mediators, is widely recognized for mediating hydrogen atom transfer (HAT). At a carbon electrode, NHPI is easily converted into the phthalimide-N-oxyl (PINO) radical, which is skilled at reacting with benzylic C–H HAT to transform back into its reduced form, NHPI, and finish one catalytic cycle (Scheme 25).

Scheme 26 demonstrates a mild electrochemical  $\alpha$ -oxygenation of a variety of linear and cyclic benzamides in an undivided cell with O<sub>2</sub> as the oxygen supply. The experiments on radical scavengers and <sup>18</sup>O labeling showed the presence of a radical route. This is gram scale approach, which is devoid of metal and bases. In the oxidation of the C(sp<sup>3</sup>)–H bond, N-hydroxyphthalimide (NHPI) has been widely used as a potent electrochemical mediator.<sup>[6,165–169]</sup>

To improve the reaction conditions, the benchmark substrate N-benzylacetamide **35a** was used. The best results were found in an undivided cell with acetone as the solvent, NHPI as the redox mediator, 2,4,6-collidine perchlorate (0.01 M) as the electrolyte, Platinum plate (Pt) as the cathode, and a graphite plate (C) as the anode under 1 atm of O<sub>2</sub> at room temperature (Scheme 26). This method produces the desired benzimide **36a** in an 89% yield. The range of feasible substrates for N-benzylamides using the optimized reaction conditions, and the outcomes are shown in Scheme 26. The corresponding benzimides (**36b–36j**) were effectively produced by the oxidation of a variety of secondary N-benzylacetamides with electron-withdrawing or electron donating substituents at the *para*-positions. The oxidation of cyclic



**Scheme 24.** Practical examples of electrophotocatalyzed multiple C–H oxygenation.

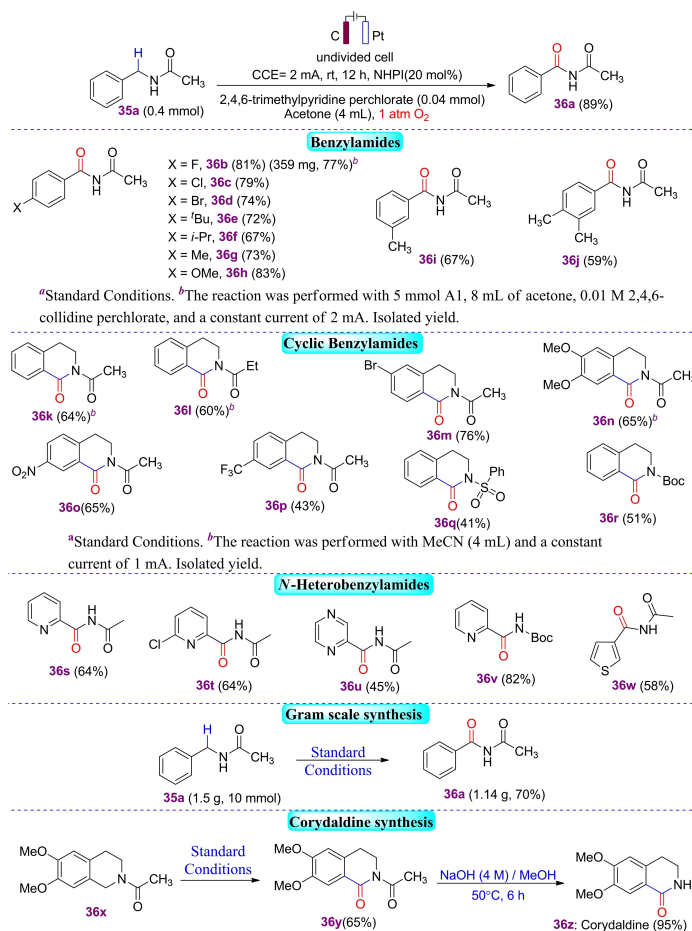


**Scheme 25.** Schematic representation of mediated oxidation to activate C–C bonds. N-Hydroxyphthalimide (NHPI) is a mediator active for hydrogen atom transfer (HAT) reactions. Reproduced from Ref. [159] Copyright (2022), with permission from European Chemical Societies Publishing.

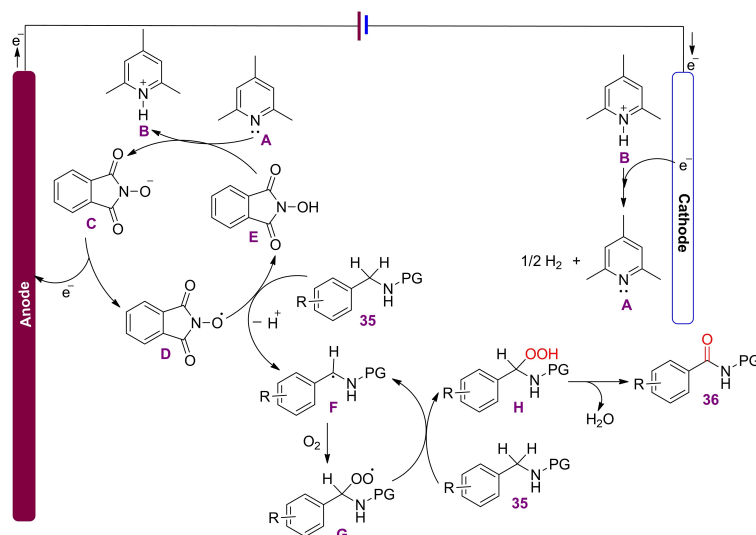
benzylamides was then explored. Following the procedure, several substituted N-acyltetrahydroisoquinolines produced the

matching tetrahydroisoquinolin-1-one products in moderate to good yields (**36k–36r**). Encouraged by these findings, more research on N-heterobenzylacetamides was done. Secondary amides generated from pyridine, pyrazine, and thiophene carried out the electrooxidation extremely successfully and produced the appropriate heterobenzimide products in moderate to high yields (**36s–36w**).<sup>[170]</sup>

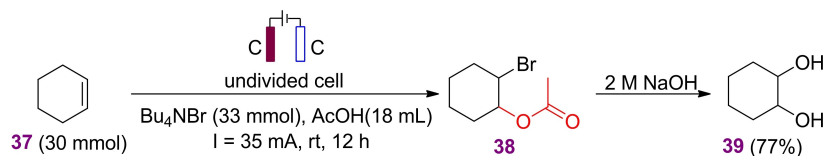
The experimental findings led to the suggestion of a potential reaction mechanism (Scheme 27). 2,4,6-collidine **A** and hydrogen gas are produced at the cathode by cathodic reduction of the electrolyte 2,4,6-collidinium **B**. In contrast, NHPI **E** generates N–O negative ions **C** by losing a proton with the help of 2,4,6-collidine **A**. Intermediate **C** is then anodically oxidized to produce PINO radical **D**, which is then followed by the abstraction of a benzylic proton from substrate **35** to generate benzylic radical **F**. A benzylic hydrogen atom can be abstracted from this radical by molecular O<sub>2</sub> to form peroxy radical **G**, which then traps the radical in order to create the intermediate hydroperoxide **H**. Dehydration of **H** results in the production of benzimide **36**.



**Scheme 26.** Electrochemical production of benzimide **36**.



**Scheme 27.** Electrochemical production of benzimide **36**.



**Scheme 28.** Anodic bromo-acetoxylation of cyclohexene **37** and hydrolysis of the adduct **38** to 1,2-cyclohexanediol **39**.

One of the crucial reactions in the synthesis of organic compounds is the oxidative cleavage of olefinic double bonds to carboxylic acids, aldehydes, or ketones. The majority of the time, ozonolysis is used for this purpose, but expensive safety precautions in technological scale conversions necessitate alternatives. Different electrochemical techniques are being researched for this purpose. No cleavage takes place during the direct oxidation of cyclohexene at a platinum or graphite anode, but substituted and rearranged products are produced instead.

This strategy does not result in double bond cleavage but rather in allylic substitution and rearrangement products. Any aliphatic alkene having an oxidation potential greater than 2.0 V will not be transformed at the boron doped diamond electrode. Ozone produced anodically from water at the lead dioxide electrode produces carboxylic acids with high material yield but low current yield. This technique is effective for producing up to 100 g O<sub>3</sub> h<sup>-1</sup> from two moles of alkene h<sup>-1</sup>. Additionally, lesser stationary ozone and ozonide concentrations result in lower safety precaution expenditures.

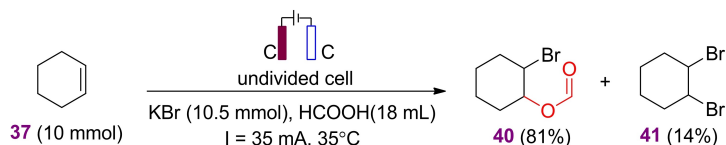
In a one-pot process, 77% of the diol **39** was produced by the condensed electrolysis of cyclohexene **37** with tetrabutylammonium bromide (TBABr) as supporting electrolyte in acetic acid (18 mL) and subsequent treatment of the crude

bromoacetate **38** with 2 M NaOH.<sup>[171]</sup> This electrolysis was done in an undivided cell setup with graphite electrodes at ambient temperature (scheme 28).<sup>[172]</sup>

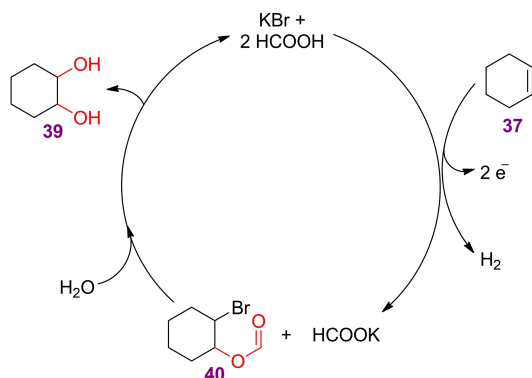
The use of the pricey, challenging to renew TBABr is less advantageous in this conversion. As a result, KBr was used in its place. The electrolysis had to be carried out in 84% aqueous acetic acid with 1.68 equivalents of KBr since KBr is poorly soluble in acetic acid. 56% conversion of cyclohexene was seen after the consumption of 3F; however, the primary product was the undesired 1,2-dibromide **41**, whose production is apparently aided by the presence of water,<sup>[172]</sup> as the yield of the required bromoacetate **38** decreased to 13%. Therefore, electrolysis in a solvent devoid of water seemed necessary. Cyclohexene was electrolyzed in formic acid at 35 °C with 35 mA and 1.05 equivalents of potassium bromide because KBr (supporting electrolyte) is easily soluble in it. An undivided cell with graphite electrodes was used. This produced just 14% of **39**, but 81% of the desired 1-bromo-2-formyloxycyclohexane **40** (Scheme 29).

The cycle below depicts the transformation of cyclohexene into cyclohexane-1,2-diol **39** (Scheme 30). After the bromoacetate **40** is produced electrochemically, formic acid can be removed from the electrolyte by distillation, and after water is added, the solution can be refluxed to produce the diol **42**.





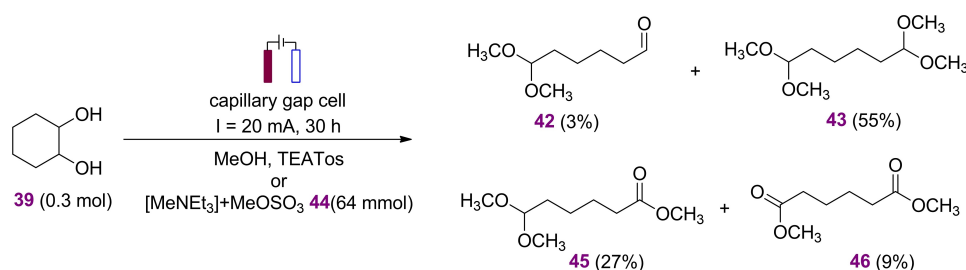
**Scheme 29.** Anodic bromo-formyloxylation of cyclohexene **37**.



**Scheme 30.** Electrochemical cycle for the conversion of cyclohexene **37** into diol **39**.

The separation of salt and diol **39** is made possible by rotaevaporation's removal of water and the addition of ethyl acetate.

Compared to chemical oxidations using hydrogen peroxide or oxygen and catalysts, this electrochemical conversion seems like a good alternative.<sup>[172]</sup> Cyclohexane-1,2-diol **39** can be broken down into 15% acetal **42** and 51% diacetal **43** with a current usage of 2 F in methanol/tetraethylammoniumtosylate (TEATos) at 20 mA cm<sup>-2</sup>.<sup>[173–174]</sup> An enhanced yield of 62% **42** and 17% **43** was obtained by increasing the charge to 2.9 F until **39** is completely consumed. 18% of **42** and 70% of **43** were isolated in an electrolysis in which TEATos, the more expensive supporting electrolyte, was substituted for methyltriethylammoniummethylsulfate **44** (Scheme 31).

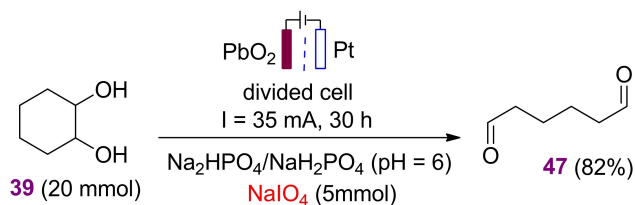


**Scheme 31.** Anodic cleavage of cyclohexane-1,2-diol **39**.

Indirect electrolysis using periodate as a mediator is another technique for the anodic cleavage of 1,2-diols.<sup>[172,175–176]</sup> To use this approach, the diol **39** was electrolyzed in a divided cell with 0.25 equivalents of NaIO<sub>4</sub> in an aqueous, phosphate buffered electrolyte (pH 6), at a lead dioxide anode. Hexanedial **47** was separated in 82% yield at 35 mA cm<sup>-2</sup> following the consumption of 3F (Scheme 32).

By oxidizing water to ozone at the lead dioxide electrode, electrochemical ozonolysis produces carboxylic acids as cleavage products with a high material yield but a low current yield. 5 mmol of 1-decene **48** was electrolyzed in a divided cell with a lead dioxide anode and a platinum cathode at 20 °C and 150 mA using dichloromethane (30 ml) and phosphate buffer (50 ml). Nonanal (44%) **49** and nonanoic acid (48%) **50** were produced using this technique (Scheme 33).<sup>[172]</sup>

The development of selective plastic depolymerization techniques has been impeded by the thermodynamic and kinetic restrictions for C–C bond cleavage. In the chemical recycling of resistant polyolefin waste, activating inert carbon(sp<sup>3</sup>)-carbon(sp<sup>3</sup>) bonds continues to be an important challenge. Redox mediators are employed in this work to activate the inactive C–C bonds. To start hydrogen atom transfer (HAT) reactions with benzylic C–H bonds, the redox mediator N-hydroxyphthalimide (NHPI) is oxidized to the radical phthalimide-N-oxyl (PINO). The resultant carbon radical is quickly absorbed by molecular oxygen to create a peroxide, which then breaks down into oxygenated C–C bond scission fragments. Compared to directly oxidizing the substrate, this indirect method lowers the oxidation potential by > 1.2 V. Studies using model compounds show that as the C–C bond dissociation energy decreases, the selectivity of the C–C bond cleavage rises. Oligomeric styrene (OS<sub>510</sub>; M<sub>n</sub> =



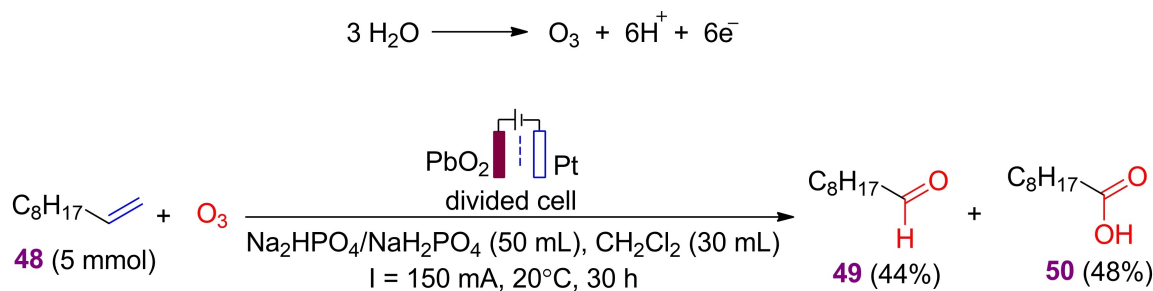
**Scheme 32.** Cleavage of cyclohexane-1,2-diol **39** by indirect anodic oxidation with  $\text{NaIO}_4$  as mediator.

510 Da) and polystyrene (PS;  $M_n \approx 10000$  Da) are transformed into oxygenated monomers, dimers, and oligomers through NHPI-mediated oxidation.<sup>[159]</sup>

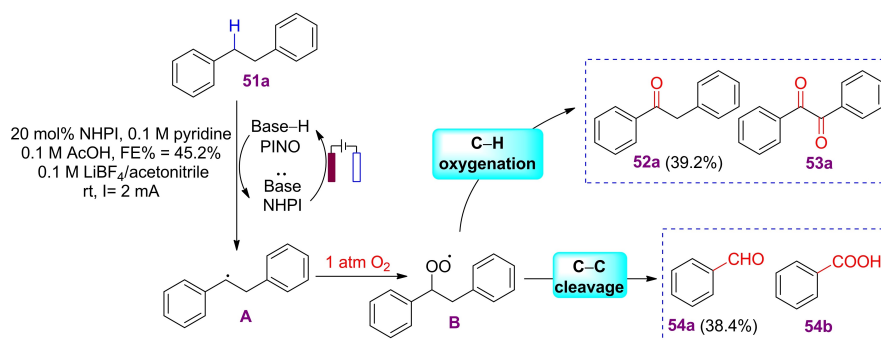
According to these findings, a bifurcated reaction pathway was proposed in which bibenzyl **51a** converts a benzylic C–H to the electrochemically produced PINO, resulting benzylic carbon radical **A** is captured by oxygen gas ( $\text{O}_2$ ) to provide a peroxide radical **B** and then peroxide radical decomposes in two parallel pathways, one resulting in C–C bond cleavage and the other C–H bond oxygenation (Scheme 34).<sup>[177]</sup> The factors affecting the ideal conditions for bulk electrolysis include the quantity of NHPI, media basicity, substituents on the NHPI phenyl ring, solvent, electrolyte types, oxidation current, oxygen partial pressure, and temperature etc. 20 mol%

NHPI solution, 1 atm of oxygen, 0.1 M HOAc, 0.1 M pyridine, 0.1 M  $\text{LiBF}_4$ /acetonitrile electrolyte, ambient temperature, and 2 mA oxidation current are the ideal NHPI-mediated oxidation conditions to achieve 61% conversion and 45.2% faradaic efficiency (FE%). Then, using these reaction conditions, model compound and samples of polystyrene were oxidized.<sup>[159]</sup>

It is generally recognized that plastic waste has a wide range of negative environmental effects, such as elevated energy consumption and exhaustion of greenhouse gases.<sup>[178–180]</sup> Particularly, fossil-based plastics like polystyrene, polyethylene, polyethylene terephthalate, and polypropylene are utilized on a regular basis, which causes an increase in the amount of waste being disposed of in landfills.<sup>[181–187]</sup> As a result, developing a strategy to address these issues that is both efficient and affordable has been difficult. Therefore, compared to landfilling and incineration, recycling technology not only minimizes toxic elements and waste pollution on the environment,<sup>[188–190]</sup> but it can also produce novel products with good mechanical and physical features. Due to their processing-related blending with other plastics and additives, these materials are not simple to recycle. The mechanical properties of recycled plastics typically change due to a number of factors, including oxidation during reprocessing, mechanical stress, and degradation from heat.<sup>[191]</sup>



**Scheme 33.** Anodic generation of ozone and ozonolysis of 1-decene **48**.



**Scheme 34.** Bifurcated pathway of C–C bond cleavage and C–H oxygenation follows PINO induced HAT and  $\text{O}_2$  addition.

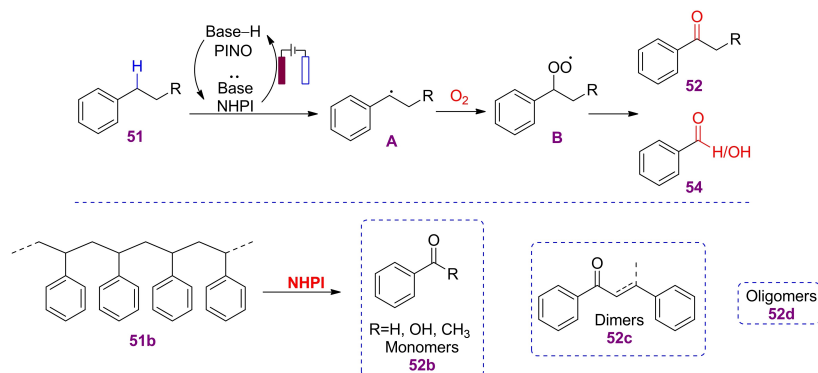
An exciting proof of concept that the mediated electrochemical bond activation technique may be practical to deconstruct polymeric substrates is the potential of NHPI/PINO to activate polystyrene substrates **51b**. However, there are still numerous obstacles to overcome before real PS waste can be effectively depolymerized. For instance, the rate of HAT from polystyrene (PS) to PINO is constrained by the sluggish diffusion and high viscosity of the PS in solution.<sup>[192–194]</sup> Polystyrene conversion may be enhanced by mass transfer techniques include raising the operational temperature, utilizing mixed solvents, and vigorous stirring. Additionally, a downstream separation strategy must be devised in order to filter the vast array of oxygenate products. To overcome the heterogeneity of the reaction products, for instance, efficient separation methods like chromatography or modified microbes could be applied.<sup>[195]</sup> A number of additives, including pigments, metals, photo-stabilizers, metal oxides, dyes, thermal stabilizers, and other polymers (such as acrylonitrile butadiene styrene (ABS); a terpolymer), are also present in PS plastic. These additives may have a significant impact on the electrochemical oxidation reactivity. Furthermore, to recognize and quantify the entire spectrum of the oxidation products, systematic characterization techniques must be developed.<sup>[196–198]</sup> NHPI to mediate the oxidative depolymerization of PS (10000 Da) as a proof-of-concept was used, and 12% yield of monomers and dimers in the process was obtained (Scheme 35). There are a variety of appealing applications for this form of industrial recycling. The product of polypropylene oxidation in acetic acid, for example, would be mostly acetic acid – the solvent and the product are the same. Polystyrene oxidation might also be carried out in benzoic acid as a solvent.<sup>[199]</sup>

If pure, distilled acetic acid is desired, benzoic acid can be used as the solvent for polypropylene oxidation. Because the reaction could be run at temperatures over the boiling point of acetic acid, the acetic acid would shoot out of the reactor as it was being produced. Polymer mixes could also be employed.

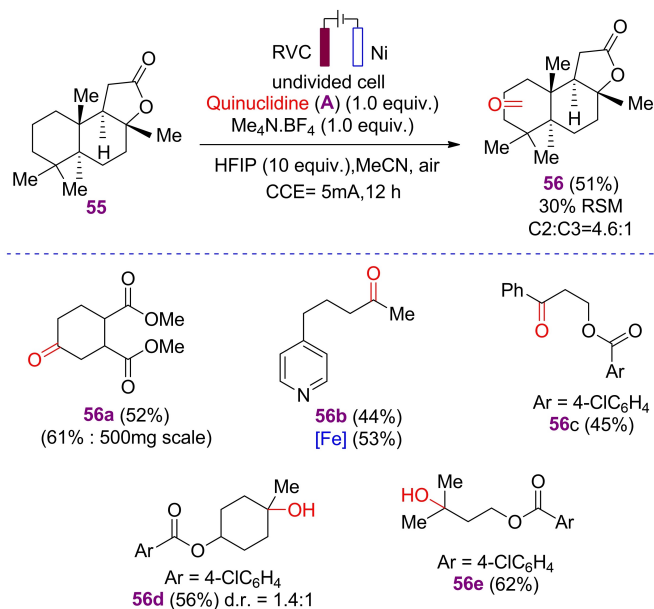
Polystyrene and polypropylene mixes in acetic acid, for example, would produce acetic acid and benzoic acid. Acetic acid and benzoic acid can be easily separated.

A simple electrochemical approach enabled the oxidation of unactivated C–H bonds, which previously required the employment of extremely reactive, scarce, and costly compounds. This effective technology used quinuclidine **A** as a mediator and a basic electrochemical setup with inexpensive carbon and nickel electrodes. This selective technique proved compatible with a wide range of functional groups. Scalability of the method proved by successfully oxidizing sclareolide **55** on a 50 g scale, demonstrating its potential to simplify the synthesis of complex compounds. Quinuclidine (**A**) mediated the selective electrochemical oxidation of C-2 methylenes at 1.8 V (compared to Ag/AgCl reference electrode). While  $\text{Me}_4\text{N}\cdot\text{BF}_4$  was chosen as an electrolyte due to its safety and lower cost. Reticulated vitreous carbon (RVC) electrode was employed for the anode, whereas nickel, copper, and stainless steel were feasible cathode materials. The reaction occurs in a simple undivided cell at room temperature with constant current (25 mA/mmol). Sclareolide electrochemical oxidation yields 51% product. After finding the best conditions, this electrochemical C–H oxidation method was explored for a range of compound (Scheme 36). It is possible to carefully change methylene groups in linear, cyclic, bicyclic, heteroarene-containing, and natural product-derived substrates into ketones. The selectivities and yields were about the same as those of TFDO oxidation<sup>[200]</sup> or Barton-Gif-type (iron-based) methods.

Electrochemical oxidation was made possible by the quinuclidine mediator at a comparatively low potential. Numerous functionalities are therefore tolerated under response conditions. Despite having two epimerizable centers, **56a** was produced with perfect stereochemical integrity. **56b** showed selective distal methylene oxidation, and both the pyridine motif and the benzylic methylene group were preserved. In contrast, TFDO oxidation only resulted in the



**Scheme 35.** Depolarization of polystyrene **51b**.



**Scheme 36.** Electrochemical production of ketone **56** by quinuclidine mediated electrochemical C–H oxidation.

synthesis of N-oxide and did not result in methylene oxidation. Effective oxidation was also possible with activated methylenes, such as benzylic **56c** C–H bonds. The corresponding alcohols could be produced by using this approach to oxidize tertiary C–H bonds (**56d** and **56e**).<sup>[35]</sup>

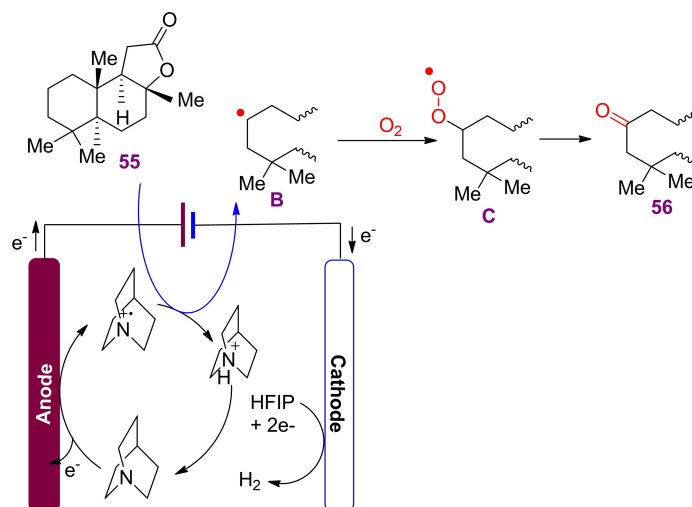
This method works well at targeting specific parts of molecules without affecting the rest and it is especially useful for making chemicals in the pharmaceutical industry. Sclareolide is a good starting material for making different types of meroterpenoid compounds.<sup>[201]</sup> So, researcher used this electro-

chemical C–H oxidation approach to produce 2-oxo-sclareolide, which is a unique version of terpenoid compounds. Alkene amino-oxygenation is common in chemistry, biology, and materials. This technique produces 1,2-aminoalcohols for medicines, natural goods, and chiral reagents.<sup>[202]</sup> The intramolecular variant produces nitrogen-containing heterocycles with biological functions.<sup>[203–206]</sup>

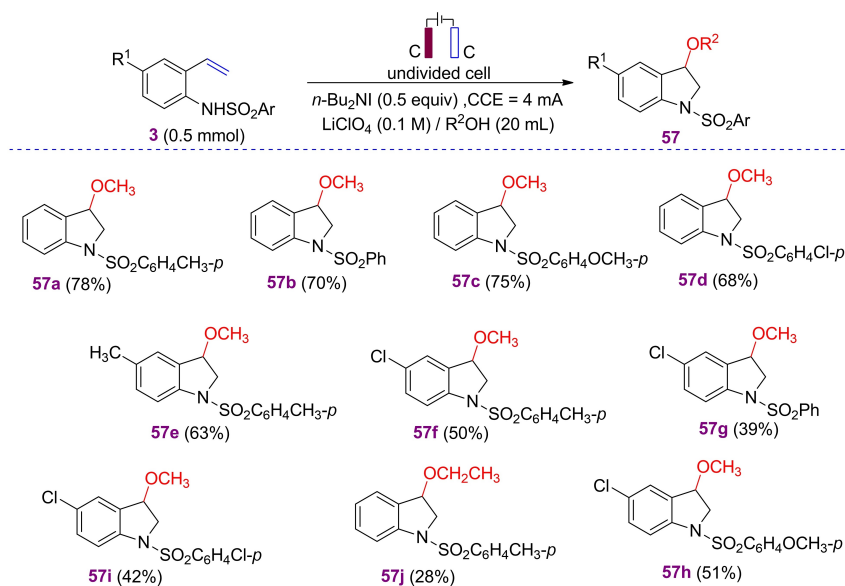
In terms of mechanism, electrochemical C–H oxidation is connected with anodic oxidation of a quinuclidine radical cation. As a high-energy entity, this radical cation has the ability to perform homolytic cleavage of an un-activated C–H bond. The resultant carbon-centered radical **B** may then combine with molecular oxygen to produce the oxidation product **56**. It is believed that HFIP functions as an electron acceptor in the cathodic process, resulting in the formation of H<sub>2</sub> (Scheme 37).

Researchers devised an effective electrochemical approach for producing 3-methoxyindolines and 3-ethoxyindolines from styrene **3**. Electrolysis was performed in an undivided cell equipped with a graphite plate anode and a graphite cathode, 0.5 equivalent of *n*-Bu<sub>4</sub>NI served as the redox catalyst, CH<sub>3</sub>OH as the solvent, and 0.1 M lithium perchlorate as a supporting electrolyte. Reaction happened at room temperature. The required products were synthesized in upto 80% yield via a C–N cascade followed by C–O bond formation (Scheme 38).

After determining the optimal reaction conditions, the range and generality of the reaction was investigated. As can be observed in scheme 38, the reaction of N-(2-vinylphenyl)sulfonamide derivatives containing various sulfonyl groups, such as benzenesulfonyl **3ab**, *p*-methoxybenzenesulfonyl **3ac**, and *p*-chlorobenzenesulfonyl **3ad**, went smoothly and produced the cyclization products in good



**Scheme 37.** Suggested mechanism for electrochemical production of ketone **56** by quinuclidine mediated electrochemical C–H oxidation.



**Scheme 38.** Electrochemical production of 3-alkoxyindoline **57**.

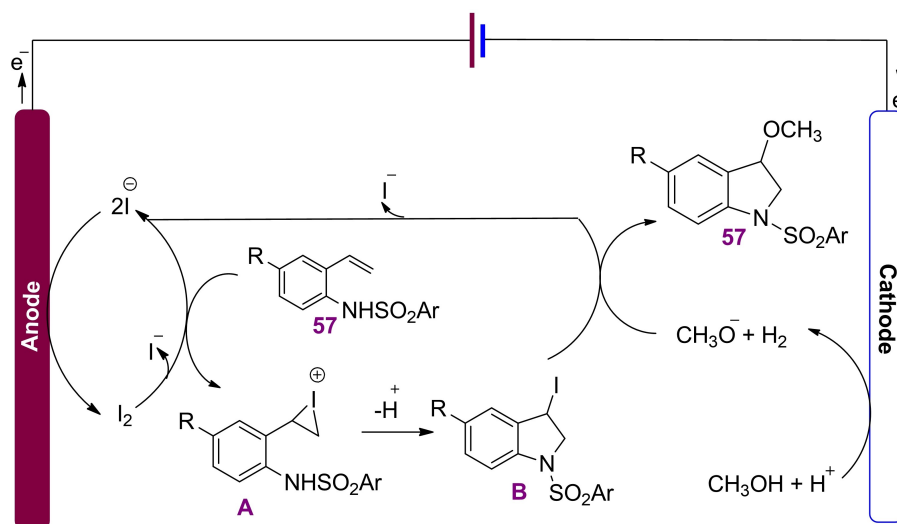
yields. When an electron-donating group is added to the benzenesulfonyl subunit, yields are typically higher. For instance, when *p*-methoxybenzenesulfonamide **3ac** was electrolyzed at a constant current under the described conditions, the adduct **57c** was isolated in 75% of the reactions. However, when an electron-withdrawing chlorine was present in the starting material, **3ad**, the yield of the adduct **57d** was lower (68%). To assess the applicability of the cyclization reaction, various 2-vinylphenyl group-containing sulfonamide derivatives were also examined. The corresponding adducts **57e** and **57f** were produced in moderate to fair yields from vinyl sulfonamide derivatives containing methyl groups (**3ae**, R1 = CH<sub>3</sub>) or chlorine groups (**3af**, R1 = Cl). Once more, it was discovered that adding an electron-donating substituent to the aromatic ring made the cyclization reaction more effective. Examples include the *p*-methoxy group-containing substrate **3ah**, which produced the adduct **57h** in a yield of 51%, and the chloro-substituted starting material **3ai**, which produced the adduct **57i** in a yield of 42%. It is noteworthy that the ethoxy-substituted adduct, 3-ethoxy-1-tosylindoline **57j**, formed when the electrolysis was carried out in ethanol rather than methanol, albeit in a yield of only 28%.

Gram-scale reaction provides additional proof that the protocol is workable. This method has several advantages. First, the anode acts as a co-oxidant but can be separated from the organic layer containing the substrate for easy removal. Second, there is no need for an additional chemical co-oxidant. Third, it does not require extra supporting electrolytes, making the workup and isolation simpler and reducing waste.

The process begins with the anodic oxidation of iodide, which produces molecular iodine, which then reacts with the starting material **3** (Scheme 39). This reaction results in the formation of an iodonium intermediate **A**. Simultaneously, the sulfonamide nitrogen conducts an intramolecular nucleophilic assault on the cyclic iodonium ion, yielding the desired product 3-iodo-1-arylsulfonylindoline, designated as **B**. Methanol is reduced in the cathodic compartment, yielding hydrogen gas and methoxide anions. As nucleophiles, the methoxide anions react with compound **B**, resulting in the production of the target product **57** and the regeneration of iodide ions. The regenerated iodide ions then re-enter the redox catalyst cycle, allowing the process to continue.<sup>[202]</sup>

### 3.6. Electrochemical C–H/C–C Bond Oxygenation Using Metal Catalysts

Through direct<sup>[17,20,91,93,207–208]</sup> or mediated electro-oxidation (mostly focusing on organic mediators) methods,<sup>[19,37,162–163,209]</sup> electrochemical organic synthesis has demonstrated its promise for benzylic C–H oxidation, being effective and environmentally benign. The restricted functional group tolerance, inadequate selectivity, sensitive group incompatibility, and the fact that most techniques only utilize oxidative half-cell reactions were still obstacles to wider adoption of this strategy. Transition metal catalysis has become one of the most significant channels for selectivity control in contemporary synthetic chemistry due to the good manipulation of reaction selectivity and the high tolerance of functional groups.<sup>[210–215]</sup> In this instance, Sanford,<sup>[216]</sup> Mei,<sup>[217–218]</sup> Ackermann,<sup>[219–222]</sup>



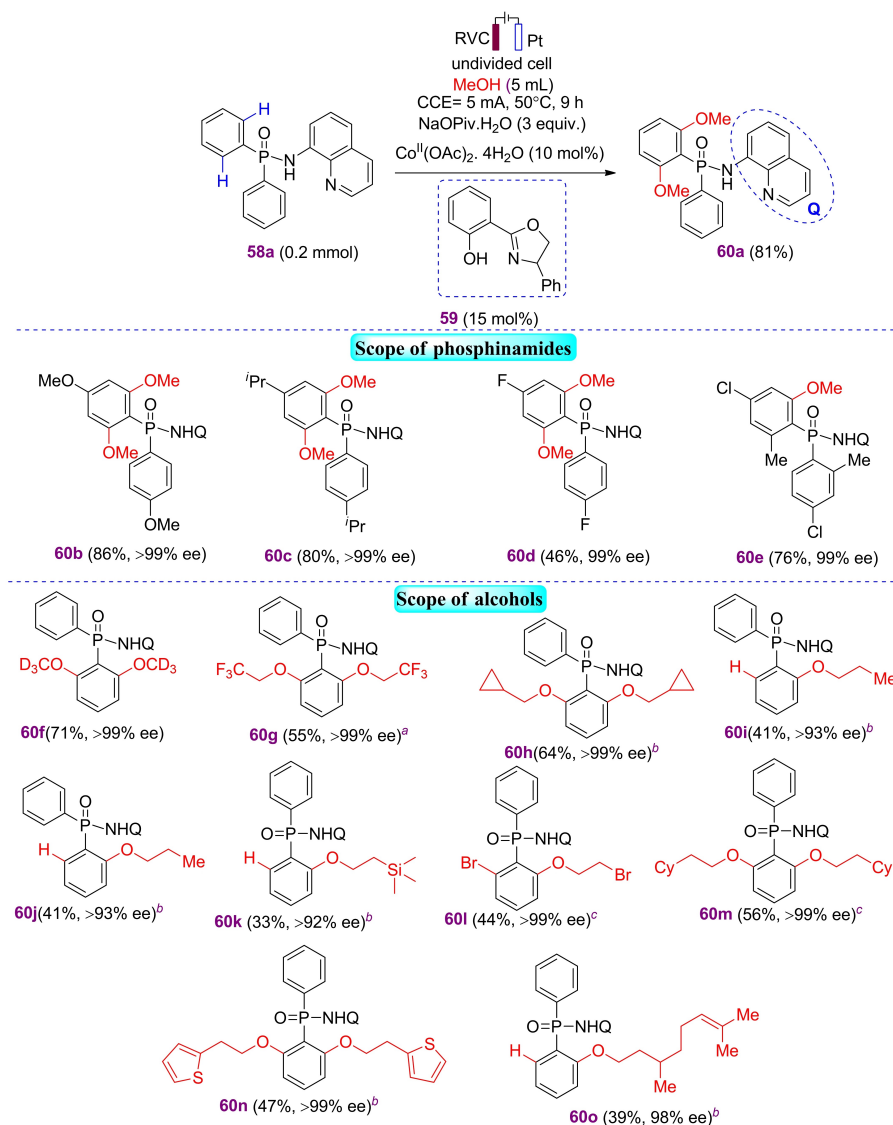
**Scheme 39.** Proposed mechanism for electrochemical production of 3-methoxyindoline **57**.

Chang,<sup>[223]</sup> Quan and Xie,<sup>[224]</sup> established transition metal-catalyzed electrochemical C–H oxygenation processes. The enantioselective electrochemical C–H oxygenation<sup>[225]</sup> is still elusive despite the fact that electrochemical C–H oxygenation has been extensively studied. The significant difficulties could be the cause of electrochemical asymmetric C–H oxygenation such as the metal–oxygen (M–O) bond exhibits strong polarity, alcohols and chiral ligands undergo oxidative breakdown under electrooxidative circumstances, and the electrolyte and active intermediates interact adversely.

As sacrificial oxidants, vast quantities of silver salts were utilized, leading to significant costs and harmful consequences.<sup>[226]</sup> The first electrochemical enantioselective C–H oxygenation catalyzed by Co<sup>II</sup> in order to resolve this flaw was described.<sup>[227–235]</sup> The use of electricity in place of stoichiometric silver salts, which only produces H<sub>2</sub> as a byproduct, good yields and excellent enantioselectivities (up to 98% yield and >99% ee), the isolation and complete characterization of cobalt(III) alcohol complex, which was discovered to be a crucial intermediate in this C–H alkoxylation process, are some main benefits of this strategy.

Enantioselective C–H methoxylation of phosphinamide **58a** and employing Salox **59** (chiral ligand) as the model reaction was chosen to investigate the ideal reaction parameters. The expected electrochemical C–H oxygenation was discovered to be achieved when utilizing RVC as the anode and Pt as the cathode in an undivided cell arrangement after the preliminary screening of reaction conditions (Scheme 40). When **59** was employed as the ligand, it was found that the required alkoxyated product **60a** was produced in 71% yield and with 99% ee.<sup>[236–238]</sup> Better yield and enantioselectivity were not achieved while testing different Salox ligands. When

the amount of NaOPiv.H<sub>2</sub>O was increased to 3.0 equivalents, the yield scaled to 75% but no desirable product was seen in the absence of NaOPiv.H<sub>2</sub>O, demonstrating the crucial function that NaOPiv.H<sub>2</sub>O plays in this process. The intended product **60a** could be produced in 81% yield with 99% ee under continuous current electrolysis at 5.0 mA in the presence of 10 mol% Co(OAc)<sub>2</sub>.4H<sub>2</sub>O, 15 mol% **59**, 3.0 equiv. of NaOPiv.H<sub>2</sub>O in MeOH at 50 °C for 9 h under air after thorough screening of various circumstances. The efficacy of electrochemically catalyzed asymmetric C–H functionalization by 3d metals is demonstrated in this scheme. It is believed that it might present novel asymmetric synthesis options. The range of phosphinamides and alcohols was tested, respectively, after determining the ideal reaction conditions (Scheme 40). In general, a wide variety of phosphinamides with various functional groups were all compatible, resulting in good yields and outstanding enantioselectivities for the methoxylation products (**60a–60e**, 46–88% yield, 99%–>99% ee). Notably, multi-substituted phosphinamide **58e** were also well tolerated and provided the required product with outstanding ee and high yield (**60e**, 76%–yield, 99% ee). The successful conversion of diverse alcohols further proved the applicability of electrochemical enantioselective C–H oxygenation. It was possible to obtain the necessary alkoxyated chiral phosphinamides with outstanding enantioselectivities (93–>99% ee) by the smooth reaction of a number of aliphatic alcohols. It was also successful to oxygenate C–H with citronellol, demonstrating the possibility of late-stage alteration of natural products. Unexpectedly, under electrochemical circumstances, 2-bromoethan-1-ol displayed a special reactivity that produced the C–H bromination product **601** in a modest yield with excellent enantiocontrol (44%, 99% ee).<sup>[239]</sup>



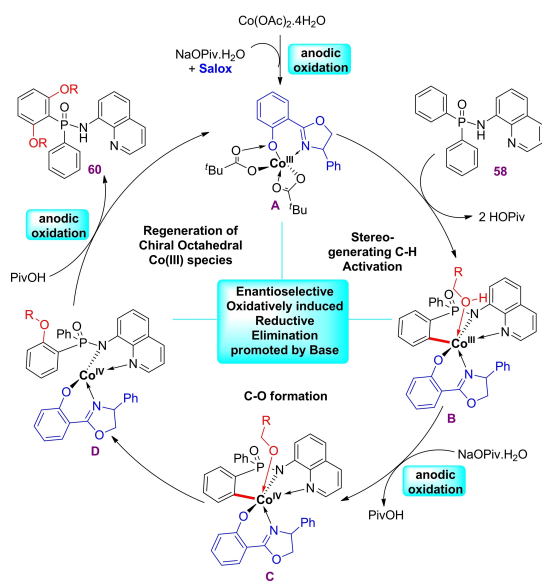
<sup>a</sup>60 °C. <sup>b</sup>*n*-Bu<sub>4</sub>NPF<sub>6</sub> (0.2 M), in MeCN, 70 °C, CCE at 2 mA. <sup>c</sup>*n*-Bu<sub>4</sub>NPF<sub>6</sub> (0.2 M), in DCE, 70 °C, CCE at 2 mA, Co(OAc)<sub>2</sub> · H<sub>2</sub>O (20 mol%), L1 (22 mol%).

**Scheme 40.** Electrochemical production of alkoxyated product **60**.

For the electrochemical enantioselective method, a reasonable catalytic cycle was suggested (scheme 41), based on our mechanistic research and precedents.<sup>[220,226,236–238]</sup> The chiral octahedral Co<sup>III</sup> complex **A** was initially produced by the anodic oxidation of Co<sup>II</sup> in the presence of Salox ligand and NaOPiv. Cobaltacycle intermediate **B** coordinated with alcohol was produced by a subsequent ligand exchange with phosphinamide **58**, followed by an enantio-determining, carboxylate-assisted C–H activation. This was categorically proven by single-crystal X-ray diffraction. At the anode promoted NaOPiv, Co<sup>III</sup> intermediate **B** was further oxidized

to Co<sup>IV</sup> intermediate **C**. Co<sup>IV</sup> intermediate **C** was reduced to give Co<sup>II</sup> species **D**. Finally, protodemetalation allowed for the release of the desired product **60** while anodic oxidation allowed for the regeneration of the catalytically active cobalt(III) species.

It is revealed how functionalized alkyl arenes can be oxygenated utilizing water in a site-specific, paired nickel electrocatalyzed reaction. The oxidation of a variety of compounds with varied degrees of complexity and drug derivatives can be accomplished using the nickel catalyst in conjunction with water in a reliable, environmentally friendly,



**Scheme 41.** Suggested mechanism for electrochemical production of alkoxy-lated product **60**.

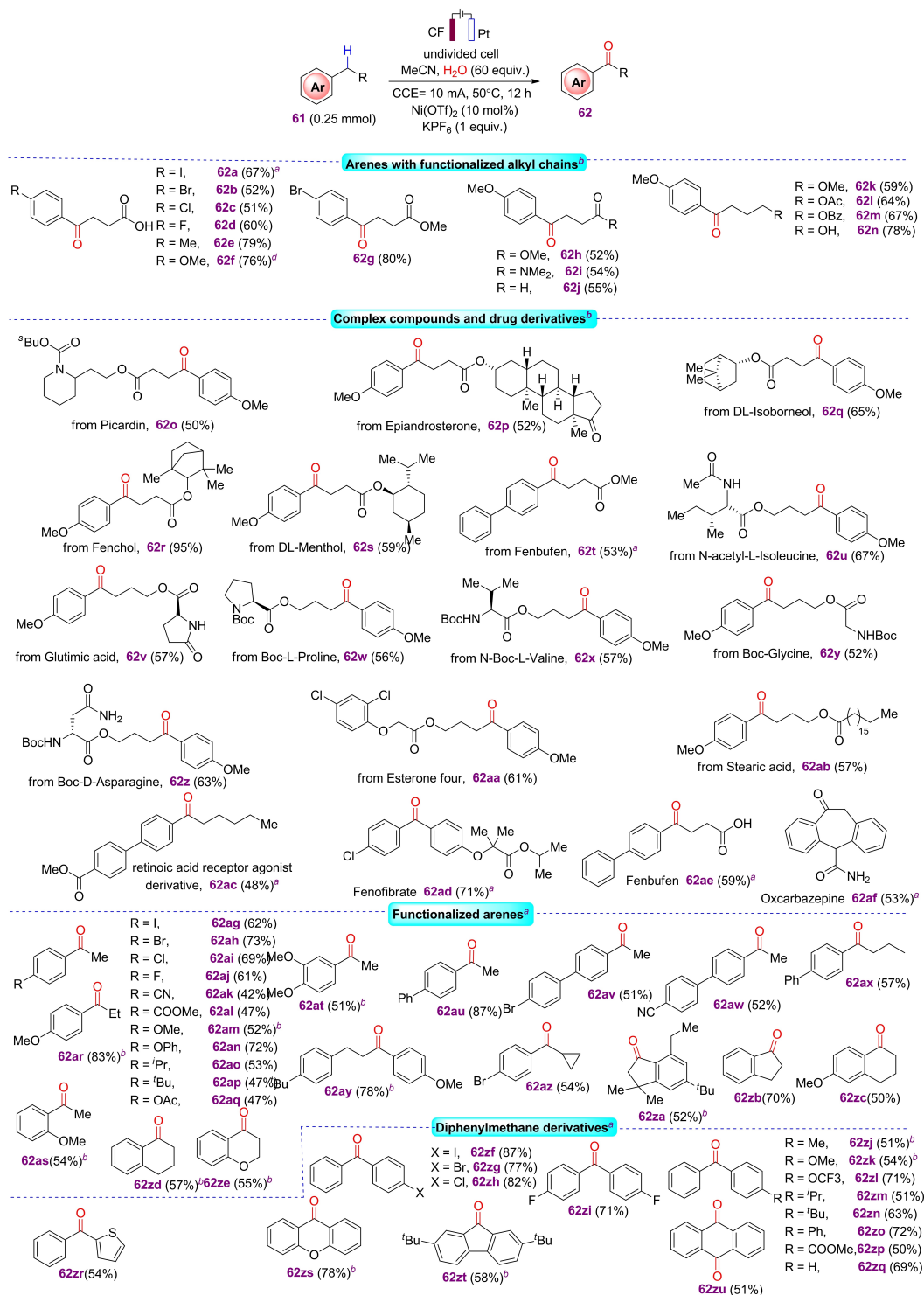
and cost-effective manner, suggesting its potential usage in organic synthesis and the pharmaceutical sector. Notably, the transition went successfully for a variety of functionalized aromatic ketones, including examples with sensitive functional groups. Iodinated aromatics, for instance, were well tolerated in this reaction. Furthermore, in this paired nickel-catalyzed system, aldehydes and alcohols, which are susceptible to over-oxidation, were also compatible. This method has several noteworthy qualities, such as excellent tolerance to a wide range of sensitive functional groups (free carboxylic acids, alcohols, amides, esters, amino acids, halogens, and aldehydes), high chemo- and site- selectivity, late-stage oxygenation of natural compounds and drug derivatives and the use of a bipolar ultramicroelectrode (BUME) in conjunction with nano-electrospray ionization mass spectrometry allowed for the collection of a transient reactive aryl radical cation intermediate. It is noteworthy that this quick and precise paired nickel-catalyzed electro-oxidation method can also be used to create natural compounds. The crucial function of the in situ Ni(II)-dioxygen species for the subsequent oxidation of C(sp<sup>3</sup>)-H bonds was highlighted by the results of the reaction and mechanistic studies. A practical method for industrial scale-up production is to use green, pure water as the source of oxygen. In the laboratory, more investigation into the selective earth-abundant metal-catalyzed C-H oxidation is being conducted by S. Tang and coworkers.

After careful optimization, the reaction was carried out in CH<sub>3</sub>CN with the addition of 60 equiv. of water, a catalytic amount (10 mol%) of Ni(OTf)<sub>2</sub>, a constant current (10 mA), KPF<sub>6</sub> (1 equiv.) as the supporting electrolyte, carbon felt as the

anode, and platinum plate as the cathode. Product **62** was obtained in good isolated yield (Scheme 42). The scope and compatibility of the reaction were examined using optimized reaction conditions. A number of typical functionalized alkyl arenes were shown to function well in the process, resulting in good to outstanding yields for the corresponding aryl ketone acids (**62 a–62 f**). Following constant current electrolysis, the sensitive groups on the substrates (precursors of **62 g–62 m**) were unaltered, and moderate to good yields of the required products were produced. With a 78% yield, the substrate with the lengthy alkyl chain and the terminal OTIPS group produced the deprotected hydroxyl product **62 n**. The late-stage functionalization of complicated molecules could be accomplished using the benzyl electro-oxidation method. With moderate to good yields and diastereoselectivities **62 o–62 z** and **62 aa–62 ac**, alkylarenes generated from pharmaceuticals like epiandrosterone, DL-isoborneol, fenbufen, stearic acid, esterone four, picaridin, fenchol, retinoic acid receptor agonist derivatives, and DL-menthol,  $\alpha$ -amino acid derivatives including glutimic acid, Boc-L-proline, N-acetyl-L-isoleucine, N-Boc-L-valine, Boc-D-asparagine, and Boc-glycine were all susceptible to the electro-oxidation transformation. Only **62 p**, **62 q**, **62 v**, **62 w**, **62 x**, and **62 z** were produced as a single diastereoisomer.

Similarly, these reaction conditions might be used to directly produce the therapeutic compounds fenofibrate **62 ad**, fenbufen **62 ae**, and oxcarbazepine **62 af**. These findings demonstrated the method's synthetic promise for the simple addition of carbonyl groups to large chemicals and medicinal molecules. The intended corresponding alkyl aryl ketones were all produced in moderate to good yields by functionalizing arenes with electron-withdrawing (**62 ag–62 al**) or electron-donating (**62 am–62 at**) substituents, and the sensitive functional groups were unaffected under the usual conditions. Similar to this, the aryl-substituted substrates on the benzene ring performed admirably under our reaction conditions and provided the required products in good yields (**62 au–62 ax**). Notably, the reaction only took place at the benzylic position of the more electron-rich methoxy-substituted aryl group when substrate **62 ay** with two benzylic positions was used. When both ring and alkyl chain reaction sites were present, it was additionally observed that the oxidation reaction took place preferentially on the ring **62 za**. When a ternary ring is connected to a benzylic position, the ternary ring did not go through a ring-opening process after electrolysis and delivered the product **62 az** directly in a modest yield. Simple 1-indanone **62 zb** and benzohexacycles **62 zc–62 ze** produced the necessary compounds with no difficulties. It is interesting to note that great yields of the target molecules were produced from substrates with diaryl substitutions **62 zf–62 zu**. Only one product was produced and no aldehyde was found for the substrate that had an aryl group attached to it, which may





<sup>a</sup> Standard conditions. <sup>b</sup> The reaction was conducted under a constant current of 5 mA for 12 h. <sup>c</sup> The starting material is triisopropyl(4-(4-methoxyphenyl)butoxy)silane. <sup>d</sup> The reaction was conducted under a constant current of 5 mA for 10 h.

**Scheme 42.** Nickel-electrocatalyzed benzylic C–H oxygenation of functionalized alkyl arenes.

have been because the two reaction sites had different densities of electron clouds **62zj**. The reaction also continued when heteroatomic ring substrates were utilized; for instance, a 52% yield of the target product **62zr** was produced. In contrast, for the substrate 9,10-dihydroanthracene, the product anthraquinone **62zu** was produced in one step under conventional reaction conditions without the presence of any mono-oxidized ketone products.<sup>[92]</sup>

A mechanism for paired electrochemical oxidation was suggested based on the outcomes of our experiments and observations in the literature.<sup>[240]</sup> Through single electron transfer (SET), the anodic oxidation of substrate **61** yields radical cation **C**, and the subsequent loss of a benzylic proton yields benzyl radical **D**. At the same time, molecular oxygen ( $O_2$ ) is activated by the Ni(I) intermediate produced by the one-electron reduction of the Ni(II) species at the cathode to produce the Ni(II)-superoxo species **A**. The catalytically active Ni(II)-peroxo species **B** is subsequently produced by additional one-electron reduction of this Ni-superoxo species **A**. This species **B** may exhibit oxygenase-like reactivity by transferring an oxygen atom to the external substrate **D**. The catalytic cycle is completed by anodic oxidation of the reduced Ni(0) species, which produces the end product **62** and regenerates the Ni(II) salt. At this point, it is not possible to completely rule out additional minor reaction paths, such as **D** being reoxidized to benzyl cation and subsequently being attacked by  $H_2O$  (Scheme 43).

An electrochemical technique was established for the selective oxidation of alkanes with  $C(sp^3)-H$  bonds utilizing water as the oxygen source. In most cases, the “high over potential” required for these electrochemical oxidations also oxidizes other functional groups in the substrate. To accom-

plish these oxidations at much lower over potentials and with good selectivity, however, the  $Fe^{III}$  complexes **Cl (A)**/ $H_2O$  (**B**) are used. By using  $[(bTAML)Fe^{III}(OH_2)]^-$  as the catalyst and water as the oxygen atom source, we demonstrate the selective electrochemical alkane hydroxylation and epoxidation in this scheme. The natural product cedryl acetate served as the substrate, and the selective hydroxylation of an inactive  $3^\circ C-H$  bond was displayed. The electrochemical oxidations were conducted in a simple undivided cell using low-cost nickel and carbon electrodes. As far as we are aware, this is the first instance of using an iron complex to catalyze the electrochemically selective oxidation of strong  $C-H$  bonds (using  $BDE \leq 97 \text{ kcal mol}^{-1}$ ) and  $C=C$  bonds using water as the O-atom donor (Scheme 44).

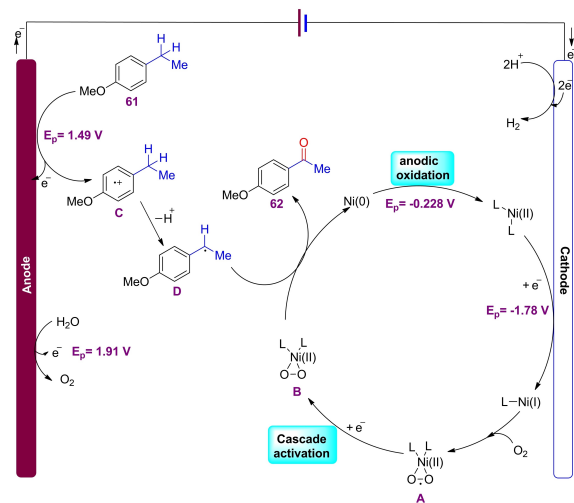
A reaction mixture of  $Cl/H_2O$  (0.75 mM) and substrate (15 mM) in acetonitrile aqueous phosphate buffer (4: 1 v/v, 5 mM,  $pH=8$ ) at a constant potential of 0.80 V (vs.  $Ag/AgNO_3$ ) at room temperature for 10 hours resulted in high conversion and yield of oxygenated compounds **64** or **65**.

The electrocatalytic cycle begins immediately after applying a constant voltage (0.80 V) to the anode (RVC), where complex  $H_2O$  undergoes an overall  $2H^+/2e^-$  (PCET) transfer reaction to create oxoiron(V) species,  $[(bTAML)Fe^V(O)]^-$  **C**. The high-valent oxoiron (V) species **C** hydroxylates the  $C-H$  bond in substrates to generate the corresponding alcohol via the standard “rebound mechanism” in the hydroxylation reaction as shown in scheme 45.<sup>[241]</sup>

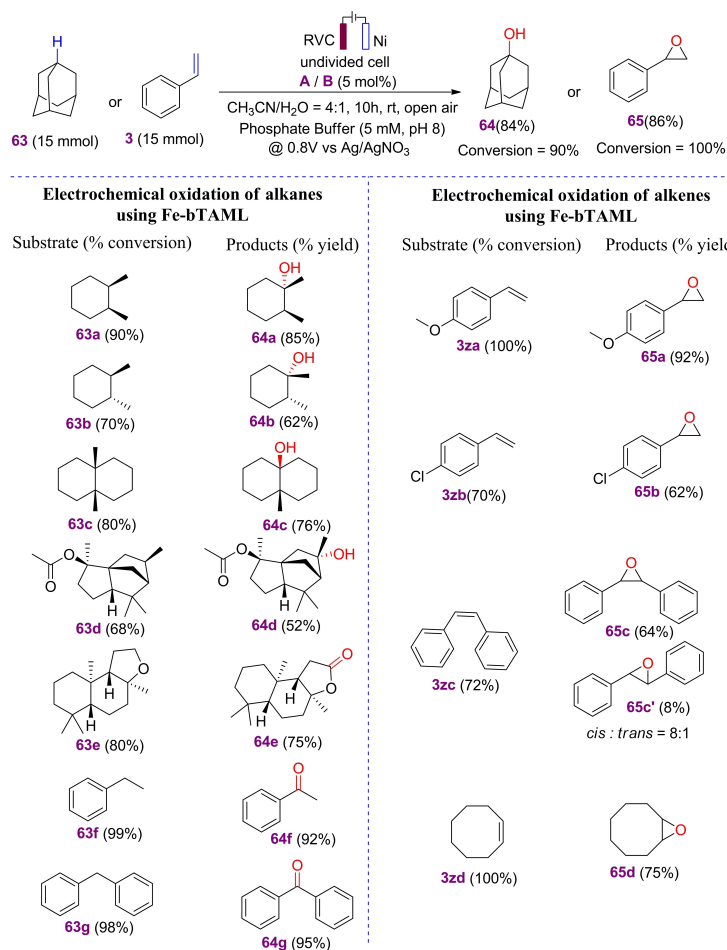
The functional group tolerance in the selective benzylic  $C-H$  oxidation of functionalized alkyl arenes is thought to be improved by transition-metal catalysis. To the best of our knowledge, the selective electrochemical benzylic  $C-H$  oxidation of functionalized alkyl arenes containing sensitive functional groups has thus far shown to be difficult.<sup>[38,242]</sup>

Under ambient conditions, electrochemical cobalt-catalyzed  $C-H$  oxygenation on arenes and alkenes with outstanding degrees of positional and diastereo-selectivity was successful by avoiding the use of stoichiometric silver(I) oxidants.<sup>[219,243–254]</sup> Ackermann and collaborators accomplished cobalt-mediated  $C-H$  oxygenation. The reliable electrochemical  $C-H$  functionalization had a wide substrate scope, and mechanistic investigations indicated a straightforward  $C-H$  cleavage. The electrochemical oxygenation occurred at  $23^\circ C$  with 3.6 F/mol, delivering the product **68**. Out of a representative group,  $Co(OAc)_2$  was the most effective cobalt precursor, with  $NaOPiv$  as the preferred base. Reaction took place in a divided cell containing RVC anode and platinum cathode.

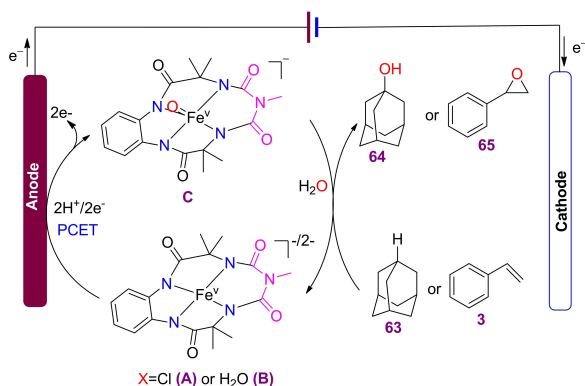
Then the viability of the improved cobalt catalyst for the  $C-H$  oxygenation of benzamides **66** was investigated (Scheme 46). As a result, a wide variety of critical functional groups, such as ketone substituents and fluoro, chloro, and bromo, were well tolerated. It is also notable that certain



**Scheme 43.** Selective nickel-electrocatalyzed benzylic  $C-H$  oxygenation of diverse functionalized alkyl arenes and its suggested mechanism.



**Scheme 44.** Electrochemical production of hydroxylation **64** and epoxidation product **65**.

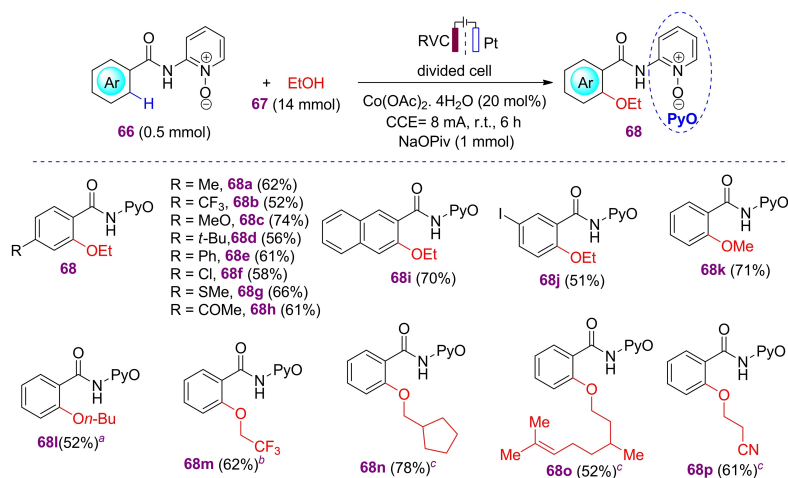


**Scheme 45.** Electrochemical approach of forming an oxoiron (V) complex from A/B followed by oxidation of alkanes **63** and alkenes **3** using water as the O-atom source.

substrates did not undergo benzylic oxidation, demonstrating the distinct chemoselectivity of the cobalt catalysis

phase.<sup>[255–256]</sup> The electrochemical C–H functionalization's positional selectivity in intramolecular competition studies was controlled by steric interactions, yielding the benzamides **68j** as the only product. The effective conversion of diverse alcohols **67**, including functionalized derivatives, further demonstrated the flexibility of the electrochemical C–H functionalization. It is particularly interesting in this case that a chemo-selective process was used to achieve a smooth transformation of the readily oxidized benzylic alcohols. The accomplishment of C–H oxygenation with naturally occurring citronellol also suggests the possibility of late-stage diversifications. Phenols have so far produced less than ideal results, but the cobalt catalyst was tolerant of functional groups like nitrile and ester. The gram-scale synthesis of product **68** was also carried out with comparable catalytic efficacy to test the stability of this approach.

An electrochemical cycle that would begin with the electrochemical SET of the aromatic benzamide **66** by anodic oxidation and end with the development of a straightforward

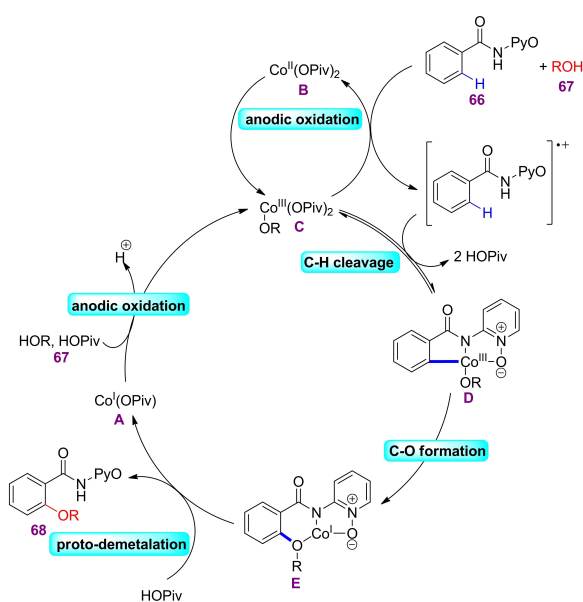


<sup>a</sup>*n*-Bu<sub>4</sub>N<sup>+</sup>OAc<sup>-</sup> (1.0 mmol in each cell). <sup>b</sup>60 °C. <sup>c</sup>In MeCN and *n*-Bu<sub>4</sub>NPF<sub>6</sub> (0.3 M).

**Scheme 46.** Electrochemical synthesis of alkyl aryl ether **68**.

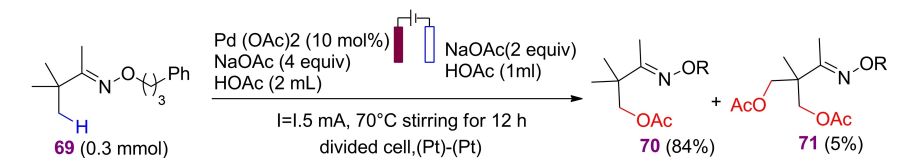
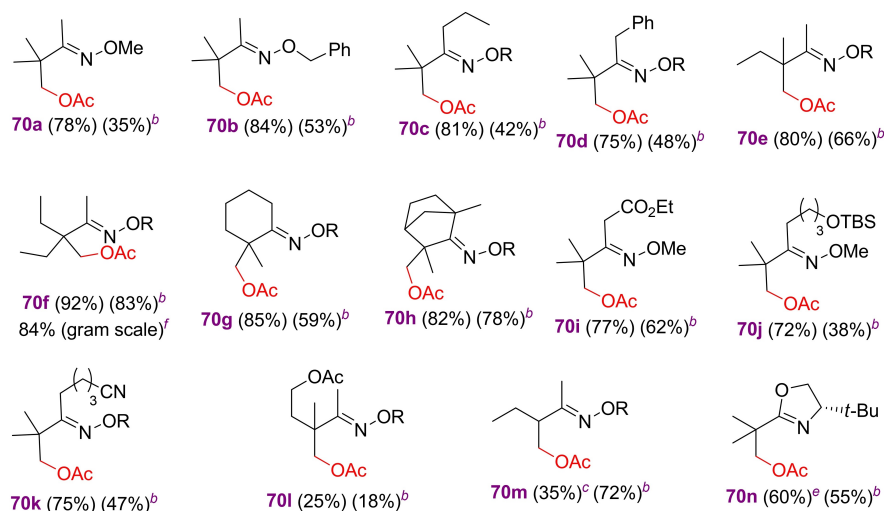
electrochemical catalyst has been proposed, focusing on fundamental studies (Scheme 47). Then, proximity-induced chelation promotes C–O synthesis and great positional selectivity. The desired product **68** is finally released as a result, and the catalytically active cobalt(III) species are renewed through anodic oxidation.<sup>[219]</sup>

Strong chemical oxidants are required for palladium-catalyzed C–H activation/C–O bond formation processes, which transform organopalladium (II) intermediates into the

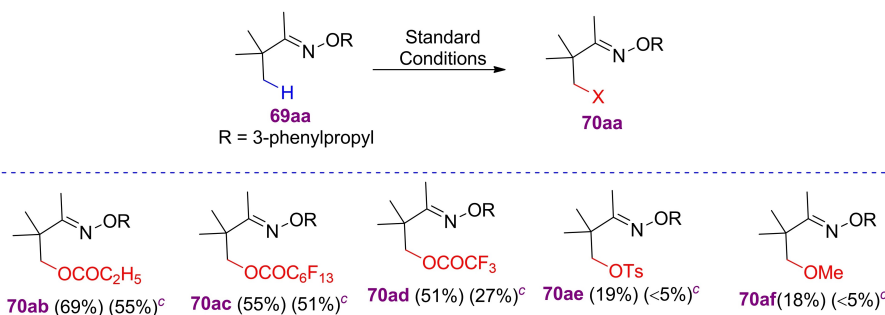


**Scheme 47.** Suggested mechanism for electrochemical synthesis of alkyl aryl ether **68**.

Pd<sup>III</sup> or Pd<sup>IV</sup> oxidation state to facilitate difficult C–O reductive elimination. However, previously described oxidants have substantial drawbacks such as poor atom economy, high cost, and the generation of undesirable byproducts. To address these difficulties, researchers reported an electrochemical approach based on anodic oxidation of Pd<sup>II</sup> that allows for selective C–O reductive elimination with multiple oxyanion-coupling partners. These reactions may lead to new disconnection approach that can be used in retrosynthetic studies. A reaction was carried out in an H-type split cell with platinum electrodes and a Nafion 117 membrane at 70 °C. There was 0.3 mmol of **69**, Pd(OAc)<sub>2</sub> (10 mol%), NaOAc (4 equiv), and 2 mL acetic acid in the anode compartment. There is NaOAc (2 equiv) and 1 mL acetic acid in the cathode compartment. This configuration separates two reactions, one at the anode and one at the cathode, each with its own set of conditions, generating monoacetoxyated product **70** (Scheme 48). After establishing optimal reaction conditions, researchers tested a series of oxime substrates with varying substitution patterns and functional groups to determine the scope of the Pd(II)-catalyzed C–H acetoxylation reaction. For example, a variety of oxime substrates with varied functional groups and substitution patterns to determine the range of the Pd(II)-catalyzed C–H acetoxylation reaction was tested. This acetoxylation process (**70a** and **70b**) was shown to work with a variety of oxime-directing groups. The reaction system (**70i–70k**) tolerated a range of functional groups, including OTBS, ester, chloro, amino, cyano, and acetoxy substituents. However, the oxime substrates **70l** having the acetoxy group on the inhibited side had a low yield. Aside from that, substrates with  $\alpha$ -hydrogen atom reacted more slowly and produced lower yields (**70m**). Fortunately, the C–H acetoxylation of oxazoline

Substrate Scope of Oximes<sup>d</sup>

<sup>a</sup>Isolated yield. <sup>b</sup>The yields in the parentheses use  $\text{NaNO}_3/\text{O}_2$  as an oxidant. <sup>c</sup>The reaction temperature is 100 °C. <sup>e</sup>The reaction temperature is 50 °C. <sup>f</sup>1.04 g (4.0 mmol) 1h is used under electrochemical oxidation.

Scope of Oxygen Nucleophiles<sup>a,b</sup>

<sup>a</sup>Isolated yield. <sup>b</sup>The corresponding carboxylic acids or sodium salts were used in lieu of HOAc and NaOAc in the anode. <sup>c</sup>The yields in the parentheses use  $\text{NaNO}_3/\text{O}_2$  as an oxidant.

**Scheme 48.** Electrochemical production of monoacetylated product **70**.

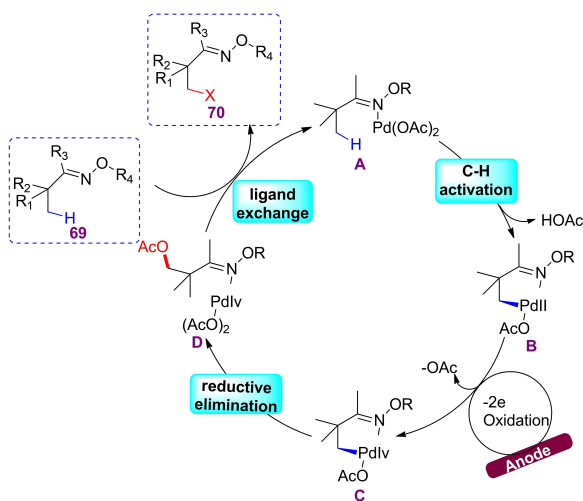
under standard circumstances was also successful, though the yield was slightly lower (**70n**). Additionally, electrolysis of 1.04 g (4.0 mmol) of substrate yielded **70f** in 84% yield, demonstrating the protocol's potential for synthetic synthesis. The  $\text{NaNO}_3/\text{O}_2$  oxidation system created by Sanford and colleagues had the best outcomes among the chemical oxidants.<sup>[257]</sup> While chemical oxidation produced higher yields with substrates containing the  $\alpha$ -H **70m**, anodic oxidation

obviously has an edge over it when it comes to producing monoacetylation products. In the reaction system, several oxygen anions were used. The generation of the acetylation product under the reaction conditions is mostly responsible for the reduced yields in these samples (**70ad**–**70af**). However, the success of these modifications illustrates clearly the potential applicability of this electrochemical oxidation strategy for permitting  $\text{C}(\text{sp}^3)\text{-H}$  functionalization with various reac-

tion partners. Anodic oxidation also produced higher yields than chemical oxidation ( $\text{NaNO}_3/\text{O}_2$ ) in all substrates.

The palladium catalyst first coordinates with a nitrogen atom in substrate **69**, bringing it near to the  $-\text{C}-\text{H}$  bond. Following that,  $\text{C}-\text{H}$  activation occurs to produce palladacycle **B**, which is the rate-limiting step in the catalytic cycle. At the anode, the resultant Pd complex **B** is immediately oxidized to create a Pd(III) or Pd(IV) species. Finally, reductive elimination from the high-valent palladium center yields palladium(II) product complex **D**, which may be ligand exchanged with a fresh substrate molecule to release the product and complete the catalytic cycle. Complex **D** can also produce another  $\text{C}-\text{H}$  activation/ $\text{C}-\text{O}$  bond formation cascade, resulting in a di or triacetoxylation product (Scheme 49).<sup>[218]</sup>

Das et al. reported the first electrochemical production of high-valent iron species from a TAML-ligated  $\text{Fe}^{\text{III}}-\text{OH}_2$  complex, as well as the application of this process to preparative electrochemical oxidation of organic molecules. Acetophenone **15** is produced in 79% yield by electrochemical oxidation of ethyl benzene **14** at 1250 mV under constant potential electrolysis conditions using **A**. When modified ethylbenzene derivatives were evaluated, the electron-rich and neutral derivatives performed well (**15a–15b**), whereas the extremely electron-deficient nitro-substituted derivative **15c** displayed decreased reactivity. There is no evidence of a tertiary  $\text{C}-\text{H}$  oxidation product as the reaction with isobutyl benzene occurs with great selectivity **15e**, exclusively occurring at the benzylic position. Comparably, in the reaction with the methyl ester of ibuprofen **15f**, no oxidation of the tertiary benzylic  $\text{C}-\text{H}$  position was seen, most likely due to both steric and electronic (i.e., electron-withdrawing ester) effects.



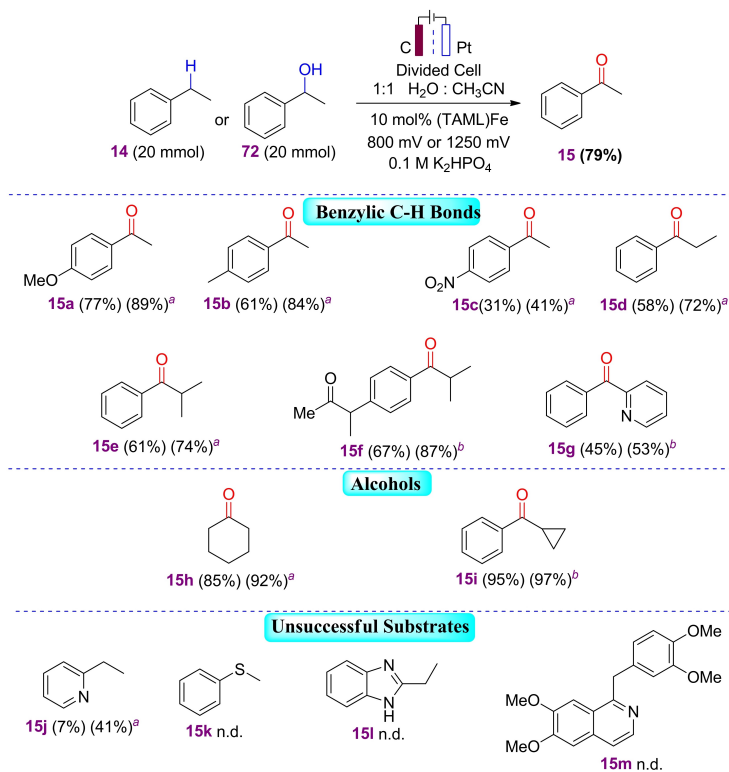
**Scheme 49.** Proposed mechanism for electrochemical production of mono-acetoxylated product **70**.

Although the less reactive 2-ethylpyridine substrate **15j** exhibits low conversion and yield, the reaction also exhibits some tolerance to a pyridine substituent **15g**. These complexes may decrease reactivity by coupling pyridine to  $\text{Fe}$ .<sup>[258]</sup> A small number of secondary alcohols were subjected to electrochemical oxidation, which was studied (Fig. 5B). Compared to benzylic  $\text{C}-\text{H}$  oxidation, this reaction is simpler, and high reactivity was observed with only a 5 mol% catalyst. Even though cyclohexanol is a straightforward substrate, the high yield obtained here (**15h**, 85%) is interesting because a recent electrochemical oxidation of cyclohexanol using a different molecular  $\text{Fe}$ -based catalyst resulted in mineralization of this substrate (i.e., the formation of  $\text{CO}_2$ ).<sup>[259]</sup> Under the electrolysis conditions, a more intriguing alcohol showed good to exceptional yield (**15i**). Electron-rich substrates **15k–15m**, are inefficient because they cannot undergo direct electron transfer.

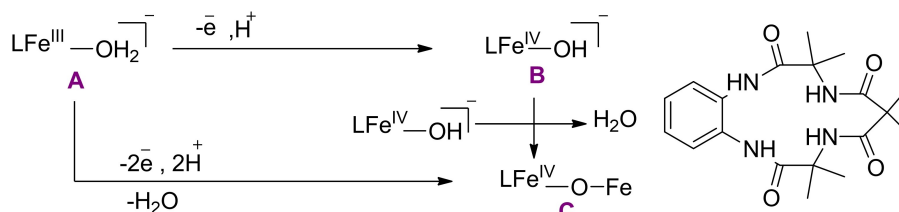
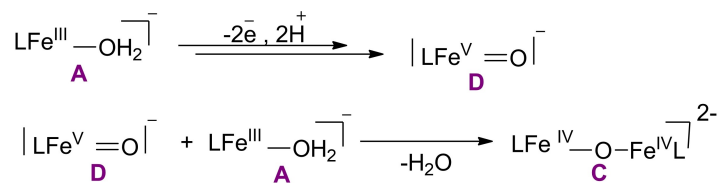
This electrocatalytic method lacks the reactivity of (TAML) $\text{Fe}$  and other catalysts using chemical oxidants.<sup>[260,261,262,263]</sup> The main constraint is the oxidative self-decomposition of the (TAML) $\text{Fe}$  catalyst during bulk electrolysis, which restricts its lifespan. The results summarized in scheme 50 provide a baseline for electrochemical oxidation of organic compounds, despite limitations. Although proton-coupled oxidation of metal-aqua complexes successfully generates transition-metal oxo species for water oxidation, it has not been shown to be effective for preparing electrochemical oxidation of organic compounds. This technique requires further research to complement the use of organic hydrogen-atom transfer (HAT) mediators such as *N*-hydroxyphthalimide<sup>[165,16,60,82]</sup> and nitrogen-centered radicals<sup>[148,35]</sup> in electrochemical oxidation of organic compounds.

Electrolysis was carried out at applied potentials of 800 and 1250 mV using a solution of **A** in 1:1  $\text{CH}_3\text{CN}:\text{H}_2\text{O}$  with  $\text{K}_2\text{HPO}_4$  (0.1 M). After 15 minutes of electrolysis at 800 mV, the spectrum data revealed that the  $\text{Fe}^{\text{III}}$  species **A** was transformed into the dimeric oxo-bridged iron (IV) complex **C**. The same spectrum modifications were obtained by electrolysis at a potential of 1250 mV, but with a more rapid formation of **C**. In a  $1\text{e}^-/1\text{H}^+$  process, electrochemical oxidation of **A** yield the  $[\text{Fe}^{\text{IV}}-\text{OH}]$  molecule **B**, and dimerization of **B** yields **C** (Scheme 51a). It has been established that the (TAML) $\text{Fe}^{\text{V}}(\text{O})$  species **D** rapidly reacts with **A** to form **C**. Complex **D** is not detectable directly under electrochemical circumstances, but it is expected to rapidly react with **A** in solution after being generated at the electrode to yield **C** (Scheme 51b).<sup>[38]</sup>

It was found that  $\text{Fe}_{30}\text{W}_{72}$ , an inorganic iron tungsten oxide capsule with a keplerate structure, is an efficient electrocatalyst for the cathodic activation of molecular oxygen in water, resulting in the oxidation of light alkanes and alkenes.



Scheme 50. Electrochemical production of ketone derivatives 15.

**a : 800 mV applied potential****b: 1250 mV applied potential**

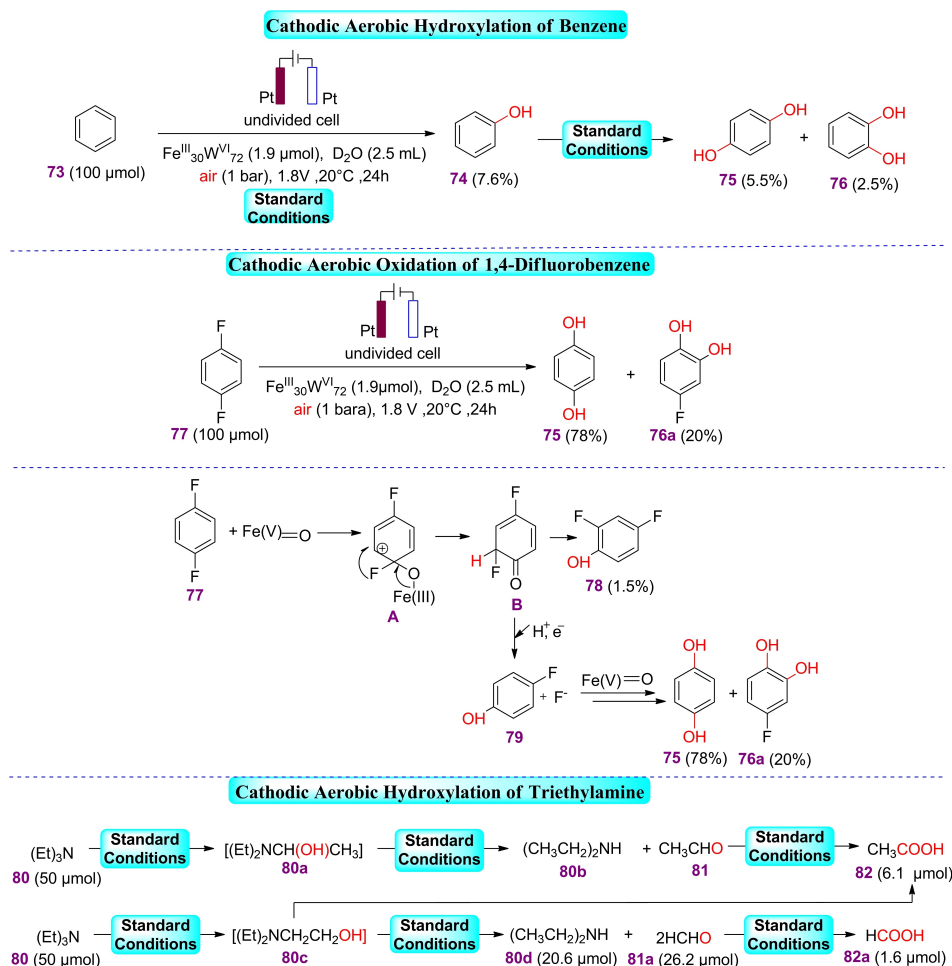
Scheme 51. Proposed mechanism for electrochemical production of ketone derivatives 15.

Heterolytic bond breakage of  $[(\text{Fe}^{\text{III}}\text{OOH})_{10}\text{Fe}^{\text{III}}_{20}\text{W}^{\text{VI}}_{72}]$  produces a Fe(V)-oxo species as shown in scheme 52. A platinum mesh cathode, a platinum wire anode, and a potential of 1.8 V were used in a reaction involving 1.9  $\mu\text{mol}$  of  $\text{Fe}^{\text{III}}_{30}\text{W}^{\text{VI}}_{72}$ , 2.5 mL of  $\text{D}_2\text{O}$ , air at 1 bar, 20 °C, and 24 hours. These are standard conditions.<sup>[264]</sup>

Alkane and alkene oxidation in water involved the efficient electrocatalytic activation of molecular oxygen using a fully inorganic iron-tungsten oxide capsule ( $\text{Fe}_{30}\text{W}_{72}$ ). This study investigated extensive reactivity, revealing processes like arene hydroxylation, alkyl C–H bond activation, dealkylation, desaturation, stereochemistry retention in cis-alkene epoxidation, and unique regioselectivity in ketones, alcohols, and carboxylic acids oxidation. These findings showed that the active intermediate in cathodic aerobic oxidation reactions is a compound I-type oxidant, and they placed  $\text{Fe}_{30}\text{W}_{72}$  as an inorganic functional analog of iron-based monooxygenases.<sup>[264]</sup>

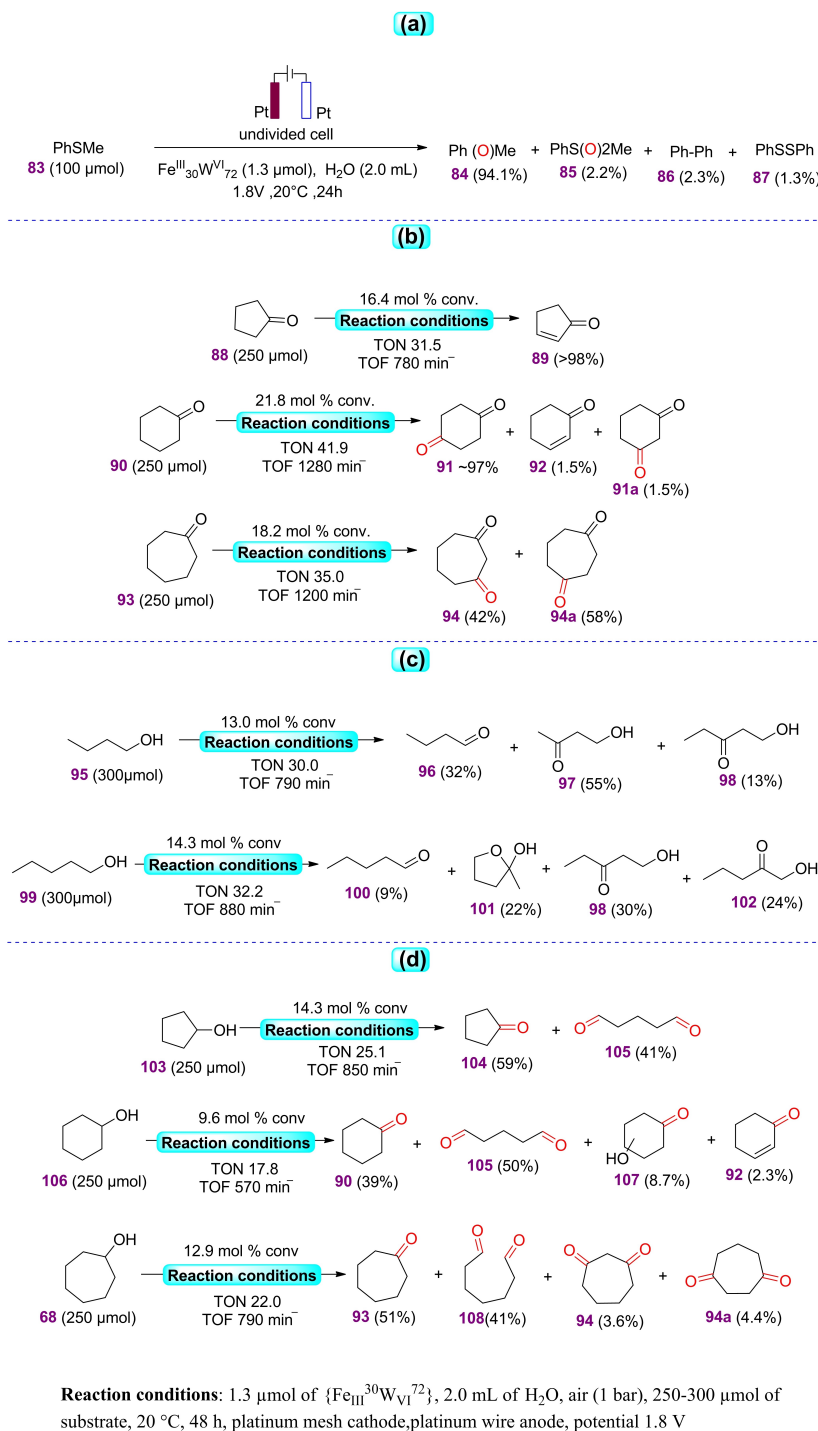
The oxidation of thioanisole **83** was also investigated to contrast S-dealkylation and S-oxidation (Scheme 53). Here, it is obvious that S-oxidation is the favored reaction because S-dealkylation products are formed in very little amounts. For a number of new functionalized molecules,  $\alpha$ -C–H bond activation and oxygenation were investigated. The predominant product (> 98%) for cyclopentanone **88** in the case of cyclic ketones is cyclopent-2-en-1-one **89**. In contrast, despite the fact that the bond dissociation energy of C–H bond to the ketone is substantially lower, no appreciable oxygenation at the carbon atom next to the ketone occurred for cyclohexanone **90** or cycloheptanone **93**. Particularly persuasive is the extremely high selectivity observed for the synthesis of 1,4-cyclohexanedione **91** from cyclohexanone **90**.

Certain cyclic alcohols can give related ketones on oxidation, considering that the bond dissociation energy of  $\alpha$ -C–H bond in a linear primary alcohol is about 5 kcal/mol weaker than the corresponding  $\beta$ -C–H bond,<sup>[265]</sup> and the



**Scheme 52.** Reductive Electrochemical Activation of Molecular Oxygen Catalyzed by an Iron-Tungstate Oxide Capsule.





**Scheme 53.** a) Cathodic Aerobic Oxidation of Thioanisole **83**; b) Cathodic Aerobic Oxidation of Cyclic Ketones (**88**, **90**, and **93**); c) Cathodic Aerobic Oxidation of Linear Alcohols (**95** and **99**); d) Cathodic Aerobic Oxidation of cyclic Alcohols (**103**, **106** and **108**).

observation that the reactivity of cyclohexanol **106** with a *t*-butylperoxy radical favors the reaction at the  $\alpha$ -C–H bond versus  $\beta$ -C–H bond by 3 orders of magnitude.<sup>[266]</sup> Unexpected-

ly, cyclic alcohols were only selectively oxidized at the  $\alpha$ -C–H bond with a selectivity of between 50% and 60%. Additionally, the  $\beta$ -C–H bond underwent substantial oxida-

tion (40–50%) to produce the  $\alpha,\omega$ -dialdehyde **105** extremely selectively. Only 4-hydroxybutanal, which in  $D_2O$  showed as a combination of the acyclic product and the intramolecular hemiacetal lactol, was produced by the oxidation of 1,4-butanediol. Therefore, it is feasible that in these “ $Fe^{III}_{30}W^{VI}_{72}$ ” catalyzed processes, the production of hydrates and hemiacetals stabilizes aldehydes for further oxidation. In contrast to what happened with the cyclic alcohols, 1,4-butanediol only underwent a reaction at the  $\alpha$ -C–H bond. As a result, examined the reactivity of linear primary alcohols as well.

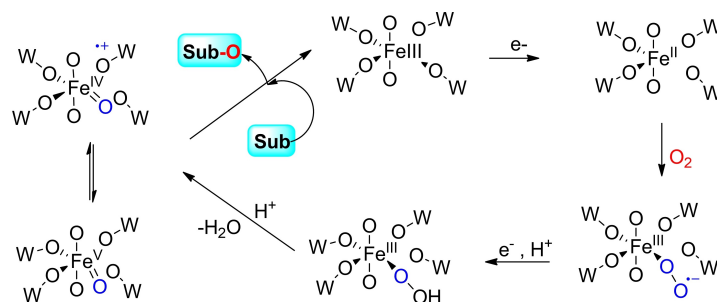
Mechanistic studies in scheme 54 reveal high-valent  $Fe(V)=O$  and the formally isoelectronic  $Fe(IV)=O$  porphyrin cation radical intermediates as active species in alkane and arene hydroxylation and alkene epoxidation reactions, often using “shunt” pathways.  $Fe^{III}_{30}W^{VI}_{72}$  has a high catalytic activity under cathodic aerobic circumstances, which motivates researchers to investigate potential active species that might be responsible for reactivity. Scheme 54 displays a similar working hypothesis for a monoiron catalytic cycle based on a standard iron-porphyrin catalytic cycle.

The selective oxidation of light hydrocarbons and their degradation using only dioxygen ( $O_2$ ) are significant steps towards the development of efficient chemical processes. An iron tungsten oxide inorganic molecular catalyst with a capsular structure stabilized inside by sulfate/bisulfate anions provides a protic environment with three iron atoms located at each of the capsule's pores, resulting in a unique and potent active site for the oxidation reactions. Researchers demonstrated the low-pressure (12 bar) hydroxylation of alkanes, especially ethane to acetic acid, and the ozone like cleavage of alkene C=C bonds at mild electrochemical conditions, 1.8 V in water at ambient temperature, using  $O_2$  from air. These findings allowed cathodic aerobic oxidation of light hydrocarbons in water utilizing air at low pressure and temperature. An iron tungsten oxide catalyst ( $Fe_{30}W_{72}$ ) molecular capsule catalyzes the reaction, resulting in a powerful oxidizing species. The oxidation of ethane to acetic acid has remarkable selectivity, addressing its underutilization. For catalytic trans-

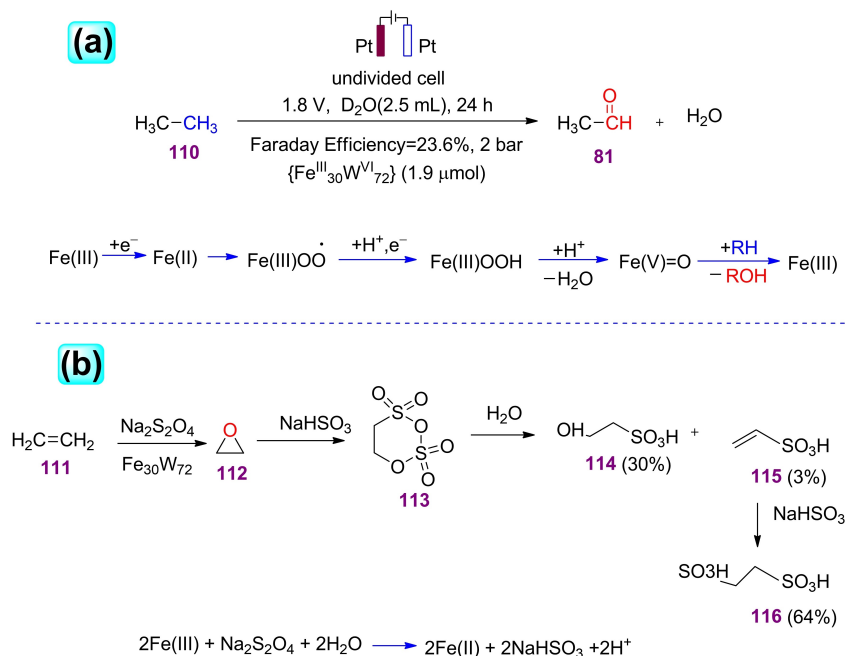
formations, electrocatalytic processes at 1.8 V offer sustainable options that could be powered by solar energy.<sup>[267]</sup> The crystal structure of  $Fe^{III}_{30}W^{VI}_{72}$  with Fe–Fe distances of around 6 suggests a mono-iron active species. Although the product of ethane **110** are commensurate with an iron-oxo active species as in scheme 55a, the signature formation of an epoxide in the oxygenation of ethane **111** and propene was not observed in the electrocatalytic reaction. In order to support the initial formation of an epoxide product **112**, a similar reaction was carried out with dithionite as a reducing agent using scheme 55b. This electrochemical process is useful to convert a simple gas called ethane (usually wasted by burning it) into a useful chemical called acetic acid powered by solar energy, which is great for the environment and can be a good alternative to current methods.<sup>[267]</sup>

#### 4. Conclusion and Future Perspectives

One advantage of electrosynthesis is that it is environmentally friendly. The use of organic electrosynthesis should be encouraged by a number of reasons from the standpoint of practical application. For example, in the absence of external oxidants or reductants, electrochemical processes often exhibit considerable functional group tolerance. In contrast to conventional processes, which generally continue at elevated temperatures or pressure, electrochemical reactions are typically carried out in milder settings, providing an energy-saving alternative. Electrochemical processes often have short reaction times because of their high reaction efficiency. By adjusting the current, the reaction time can be decreased even more. By altering the voltage or current, it is possible to vary the electrochemical technique's capacity for oxidation or reduction, opening up operations that are not conceivable with chemical oxidants or reductants. In contrast to traditional reactions, which often need quenching, electrochemical processes can be easily stopped at any time by switching the power switch. The bulk of electrochemical reactions can be easily



**Scheme 54.** Possible catalytic cycle or hypothesis for cathodic activation of  $O_2$  and oxygenation. The electron distribution for the active species is unknown. The presentation of  $Fe(V)=O$  versus  $Fe(IV)-O^{\bullet+}$  is a formalism. Other reactive intermediates can also be considered.



**Scheme 55.** Electrochemical production of aldehyde **81** and epoxide **112**.

scaled up and have a ton of potential for commercial applications, which is a final point worth mentioning.<sup>[268]</sup>

A possible method for mild-conditions activation of inert C–H/C–C bonds is electrochemical oxidation. Such electrochemical methods can be divided into direct and indirect types. Due to unintentional over-oxidation of the product, direct selective oxidation is particularly challenging. A variety of challenging oxidative processes have also been carried out selectively using water, air, visible light, transition metal catalysts, or mediators. Electrophotocatalysis (EPC), which induces reactions using both electrochemical and photochemical energy. Due to the excellent modulation of reaction selectivity and the high functional group tolerance, transition metal catalysis has emerged as one of the most important mechanisms for selectivity control in modern synthetic chemistry. In chemical syntheses, oxidative C–H activation has become an increasingly potent technique. The overall sustainability of the C–H activation method is compromised despite significant advancements toward atom and step economies since these transformations heavily rely on precious metal catalysts and stoichiometric concentrations of hazardous metal oxidants. Utilizing electro-oxidation instead of reactive chemical oxidants, on the other hand, allows efficient use of renewable energies from sustainable sources for the creation of chemical bonds and eliminates the formation of unwanted waste through oxidant economy.<sup>[269]</sup>

In this study, we have also established electrochemical techniques for initiating inert C–C bonds at ambient pressure

and temperature. We demonstrated the existence of a mediator that starts HAT reactions with C–H bond. The C–C bonds were broken by the mediated oxidation method. The facilitated oxidation strategies show how electrocatalysis can be used to activate chemical bonds that are inert in low-stress situations. This discovery paves the way for the use of specific redox mediators and renewable power to accelerate difficult chemical transformations because of the diversity of redox mediators. Choosing a solvent for electrosynthesis can occasionally be difficult because poorly conductive solvents like tetrahydrofuran, toluene, etc. must typically be employed to aid the transfer of electrons in solution. Because the majority of metal cations are easily reduced to zero-valent metals at the cathode and expensive ion exchange membranes are needed to separate the anode and cathode when electrochemical reactions are conducted in divided cells, the use of metal catalysts in electrochemical reactions under readily accessible undivided cells is relatively limited. Modern method for chemically recycling commercial plastics and workable C–C/H bond oxygenation pathways for industrial scale-up are covered in this review.

In order to increase the conversion and product selectivity, future research will concentrate on functionalizing the redox mediator to increase its stability. Furthermore, techniques used to immobilize redox mediators onto a support or to create heterogeneous mediators will lessen the redox mediators' tendency to self-degrade and will make the procedures of product separation and purification easier, especially for large-

scale applications. Additionally, a flow electrochemical cell with high volumes and electrode surface areas can be devised in order to practically scale up the oxidation method.<sup>[270]</sup>

Electrochemical generation of high-valent iron species and their utilization in selective oxidation reactions open doors to more sustainable and versatile synthetic processes. Addressing the challenges of catalyst stability and functional group compatibility underlines the exciting future prospects for this research, with potential implications in the development of greener and more efficient chemical transformations.<sup>[38]</sup>

The electrocatalytic reactions observed at 1.8 V, with the potential for using solar energy as a driving force for catalytic transformations, hold tremendous promise for sustainability. Utilizing renewable energy sources for catalytic reactions is a forward-looking approach that aligns with the global shift towards clean and green technologies. Future research could focus on optimizing and scaling up these electrocatalytic processes to make them viable alternatives to current energy-intensive technologies.<sup>[267]</sup> The electrochemistry-driven aerobic cleavage of indoles represents a sustainable, scalable, and metal-free approach with significant potential for synthetic chemistry.<sup>[94]</sup> Future research endeavors will help refine and expand the utility of this method, making it a valuable tool for chemists seeking efficient and environmentally friendly synthetic routes.

The electrochemical process for C–H bond oxidation is a game-changing innovation in synthetic chemistry. Its simplicity, affordability, compatibility with diverse functional groups, and scalability make it a powerful tool for organic synthesis and industrial applications.<sup>[35]</sup> The future holds exciting possibilities for the refinement and expansion of this method, promising to drive advancements in the field of chemical synthesis and material science.

### Acknowledgements

Support from Cardiff University to Dr. Nisar Ahmed is gratefully acknowledged.

### References

- [1] M. Yan, Y. Kawamata, P. S. Baran, *Chem. Rev.* **2017**, *117*, 13230–13319.
- [2] Y. Jiang, K. Xu, C. Zeng, *Chem. Rev.* **2017**, *118*, 4485–4540.
- [3] K. D. Moeller, *Chem. Rev.* **2018**, *118*, 4817–4833.
- [4] P. Xiong, H.-C. Xu, *Acc. Chem. Res.* **2019**, *52*, 3339–3350.
- [5] J. C. Siu, N. Fu, S. Lin, *Acc. Chem. Res.* **2020**, *53*, 547–560.
- [6] F. Wang, S. S. Stahl, *Acc. Chem. Res.* **2020**, *53*, 561–574.
- [7] C. Zhu, N. W. Ang, T. H. Meyer, Y. Qiu, L. Ackermann, *ACS Cent. Sci.* **2021**, *7*, 415–431.
- [8] E. C. McKenzie, S. Hosseini, A. G. C. Petro, K. K. Rudman, B. H. Gerroll, M. S. Mubarak, L. A. Baker, R. D. Little, *Chem. Rev.* **2021**, *122*, 3292–3335.
- [9] X. Cheng, A. Lei, T.-S. Mei, H.-C. Xu, K. Xu, C. Zeng, *CCS Chem.* **2022**, *4*, 1120–1152.
- [10] E. J. Horn, B. R. Rosen, P. S. Baran, *ACS Cent. Sci.* **2016**, *2*, 302–308.
- [11] R. Francke, R. D. Little, *Chem. Soc. Rev.* **2014**, *43*, 2492–2521.
- [12] J.-i. Yoshida, K. Kataoka, R. Horcajada, A. Nagaki, *Chem. Rev.* **2008**, *108*, 2265–2299.
- [13] A. Jutand, *Chem. Rev.* **2008**, *108*, 2300–2347.
- [14] C. Li, Y. Kawamata, H. Nakamura, J. C. Vantourout, Z. Liu, Q. Hou, D. Bao, J. T. Starr, J. Chen, M. Yan, *Angew. Chem.* **2017**, *129*, 13268–13273.
- [15] A. Badalyan, S. S. Stahl, *Nature* **2016**, *535*, 406–410.
- [16] D. P. Hruszkewycz, K. C. Miles, O. R. Thiel, S. S. Stahl, *Chem. Sci.* **2017**, *8*, 1282–1287.
- [17] P. Xiong, H.-B. Zhao, X.-T. Fan, L.-H. Jie, H. Long, P. Xu, Z.-J. Liu, Z.-J. Wu, J. Cheng, H.-C. Xu, *Nat. Commun.* **2020**, *11*, 2706.
- [18] S. Zhang, Y. Li, T. Wang, M. Li, L. Wen, W. Guo, *Org. Lett.* **2022**, *24*, 1742–1746.
- [19] Z. Li, Y. Zhang, K. Li, Z. Zhou, Z. Zha, Z. Wang, *Sci. China Chem.* **2021**, *64*, 2134–2141.
- [20] Z.-W. Hou, M.-M. Zhang, W.-C. Yang, L. Wang, *J. Org. Chem.* **2022**, *87*, 7806–7817.
- [21] C.-Y. Cai, X.-L. Lai, Y. Wang, H.-H. Hu, J. Song, Y. Yang, C. Wang, H.-C. Xu, *Nat. Catal.* **2022**, *5*, 943–951.
- [22] G. Yang, Y. Ma, J. Xu, *J. Am. Chem. Soc.* **2004**, *126*, 10542–10543.
- [23] R. A. Tomas, J. o. C. Bordado, J. F. Gomes, *Chem. Rev.* **2013**, *113*, 7421–7469.
- [24] K. Chen, P. Zhang, Y. Wang, H. Li, *Green Chem.* **2014**, *16*, 2344–2374.
- [25] D. I. Enache, J. K. Edwards, P. Landon, B. Solsona-Espriu, A. F. Carley, A. A. Herzing, M. Watanabe, C. J. Kiely, D. W. Knight, G. J. Hutchings, *Science* **2006**, *311*, 362–365.
- [26] B. P. Hereijgers, B. M. Weckhuysen, *J. Catal.* **2010**, *270*, 16–25.
- [27] Y. Zhang, W. Schilling, S. Das, *ChemSusChem* **2019**, *12*, 2898–2910.
- [28] U. Schuchardt, D. Cardoso, R. Sercheli, R. Pereira, R. S. Da Cruz, M. C. Guerreiro, D. Mandelli, E. V. Spinacé, E. L. Pires, *Appl. Catal. A* **2001**, *211*, 1–17.
- [29] Z. Guo, B. Liu, Q. Zhang, W. Deng, Y. Wang, Y. Yang, *Chem. Soc. Rev.* **2014**, *43*, 3480–3524.
- [30] A. K. Suresh, M. M. Sharma, T. Sridhar, *Ind. Eng. Chem. Res.* **2000**, *39*, 3958–3997.
- [31] A. N. Campbell, S. S. Stahl, *Acc. Chem. Res.* **2012**, *45*, 851–863.
- [32] K. Nair, D. P. Sawant, G. Shanbhag, S. Halligudi, *Catal. Commun.* **2004**, *5*, 9–13.
- [33] H. Huang, X. Ji, W. Wu, H. Jiang, *Chem. Soc. Rev.* **2015**, *44*, 1155–1171.
- [34] M. D. Kärkäs, *Chem. Soc. Rev.* **2018**, *47*, 5786–5865.

- [35] Y. Kawamata, M. Yan, Z. Liu, D.-H. Bao, J. Chen, J. T. Starr, P. S. Baran, *J. Am. Chem. Soc.* **2017**, *139*, 7448–7451.
- [36] B. You, X. Liu, N. Jiang, Y. Sun, *J. Am. Chem. Soc.* **2016**, *138*, 13639–13646.
- [37] Y. Mo, K. F. Jensen, *Chem. Eur. J.* **2018**, *24*, 10260–10265.
- [38] A. Das, J. E. Nutting, S. S. Stahl, *Chem. Sci.* **2019**, *10*, 7542–7548.
- [39] J. Zheng, X. Chen, X. Zhong, S. Li, T. Liu, G. Zhuang, X. Li, S. Deng, D. Mei, J. G. Wang, *Adv. Funct. Mater.* **2017**, *27*, 1704169.
- [40] W. Liu, W. You, Y. Gong, Y. Deng, *Energy Environ. Sci.* **2020**, *13*, 917–927.
- [41] Y. Adeli, K. Huang, Y. Liang, Y. Jiang, J. Liu, S. Song, C.-C. Zeng, N. Jiao, *ACS Catal.* **2019**, *9*, 2063–2067.
- [42] F. N. Khan, R. Jayakumar, C. Pillai, *J. Mol. Catal. A* **2003**, *195*, 139–145.
- [43] M. Rafiee, M. Alherech, S. D. Karlen, S. S. Stahl, *J. Am. Chem. Soc.* **2019**, *141*, 15266–15276.
- [44] D. Zollinger, U. Griesbach, H. Pütter, C. Comninellis, *Electrochem. Commun.* **2004**, *6*, 605–608.
- [45] S.-H. Shi, Y. Liang, N. Jiao, *Chem. Rev.* **2020**, *121*, 485–505.
- [46] C. J. Allpress, L. M. Berreau, *Coord. Chem. Rev.* **2013**, *257*, 3005–3029.
- [47] J. Zakzeski, P. C. Bruijninx, A. L. Jongerius, B. M. Weckhuysen, *Chem. Rev.* **2010**, *110*, 3552–3599.
- [48] A. J. Martín, C. Mondelli, S. D. Jaydev, J. Perez-Ramirez, *Chem* **2021**, *7*, 1487–1533.
- [49] A. Rahimi, J. M. García, *Nat. Chem. Rev.* **2017**, *1*, 0046.
- [50] I. Vollmer, M. Jenks, M. Roelands, R. White, T. van Harmelen, P. de Wild, *Angew. Chem. Int. Ed.* **2020**, *59*, 15402–15423.
- [51] L. D. Ellis, N. A. Rorrer, K. P. Sullivan, M. Otto, J. E. McGeehan, Y. Román-Leshkov, N. Wierckx, G. T. Beckham, *Nat. Catal.* **2021**, *4*, 539–556.
- [52] J. E. Rorrer, G. T. Beckham, Y. Román-Leshkov, *JACS Au* **2020**, *1*, 8–12.
- [53] D. M. Wiles, G. Scott, *Polym. Degrad. Stab.* **2006**, *91*, 1581–1592.
- [54] C.-H. Jun, *Chem. Soc. Rev.* **2004**, *33*, 610–618.
- [55] B. Yan, C. Shi, G. T. Beckham, E. Y.-X. Chen, Y. Román-Leshkov, *ACS Sustainable Chem. Eng.* **2021**, *9*, 623–628.
- [56] P. Sivaguru, Z. Wang, G. Zanoni, X. Bi, *Chem. Soc. Rev. Chemical Society Reviews* **2019**, *48*, 2615–2656.
- [57] T. Kondo, T.-a. Mitsudo, *Chem. Lett.* **2005**, *34*, 1462–1467.
- [58] Y. Terao, H. Wakui, T. Satoh, M. Miura, M. Nomura, *J. Am. Chem. Soc.* **2001**, *123*, 10407–10408.
- [59] B. Rybtchinski, D. Milstein, *Angew. Chem.* **1999**, *111*, 918–932.
- [60] J. E. Nutting, M. Rafiee, S. S. Stahl, *Chem. Rev.* **2018**, *118*, 4834–4885.
- [61] T. Xu, A. Dermenci, G. Dong, In *Top. Curr. Chem.* **2014**, *346*, 233–257, Springer Berlin, Germany.
- [62] D.-S. Kim, W.-J. Park, C.-H. Jun, *Chem. Rev.* **2017**, *117*, 8977–9015.
- [63] G. Fumagalli, S. Stanton, J. F. Bower, *Chem. Rev.* **2017**, *117*, 9404–9432.
- [64] F. Song, T. Gou, B.-Q. Wang, Z.-J. Shi, *Chem. Soc. Rev.* **2018**, *47*, 7078–7115.
- [65] B. Wang, M. A. Perea, R. Sarpong, *Angew. Chem. Int. Ed.* **2020**, *59*, 18898–18919.
- [66] P.-F. Dai, H. Wang, X.-C. Cui, J.-P. Qu, Y.-B. Kang, *Org. Chem. Front.* **2020**, *7*, 896–904.
- [67] X.-Y. Yu, J.-R. Chen, W.-J. Xiao, *Chem. Rev.* **2020**, *121*, 506–561.
- [68] J. Wang, S. A. Blaszczyk, X. Li, W. Tang, *Chem. Rev.* **2020**, *121*, 110–139.
- [69] M. Murakami, N. Ishida, *Chem. Rev. s* **2020**, *121*, 264–299.
- [70] S. Gazi, M. Đokić, K. F. Chin, P. R. Ng, H. S. Soo, *Adv. Sci.* **2019**, *6*, 1902020.
- [71] S. Caron, R. W. Dugger, S. G. Ruggeri, J. A. Ragan, D. H. B. Ripin, *Chem. Rev.* **2006**, *106*, 2943–2989.
- [72] Y. Liang, J. Wei, X. Qiu, N. Jiao, *Chem. Rev.* **2018**, *118*, 4912–4945.
- [73] H. Sterckx, B. Morel, B. U. Maes, *Angew. Chem. Int. Ed.* **2019**, *58*, 7946–7970.
- [74] J. Zhao, T. Nanjo, E. C. de Lucca Jr, M. C. White, *Nat. Chem.* **2019**, *11*, 213–221.
- [75] J. B. Zimmerman, P. T. Anastas, H. C. Erythropel, W. Leitner, *Science* **2020**, *367*, 397–400.
- [76] T. Dalton, T. Faber, F. Glorius, *ACS Cent. Sci.* **2021**, *7*, 245–261.
- [77] B. Cornils, W. A. Herrmann, M. Beller, R. Paciello, *Applied homogeneous catalysis with organometallic compounds: a comprehensive handbook in four volumes*. Editor, John Wiley & Sons, **2017**, Vol. 4.
- [78] R. Irie, *Compr. Chirality* **2012**, 36–68.
- [79] L. Que Jr, W. B. Tolman, *Nature* **2008**, *455*, 333–340.
- [80] M. S. Chen, M. C. White, *ChemInform* **2008**, *39*.
- [81] M. S. Chen, M. C. White, *Science* **2010**, *327*, 566–571.
- [82] E. J. Horn, B. R. Rosen, Y. Chen, J. Tang, K. Chen, M. D. Eastgate, P. S. Baran, *Nature* **2016**, *533*, 77–81.
- [83] H. Huang, K. A. Steiniger, T. H. Lambert, *J. Am. Chem. Soc.* **2022**, *144*, 12567–12583.
- [84] C. J. Paddon, P. J. Westfall, D. J. Pitera, K. Benjamin, K. Fisher, D. McPhee, M. Leavell, A. Tai, A. Main, D. Eng, *Nature* **2013**, *496*, 528–532.
- [85] M. C. White, J. Zhao, *J. Am. Chem. Soc.* **2018**, *140*, 13988–14009.
- [86] X. Huang, J. T. Groves, *JBIC J. Biol. Inorg. Chem.* **2017**, *22*, 185–207.
- [87] T. Shen, Y.-L. Li, K.-Y. Ye, T. H. Lambert, *Nature* **2023**, *614*, 275–280.
- [88] S. Das, C. D. Incarvito, R. H. Crabtree, G. W. Brudvig, *Science* **2006**, *312*, 1941–1943.
- [89] G. Hilt, *ChemElectroChem* **2020**, *7*, 395–405.
- [90] C. Schotten, T. P. Nicholls, R. A. Bourne, N. Kapur, B. N. Nguyen, C. E. Willans, *Green Chem.* **2020**, *22*, 3358–3375.
- [91] X. Li, F. Bai, C. Liu, X. Ma, C. Gu, B. Dai, *Org. Lett.* **2021**, *23*, 7445–7449.
- [92] S. Tang, S. Wang, D. Zhang, X. Zhang, G. Yang, Y. Wang, Y. Qiu, *Chin. Chem. Lett.* **2023**, 108660.
- [93] Y. Sun, X. Li, M. Yang, W. Xu, J. Xie, M. Ding, *Green Chem.* **2020**, *22*, 7543–7551.

- [94] J. Wu, Z. Peng, T. Shen, Z. Q. Liu, *Adv. Synth. Catal.* **2022**, *364*, 2565–2570.
- [95] J. Genovino, S. Lütz, D. Sames, B. B. Touré, *J. Am. Chem. Soc.* **2013**, *135*, 12346–12352.
- [96] Y.-D. Du, C.-W. Tse, Z.-J. Xu, Y. Liu, C.-M. Che, *Chem. Commun.* **2014**, *50*, 12669–12672.
- [97] S. Nakai, T. Yatabe, K. Suzuki, Y. Sasano, Y. Iwabuchi, J. Y. Hasegawa, N. Mizuno, K. Yamaguchi, *Angew. Chem. Int. Ed.* **2019**, *58*, 16651–16659.
- [98] Y. Liu, Y. Yan, D. Xue, Z. Wang, J. Xiao, C. Wang, *ChemCatChem* **2020**, *12*, 2221–2225.
- [99] S. Yang, P. Li, Z. Wang, L. Wang, *Org. Lett.* **2017**, *19*, 3386–3389.
- [100] W. Ji, P. Li, S. Yang, L. Wang, *Chem. Commun.* **2017**, *53*, 8482–8485.
- [101] Y. Zhang, D. Riemer, W. Schilling, J. Kollmann, S. Das, *ACS Catal.* **2018**, *8*, 6659–6664.
- [102] J. Zhou, S. Wang, W. Duan, Q. Lian, W. Wei, *Green Chem.* **2021**, *23*, 3261–3267.
- [103] M. J. P. Mandigma, J. Žurauskas, C. I. MacGregor, L. J. Edwards, A. Shahin, L. d'Heureuse, P. Yip, D. J. Birch, T. Gruber, J. Heilmann, *Chem. Sci.* **2022**, *13*, 1912–1924.
- [104] P. Lian, R. Li, L. Wang, X. Wan, Z. Xiang, X. Wan, *Org. Chem. Front.* **2022**, *9*, 4924–4931.
- [105] E. Tsurumaki, S. Saito, K. S. Kim, J. M. Lim, Y. Inokuma, D. Kim, A. Osuka, *J. Am. Chem. Soc.* **2008**, *130*, 438–439.
- [106] P. Liu, P. Neuhaus, D. V. Kondratuk, T. S. Balaban, H. L. Anderson, *Angew. Chem. Int. Ed.* **2014**, *53*, 7770–7773.
- [107] R. B. Teponno, S. Kusari, M. Spittler, *Nat. Prod. Rep.* **2016**, *33*, 1044–1092.
- [108] Q. Li, C. Batchelor-McAuley, N. S. Lawrence, R. S. Hartshorne, R. G. Compton, *J. Electroanal. Chem.* **2013**, *688*, 328–335.
- [109] Y. Imada, Y. Okada, K. Noguchi, K. Chiba, *Angew. Chem. Int. Ed.* **2019**, *58*, 125–129.
- [110] G. Landelle, A. Panossian, F. R. Leroux, *Curr. Top. Med. Chem.* **2014**, *14*, 941–951.
- [111] P. Bhutani, G. Joshi, N. Raja, N. Bachhav, P. K. Rajanna, H. Bhutani, A. T. Paul, R. Kumar, *J. Med. Chem.* **2021**, *64*, 2339–2381.
- [112] C. B. Burness, *Drugs* **2015**, *75*, 1559–1566.
- [113] K. M. Nelson, *PhD diss., University of Minnesota* **2013**.
- [114] R. Singh, U. Manjunatha, H. I. Boshoff, Y. H. Ha, P. Niyomrattanakit, R. Ledwidge, C. S. Dowd, I. Y. Lee, P. Kim, L. Zhang, S. Kang, *Science* **2008**, *322*, 1392–1395.
- [115] J. Qiao, Y.-S. Li, R. Zeng, F.-L. Liu, R.-H. Luo, C. Huang, Y.-F. Wang, J. Zhang, B. Quan, C. Shen, *Science* **2021**, *371*, 1374–1378.
- [116] H. Sawada, *Chem. Rev.* **1996**, *96*, 1779–1808.
- [117] Y. Zheng, Z. J. Wang, Z. P. Ye, K. Tang, Z. Z. Xie, J. A. Xiao, H. Y. Xiang, K. Chen, X. Q. Chen, H. Yang, *Angew. Chem. Int. Ed.* **2022**, *61*, e202212292.
- [118] M. Dörr, J. L. Röckl, J. Rein, D. Schollmeyer, S. R. Waldvogel, *Chem. Eur. J.* **2020**, *26*, 10195–10198.
- [119] Y. Ouyang, X. H. Xu, F. L. Qing, *Angew. Chem. Int. Ed.* **2022**, *61*, e202114048.
- [120] W. Zheng, J. W. Lee, C. A. Morales-Rivera, P. Liu, M. Y. Ngai, *Angew. Chem. Int. Ed.* **2018**, *57*, 13795–13799.
- [121] J. W. Lee, S. Lim, D. N. Maienshein, P. Liu, M. Y. Ngai, *Angew. Chem.* **2020**, *132*, 21659–21664.
- [122] B. J. Jelier, P. F. Tripet, E. Pietrasiak, I. Franzoni, G. Jeschke, A. Togni, *Angew. Chem. Int. Ed.* **2018**, *57*, 13784–13789.
- [123] T. Duhaill, T. Bortolato, J. Mateos, E. Anselmi, B. Jelier, A. Togni, E. Magnier, G. Dagousset, L. Dell'Amico, *Org. Lett.* **2021**, *23*, 7088–7093.
- [124] J. Rong, L. Deng, P. Tan, C. Ni, Y. Gu, J. Hu, *Angew. Chem. Int. Ed.* **2016**, *55*, 2743–2747.
- [125] V. Saheb, M. Javanmardi, *J. Fluorine Chem.* **2018**, *211*, 154–158.
- [126] M. A. Burgos Paci, G. A. Argüello, *Chem. Eur. J.* **2004**, *10*, 1838–1844.
- [127] M.-J. Luo, W. Zhou, R. Yang, H. Ding, X.-R. Song, Q. Xiao, *Org. Biomol. Chem.* **2023**, *21*, 2917–2921.
- [128] Z. Li, C. Liu, W. Geng, J. Dong, Y. Chi, C. Hu, *Chem. Commun.* **2021**, *57*, 7430–7433.
- [129] M. A. Drahl, M. Manpadi, L. J. Williams, *Angew. Chem. Int. Ed.* **2013**, *52*, 11222–11251.
- [130] F. Chen, T. Wang, N. Jiao, *Chem. Rev.* **2014**, *114*, 8613–8661.
- [131] P.-h. Chen, B. A. Billett, T. Tsukamoto, G. Dong, *ACS Catal.* **2017**, *7*, 1340–1360.
- [132] C. T. To, K. S. Chan, *Acc. Chem. Res.* **2017**, *50*, 1702–1711.
- [133] X. Wu, C. Zhu, *Acc. Chem. Res.* **2020**, *53*, 1620–1636.
- [134] T. R. McDonald, L. R. Mills, M. S. West, S. A. Rousseaux, *Chem. Rev.* **2020**, *121*, 3–79.
- [135] M. D. Lutz, B. Morandi, *Chem. Rev.* **2020**, *121*, 300–326.
- [136] M. Iwakubo, A. Takami, Y. Okada, T. Kawata, Y. Tagami, H. Ohashi, M. Sato, T. Sugiyama, K. Fukushima, H. Iijima, *Bioorg. Med. Chem.* **2007**, *15*, 350–364.
- [137] T. Shen, S. Liu, J. Zhao, N. Wang, L. Yang, J. Wu, X. Shen, Z.-Q. Liu, *J. Org. Chem.* **2022**, *87*, 3286–3295.
- [138] W. Zhuang, J. Zhang, C. Ma, J. S. Wright, X. Zhang, S.-F. Ni, Q. Huang, *Org. Lett.* **2022**, *24*, 4229–4233.
- [139] J.-C. Moutet, G. Reverdy, *Journal of the Chemical Society, Chem. Commun.* **1982**, 654–655.
- [140] R. Scheffold, R. Orlinski, *J. Am. Chem. Soc.* **1983**, *105*, 7200–7202.
- [141] J. P. Barham, B. König, *Angew. Chem. Int. Ed.* **2020**, *59*, 11732–11747.
- [142] H. Huang, Z. M. Strater, M. Rauch, J. Shee, T. J. Sisto, C. Nuckolls, T. H. Lambert, *Angew. Chem. Int. Ed.* **2019**, *58*, 13318–13322.
- [143] H. Huang, Z. M. Strater, T. H. Lambert, *J. Am. Chem. Soc.* **2020**, *142*, 1698–1703.
- [144] H. Huang, T. H. Lambert, *J. Am. Chem. Soc.* **2021**, *143*, 7247–7252.
- [145] T. Shen, T. H. Lambert, *Science* **2021**, *371*, 620–626.
- [146] T. Shen, T. H. Lambert, *J. Am. Chem. Soc.* **2021**, *143*, 8597–8602.
- [147] H. Huang, T. H. Lambert, *Angew. Chem. Int. Ed.* **2020**, *59*, 658.
- [148] F. Wang, S. S. Stahl, *Angew. Chem. Int. Ed.* **2019**, *58*, 6385–6390.

- [149] H. Yan, Z. W. Hou, H. C. Xu, *Angew. Chem.* **2019**, *131*, 4640–4643.
- [150] L. Zhang, L. Liardet, J. Luo, D. Ren, M. Grätzel, X. Hu, *Nat. Catal.* **2019**, *2*, 366–373.
- [151] W. Zhang, K. L. Carpenter, S. Lin, *Angew. Chem.* **2020**, *132*, 417–425.
- [152] L. Niu, C. Jiang, Y. Liang, D. Liu, F. Bu, R. Shi, H. Chen, A. D. Chowdhury, A. Lei, *J. Am. Chem. Soc.* **2020**, *142*, 17693–17702.
- [153] H. Kim, H. Kim, T. H. Lambert, S. Lin, *J. Am. Chem. Soc.* **2020**, *142*, 2087–2092.
- [154] N. G. Cowper, C. P. Chernowsky, O. P. Williams, Z. K. Wickens, *J. Am. Chem. Soc.* **2020**, *142*, 2093–2099.
- [155] Y. Qiu, A. Scheremetjew, L. H. Finger, L. Ackermann, *Chem. Eur. J.* **2020**, *26*, 3241–3246.
- [156] A. K. Ghosh, M. Brindisi, Y. C. Yen, E. K. Lendy, S. Kovala, E. L. Cárdenas, B. S. Reddy, K. V. Rao, D. Downs, X. Huang, *ChemMedChem* **2019**, *14*, 545–560.
- [157] M. S. Chambers, R. Baker, D. C. Billington, A. K. Knight, D. Middlemiss, E. H. Wong, *J. Med. Chem.* **1992**, *35*, 2033–2039.
- [158] B. W. Lund, F. Piu, N. K. Gauthier, A. Eeg, E. Currier, V. Sherbukhin, M. R. Brann, U. Hacksell, R. Olsson, *J. Med. Chem.* **2005**, *48*, 7517–7519.
- [159] B. Yan, C. Shi, G. T. Beckham, E. Y. X. Chen, Y. Román-Leshkov, *ChemSusChem* **2022**, *15*, e202102317.
- [160] C. Li, C.-C. Zeng, L.-M. Hu, F.-L. Yang, S. J. Yoo, R. D. Little, *Electrochim. Acta* **2013**, *114*, 560–566.
- [161] J. Utley, G. Rozenberg, *J. Appl. Electrochem.* **2003**, *33*, 525–532.
- [162] M. Balaganesh, S. Lawrence, C. Christopher, A. J. Bosco, K. Kulangiappar, K. J. S. Raj, *Electrochim. Acta* **2013**, *111*, 384–389.
- [163] C.-c. Zeng, N.-t. Zhang, C. M. Lam, R. D. Little, *Org. Lett.* **2012**, *14*, 1314–1317.
- [164] G. Celik, R. M. Kennedy, R. A. Hackler, M. Ferrandon, A. Tennakoon, S. Patnaik, A. M. LaPointe, S. C. Ammal, A. Heyden, F. A. Perras, *ACS Cent. Sci.* **2019**, *5*, 1795–1803.
- [165] M. Rafiee, F. Wang, D. P. Hruszkewycz, S. S. Stahl, *J. Am. Chem. Soc.* **2018**, *140*, 22–25.
- [166] H. Zhang, T. Wang, K. Xu, C. Zeng, *J. Org. Chem.* **2021**, *86*, 16171–16176.
- [167] C. Yang, L. A. Farmer, D. A. Pratt, S. Maldonado, C. R. Stephenson, *J. Am. Chem. Soc.* **2021**, *143*, 10324–10332.
- [168] M. A. Hoque, J. Twilton, J. Zhu, M. D. Graaf, K. C. Harper, E. Tuca, G. A. DiLabio, S. S. Stahl, *J. Am. Chem. Soc.* **2022**, *144*, 15295–15302.
- [169] Z.-X. Wu, G.-W. Hu, Y.-X. Luan, *ACS Catal.* **2022**, *12*, 11716–11733.
- [170] F. Bai, N. Wang, Y. Bai, X. Ma, C. Gu, B. Dai, J. Chen, *J. Org. Chem.* **2023**, *88*, 2985–2998.
- [171] T. Shono, A. Ikeda, *J. Am. Chem. Soc.* **1972**, *94*, 7892–7898.
- [172] U.-S. Bäumer, H. Schäfer, *J. Appl. Electrochem.* **2005**, *35*, 1283–1292.
- [173] T. Shono, Y. Matsumura, T. Hashimoto, K. I. Hibino, H. Hamaguchi, T. Aoki, *J. Am. Chem. Soc.* **1975**, *97*, 2546–2548.
- [174] T. Shono, H. Hamaguchi, Y. Matsumura, K. Yoshida, *Tetrahedron Lett.* **1977**, *18*, 3625–3628.
- [175] V. Pfeifer, V. Sohns, H. Conway, E. Lancaster, S. Dabic, E. Griffin, *Ind. Eng. Chem.* **1960**, *52*, 201–206.
- [176] A. Yoshiyama, T. Nonaka, M. M. Baizer, T.-C. Chou, *Bull. Chem. Soc. Jpn.* **1985**, *58*, 201–206.
- [177] W. Partenheimer, *Catal. Today* **2003**, *81*, 117–135.
- [178] L. Cabernard, S. Pfister, C. Oberschelp, S. Hellweg, *Nat. Sustain.* **2022**, *5*, 139–148.
- [179] Q. Huang, G. Chen, Y. Wang, S. Chen, L. Xu, R. Wang, *Resour. Conserv. Recycl.* **2020**, *154*, 104607.
- [180] M. A. Morales, A. Maranon, C. Hernandez, A. Porras, *Polymer* **2021**, *13*, 3162.
- [181] H. Alhazmi, F. H. Almansour, Z. Aldhfeeri, *Sustainability* **2021**, *13*, 5340.
- [182] A. Aboulkas, A. El Bouadili, *Energy Convers. Manage.* **2010**, *51*, 1363–1369.
- [183] R. C. Vázquez Fletes, E. O. Cisneros Lopez, F. J. Moscoso Sanchez, E. Mendizábal, R. González Núñez, D. Rodrigue, P. Ortega Gudiño, *Polymer* **2020**, *12*, 503.
- [184] S. Oh, E. E. Stache, *J. Am. Chem. Soc.* **2022**, *144*, 5745–5749.
- [185] K. Lewandowski, K. Skórczewska, *Polymer* **2022**, *14*, 3035.
- [186] J. J. Assaad, M. Khalil, J. Khatib, *Environments* **2022**, *9*, 37.
- [187] J. J. Assaad, J. M. Khatib, R. Ghanem, *Environments* **2022**, *9*, 8.
- [188] P. He, L. Chen, L. Shao, H. Zhang, F. Lü, *Water Res.* **2019**, *159*, 38–45.
- [189] Y. Kim, J. Lim, H. Cho, J. Kim, *Int. J. Energy Res.* **2022**, *46*, 3409–3427.
- [190] J. Lee, Y. Ahn, H. Cho, J. Kim, *Process Saf. Environ. Prot.* **2022**, *158*, 123–133.
- [191] D. Fico, D. Rizzo, V. De Carolis, F. Montagna, C. Esposito Corcione, *Polymer* **2022**, *14*, 3756.
- [192] S. Li, J. Gainer, *Ind. Eng. Chem. Fundam.* **1968**, *7*, 433–440.
- [193] O. Urakawa, S. F. Swallen, M. Ediger, E. D. von Meerwall, *Macromolecules* **2004**, *37*, 1558–1564.
- [194] J. Rauch, W. Köhler, *J. Chem. Phys.* **2003**, *119*, 11977–11988.
- [195] J. G. Linger, D. R. Vardon, M. T. Guarnieri, E. M. Karp, G. B. Hunsinger, M. A. Franden, C. W. Johnson, G. Chupka, T. J. Strathmann, P. T. Pienkos, *Proc. Nat. Acad. Sci.* **2014**, *111*, 12013–12018.
- [196] A. Turner, *Environ. Sci. Technol.* **2020**, *54*, 10411–10420.
- [197] E. Jakab, M. A. Uddin, T. Bhaskar, Y. Sakata, *J. Anal. Appl. Pyrolysis* **2003**, *68*, 83–99.
- [198] E. Yousif, R. Haddad, *Springerplus* **2013**, *2*, 1–32.
- [199] W. Partenheimer, *Catal. Today* **1995**, *23*, 69–158.
- [200] G. Asensio, G. Castellano, R. Mello, M. González Núñez, *J. Org. Chem.* **1996**, *61*, 5564–5566.
- [201] D. D. Dixon, J. W. Lockner, Q. Zhou, P. S. Baran, *J. Am. Chem. Soc.* **2012**, *134*, 8432–8435.
- [202] S. Liang, C.-C. Zeng, X.-G. Luo, F.-z. Ren, H.-Y. Tian, B.-G. Sun, R. D. Little, *Green Chem.* **2016**, *18*, 2222–2230.
- [203] M. Baumann, I. R. Baxendale, S. V. Ley, N. Nikbin, *Beilstein J. Org. Chem.* **2011**, *7*, 442–495.
- [204] L. M. Blair, J. Sperry, *J. Nat. Prod.* **2013**, *76*, 794–812.
- [205] C. T. Walsh, *Tetrahedron Lett.* **2015**, *56*, 3075–3081.

- [206] P. Majumdar, A. Pati, M. Patra, R. K. Behera, A. K. Behera, *Chem. Rev.* **2014**, *114*, 2942–2977.
- [207] J. Kong, F. Zhang, C. Zhang, W. Chang, L. Liu, J. Li, *J. Mol. Catal.* **2022**, *530*, 112633.
- [208] L. Meng, J. Su, Z. Zha, L. Zhang, Z. Zhang, Z. Wang, *Chem. Eur. J.* **2013**, *19*, 5542–5545.
- [209] J. A. Marko, A. Durgham, S. L. Bretz, W. Liu, *Chem. Commun.* **2019**, *55*, 937–940.
- [210] A. H. Cherney, N. T. Kadunce, S. E. Reisman, *Chem. Rev.* **2015**, *115*, 9587–9652.
- [211] P. Gandeepan, T. Müller, D. Zell, G. Cera, S. Warratz, L. Ackermann, *Chem. Rev.* **2018**, *119*, 2192–2452.
- [212] R. Jana, T. P. Pathak, M. S. Sigman, *Chem. Rev.* **2011**, *111*, 1417–1492.
- [213] S. W. Roh, K. Choi, C. Lee, *Chem. Rev.* **2019**, *119*, 4293–4356.
- [214] B. Liu, A. M. Romine, C. Z. Rubel, K. M. Engle, B.-F. Shi, *Chem. Rev.* **2021**, *121*, 14957–15074.
- [215] B. Yang, Y. Qiu, J.-E. Bäckvall, *Acc. Chem. Res.* **2018**, *51*, 1520–1531.
- [216] A. Shrestha, M. Lee, A. L. Dunn, M. S. Sanford, *Org. Lett.* **2018**, *20*, 204–207.
- [217] Y.-Q. Li, Q.-L. Yang, P. Fang, T.-S. Mei, D. Zhang, *Org. Lett.* **2017**, *19*, 2905–2908.
- [218] Q.-L. Yang, Y.-Q. Li, C. Ma, P. Fang, X.-J. Zhang, T.-S. Mei, *J. Am. Chem. Soc.* **2017**, *139*, 3293–3298.
- [219] N. Sauermaun, T. H. Meyer, C. Tian, L. Ackermann, *J. Am. Chem. Soc.* **2017**, *139*, 18452–18455.
- [220] T. H. Meyer, J. C. Oliveira, D. Ghorai, L. Ackermann, *Angew. Chem. Int. Ed.* **2020**, *59*, 10955–10960.
- [221] L. Massignan, X. Tan, T. H. Meyer, R. Kuniyil, A. M. Messinis, L. Ackermann, *Angew. Chem. Int. Ed.* **2020**, *59*, 3184–3189.
- [222] X. Tan, L. Massignan, X. Hou, J. Frey, J. C. Oliveira, M. N. Hussain, L. Ackermann, *Angew. Chem. Int. Ed.* **2021**, *60*, 13264–13270.
- [223] S. Jin, J. Kim, D. Kim, J. Park, *J. Am. Chem. Soc.* **2020**, *142*, 19052–19057.
- [224] Y. K. Au, H. Lyu, Y. Quan, Z. Xie, *J. Am. Chem. Soc.* **2020**, *142*, 6940–6945.
- [225] Q. J. Yao, F. R. Huang, J. H. Chen, M. Y. Zhong, B. F. Shi, *Angew. Chem.* **2023**, *135*, e202218533.
- [226] J. H. Chen, M. Y. Teng, F. R. Huang, H. Song, Z. K. Wang, H. L. Zhuang, Y. J. Wu, X. Wu, Q. J. Yao, B. F. Shi, *Angew. Chem.* **2022**, *134*, e202210106.
- [227] S. Fukagawa, Y. Kato, R. Tanaka, M. Kojima, T. Yoshino, S. Matsunaga, *Angew. Chem. Int. Ed.* **2019**, *58*, 1153–1157.
- [228] Y.-H. Liu, P.-X. Li, Q.-J. Yao, Z.-Z. Zhang, D.-Y. Huang, M. D. Le, H. Song, L. Liu, B.-F. Shi, *Org. Lett.* **2019**, *21*, 1895–1899.
- [229] K. Ozols, Y.-S. Jang, N. Cramer, *J. Am. Chem. Soc.* **2019**, *141*, 5675–5680.
- [230] A. Whyte, A. Torelli, B. Mirabi, L. Prieto, J. F. Rodriguez, M. Lautens, *J. Am. Chem. Soc.* **2020**, *142*, 9510–9517.
- [231] Y.-H. Liu, P.-P. Xie, L. Liu, J. Fan, Z.-Z. Zhang, X. Hong, B.-F. Shi, *J. Am. Chem. Soc.* **2021**, *143*, 19112–19120.
- [232] W. K. Yuan, B. F. Shi, *Angew. Chem.* **2021**, *133*, 23371–23376.
- [233] K. Ozols, S. Onodera, Ł. Woźniak, N. Cramer, *Angew. Chem. Int. Ed.* **2021**, *60*, 655–659.
- [234] Y.-B. Zhou, T. Zhou, P.-F. Qian, J.-Y. Li, B.-F. Shi, *ACS Catal.* **2022**, *12*, 9806–9811.
- [235] Y. Hirata, D. Sekine, Y. Kato, L. Lin, M. Kojima, T. Yoshino, S. Matsunaga, *Angew. Chem. Int. Ed.* **2022**, *61*, e202205341.
- [236] Q. J. Yao, J. H. Chen, H. Song, F. R. Huang, B. F. Shi, *Angew. Chem. Int. Ed.* **2022**, *61*, e202202892.
- [237] B. J. Wang, G. X. Xu, Z. W. Huang, X. Wu, X. Hong, Q. J. Yao, B. F. Shi, *Angew. Chem. Int. Ed.* **2022**, *61*, e202208912.
- [238] X.-J. Si, D. Yang, M.-C. Sun, D. Wei, M.-P. Song, J.-L. Niu, *Nat. Synth.* **2022**, *1*, 709–718.
- [239] G. Zhou, J. H. Chen, Q. J. Yao, F. R. Huang, Z. K. Wang, B. F. Shi, *Angew. Chem.* **2023**, *135*, e202302964.
- [240] Y. Liang, S.-H. Shi, R. Jin, X. Qiu, J. Wei, H. Tan, X. Jiang, X. Shi, S. Song, N. Jiao, *Nat. Catal.* **2021**, *4*, 116–123.
- [241] B. Chandra, K. Hellan, S. Pattanayak, S. S. Gupta, *Chem. Sci.* **2020**, *11*, 11877–11885.
- [242] C. Amatore, C. Cammoun, A. Jutand, *Synlett* **2007**, *2007*, 2173–2178.
- [243] T. T. Nguyen, L. Grigorjeva, O. Daugulis, *Chem. Commun.* **2017**, *53*, 5136–5138.
- [244] X. Zhu, J.-H. Su, C. Du, Z.-L. Wang, C.-J. Ren, J.-L. Niu, M.-P. Song, *Org. Lett.* **2017**, *19*, 596–599.
- [245] T. Gensch, F. J. Klauk, F. Glorius, *Angew. Chem. Int. Ed.* **2016**, *55*, 11287–11291.
- [246] A. Murtaza, Z. Ulhaq, B. Shirinfar, S. Rani, S. Aslam, G. M. Martins, N. Ahmed, *Chem. Rec.* **2023**, e202300119.
- [247] L.-B. Zhang, S.-K. Zhang, D. Wei, X. Zhu, X.-Q. Hao, J.-H. Su, J.-L. Niu, M.-P. Song, *Org. Lett.* **2016**, *18*, 1318–1321.
- [248] R. Mei, H. Wang, S. Warratz, S. A. Macgregor, L. Ackermann, *Chem. Eur. J.* **2016**, *22*, 6759–6763.
- [249] C. Du, P. X. Li, X. Zhu, J. F. Suo, J. L. Niu, M. P. Song, *Angew. Chem.* **2016**, *128*, 13769–13773.
- [250] L. B. Zhang, X. Q. Hao, S. K. Zhang, Z. J. Liu, X. X. Zheng, J. F. Gong, J. L. Niu, M. P. Song, *Angew. Chem. Int. Ed.* **2015**, *54*, 272–275.
- [251] W. Ma, L. Ackermann, *ACS Catal.* **2015**, *5*, 2822–2825.
- [252] X. Guo, L. Zhang, D. Wei, J. Niu, *Chem. Sci.* **2015**, *6*, 7059–7071.
- [253] Y. Suzuki, B. Sun, K. Sakata, T. Yoshino, S. Matsunaga, M. Kanai, *Angew. Chem. Int. Ed.* **2015**, *54*, 9944–9947.
- [254] L. Grigorjeva, O. Daugulis, *Angew. Chem.* **2014**, *126*, 10373–10376.
- [255] T. Gieshoff, A. Kehl, D. Schollmeyer, K. D. Moeller, S. R. Waldvogel, *J. Am. Chem. Soc.* **2017**, *139*, 12317–12324.
- [256] B. Elsler, A. Wiebe, D. Schollmeyer, K. M. Dybala, R. Franke, S. R. Waldvogel, *Chem. Eur. J.* **2015**, *21*, 12321–12325.
- [257] K. J. Stowers, A. Kubota, M. S. Sanford, *Chem. Sci.* **2012**, *3*, 3192–3195.
- [258] A. Ghosh, D. A. Mitchell, A. Chanda, A. D. Ryabov, D. L. Popescu, E. C. Upham, G. J. Collins, T. J. Collins, *J. Am. Chem. Soc.* **2008**, *130*, 15116–15126.



- [259] D. P. de Sousa, C. J. Miller, Y. Chang, T. D. Waite, C. J. McKenzie, *Inorg. Chem.* **2017**, *56*, 14936–14947.
- [260] M. J. Bartos, S. W. Gordon-Wylie, B. G. Fox, L. J. Wright, S. T. Weintraub, K. E. Kauffmann, E. Münck, K. L. Kostka, E. S. Uffelman, C. E. Rickard, *Coord. Chem. Rev.* **1998**, *174*, 361–390.
- [261] T. J. Collins, *Acc. Chem. Res.* **2002**, *35*, 782–790.
- [262] T. J. Collins, A. D. Ryabov, *Chem. Rev.* **2017**, *117*, 9140–9162.
- [263] S. Jana, M. Ghosh, M. Ambule, S. Sen Gupta, *Org. Lett.* **2017**, *19*, 746–749.
- [264] M. Bugnola, K. Shen, E. Haviv, R. Neumann, *ACS Catal.* **2020**, *10*, 4227–4237.
- [265] S. Puchkov, E. Buneeva, A. Perkel', *Kinet. Catal.* **2002**, *43*, 756–763.
- [266] J. M. Mayer, *Acc. Chem. Res.* **2011**, *44*, 36–46.
- [267] M. Bugnola, R. Carmieli, R. Neumann, *ACS Catal.* **2018**, *8*, 3232–3236.
- [268] Y. Yuan, A. Lei, *Nat. Commun.* **2020**, *11*, 802.
- [269] T. H. Meyer, L. H. Finger, P. Gandeepan, L. Ackermann, *Trends Chem.* **2019**, *1*, 63–76.
- [270] a) A. Murtaza, Z. Ulhaq, B. Shirinfar, S. Aslam, S. Rani, G. M. Martins, N. Ahmed, *Chem. Rec.* **2023**, *23*, e202300119; b) T. Pokhrel, B. K. Bijaya, R. Giri, A. Adhikari, N. Ahmed, *Chem. Rec.* **2022**, *22* (6), e202100338; c) A. Murtaza, M. A. Qamar, K. Saleem, T. Hardwick, Z. Ulhaq, B. Shirinfar, N. Ahmed, *Chem. Rec.* **2022**, *22* (5), e202100296; d) N. Sbei, S. Aslam, N. Ahmed, *React. Chem. Eng.* **2021**, *6*, 1342–1366; e) T. Hardwick, N. Ahmed, *Chem. Sci.* **2020**, *11*, 11973–11988; f) T. Hardwick, R. Cicala, N. Ahmed, *Scientific Reports* **2020**, *10*, 16627 (10.1038/s41598-020-73957-6); g) M. Islam, B. M. Kariuki, Z. Shafiq, T. Wirth, N. Ahmed, *Eur. J. Org. Chem.* **2019**, 1371–1376; h) T. Hardwick, N. Ahmed, *RSC Advances* **2018**, *8*, 22233–22249.

---

*Manuscript received: October 27, 2023*

*Revised manuscript received: November 23, 2023*

*Version of record online: December 8, 2023*